PUCRS

FACULDADE OU ESCOLA

PROGRAMA DE PÓS-GRADUAÇÃO

TESE PARA OBTENÇÃO DO TÍTIULO DE DOUTORADO EM ENGENHARIA E TECNOLOGIA DOS MATERIAIS

SÉRGIO ROBERTO DA SILVA

USO DE RESÍDUO DE CONSTRUÇÃO E DEMOLIÇÃO (RCD), CINZA VOLANTE E CAL HIDRATADA PARA PRODUÇÃO DE CONCRETOS APLICADOS NA CONSTRUÇÃO CIVIL

Porto Alegre

Agosto/2022

PÓS-GRADUAÇÃO - *STRICTO SENSU*

Pontifícia Universidade Católica
do Rio Grande do Sul

ESCOLA POLITÉCNICA
PUCRS
Pontifícia Universidade Católica do Rio Grande do Sul
Programa de Pós-Graduação em Engenharia e Tecnologia de Materiais

USO DE RESÍDUO DE CONSTRUÇÃO E DEMOLIÇÃO (RCD), CINZA VOLANTE E CAL HIDRATADA PARA PRODUÇÃO DE CONCRETOS APLICADOS NA CONSTRUÇÃO CIVIL

SÉRGIO ROBERTO DA SILVA

BACHAREL EM ENGENHARIA CIVIL

MESTRE EM ENGENHARIA E TECNOLOGIA DOS MATERIAIS

ORIENTADOR: PROF. DR. JAIRO JOSÉ DE OLIVEIRA ANDRADE

Tese realizada no Programa de Pós-Graduação em Engenharia e Tecnologia de Materiais (PGETEMA) da Pontifícia Universidade Católica do Rio Grande do Sul, como parte dos requisitos para a obtenção do título de Mestre/Doutor em Engenharia e Tecnologia de Materiais.

Porto Alegre

Agosto, 2022

Ficha Catalográfica

da Silva, Sérgio Roberto

Uso de Resíduo de Construção e Demolição (RCD), Cinza Volante e Cal Hidratada para Produção de Concretos Aplicados na Construção Civil / Sérgio Roberto da Silva. – 2022.

118 f.

Tese (Doutorado) – Programa de Pós-Graduação em Engenharia e Tecnologia de Materiais, PUCRS.

Orientador: Prof. Dr. Jairo José de Oliveira Andrade.

1. Cimento Portland. 2. Cal Hidratada. 3. Cinza volante. 4. RCD. 5. Escola Politécnica da PUCRS - PGETEMA. I. de Oliveira Andrade, Jairo José. II. Título.

Elaborada pelo Sistema de Geração Automática de Ficha Catalográfica da PUCRS
com os dados fornecidos pelo(a) autor(a).
Bibliotecária responsável: Clarissa Jesinska Selbach CRB-10/2051

Pontifícia Universidade Católica do Rio Grande do Sul
ESCOLA POLITÉCNICA
PROGRAMA DE PÓS-GRADUAÇÃO EM ENGENHARIA E TECNOLOGIA DE MATERIAIS

Uso de resíduo de construção e demolição (RCD), cinza volante e cal hidratada para produção de concretos aplicados na construção civil

CANDIDATO: SERGIO ROBERTO DA SILVA

Esta Tese de Doutorado foi julgada para obtenção do título de DOUTOR EM ENGENHARIA E TECNOLOGIA DE MATERIAIS e aprovada em sua forma final pelo Programa de Pós-Graduação em Engenharia e Tecnologia de Materiais da Pontifícia Universidade Católica do Rio Grande do Sul.

DR. JAIRO JOSÉ DE OLIVEIRA ANDRADE - ORIENTADOR

BANCA EXAMINADORA

DRA. EDNA POSSAN - PPGECI - ILATTI/UNILA

DR. MAURICIO MANCIO - PROGRAMA DE PÓS-GRADUAÇÃO EM ENGENHARIA CIVIL - PPGEC - UNISINOS

DRA. ELEANI MARIA DA COSTA - PGETEMA - PUCRS

DEDICATÓRIA

Dedico este trabalho, primeiramente, à Deus que me deu saúde para poder desenvolver este trabalho. Foi pensando nas pessoas que executei este projeto, por isso o dedico a todos aqueles a quem esta pesquisa possa ajudar de alguma forma.

Dedico também este trabalho ao Programa de Pós-graduação em Engenharia e Tecnologia dos Materiais (PGETEMA), corpo docente e discente, a quem fico lisonjeado por dele ter feito parte. Em especial, dedico este trabalho à minha esposa que, por muitas vezes, compreendeu minha ausência em sua vida.

AGRADECIMENTOS

Apesar da grande dificuldade de desenvolver este trabalho em virtude do período pandêmico, em que toda a população brasileira teve que ficar isolada e impossibilitada de executar trabalhos externos, foi possível dar uma contribuição a um tema inovador, visando o contexto da sustentabilidade. Além deste trabalho ter contribuído para o enriquecimento na minha formação como engenheiro, construí grandes amizades durante esta caminhada.

Primeiramente, gostaria de agradecer à CAPES e a esta Universidade pela bolsa de estudos que permitiu minha permanência no Programa de Pós-graduação em Engenharia e Tecnologia dos Materiais (PGETEMA). “O presente trabalho foi realizado com apoio da Coordenação de Aperfeiçoamento de Pessoal Nível Superior – Brasil (CAPES) – Código de Financiamento 88887.091736/2014-01”.

Agradeço ao auxílio e sobretudo a amizade:

Ao meu orientador Professor Dr. Jairo José de Oliveira Andrade por aceitar este desafio e sempre estar pronto para esclarecimentos de dúvidas. Sua maior virtude é a sua disposição em nos passar seus preciosos conhecimentos.

Ao meu grande amigo e Professor Pós-Doutor Alexandre Silva de Vargas, que, atualmente, é professor do Programa de Pós-graduação em Engenharia Civil da Universidade Federal de Santa Maria. Sua contribuição para o desenvolvimento do tema escolhido neste trabalho foi muito relevante.

Aos meus colegas engenheiros e engenheiras Pietra Moraes Borges, Jessica Zamboni Schiavon e Tiago Ortolan pelos bons momentos compartilhados durante o desenvolvimento deste trabalho.

À professora Dra. Edna Possan, professora do Programa de Pós-Graduação em Tecnologias Ambientais na Universidade Tecnológica Federal do Paraná, que contribuiu com diversas análises de laboratório constantes neste trabalho.

Aos técnicos do Laboratório de Materiais de Construção (LAMAT), engenheiro Douglas Tischner Rodeghiero e José Eduardo R. da Cruz.

“Se a educação sozinha não transforma a sociedade, sem ela tampouco a sociedade muda.”
(Paulo Freire)

RESUMO

DA SILVA, Sérgio Roberto. **Uso de resíduo de construção e demolição (RCD), cinza volante e cal hidratada para produção de concretos aplicados na construção civil.** Porto Alegre. 2022. Tese. Programa de Pós-Graduação em Engenharia e Tecnologia de Materiais, PONTIFÍCIA UNIVERSIDADE CATÓLICA DO RIO GRANDE DO SUL.

A pesquisa foi desenvolvida em duas etapas: Etapa 1, o objetivo foi avaliar o efeito do agregado reciclado misto (ARM) como agregado graúdo nas propriedades mecânicas (resistência à compressão e módulo de elasticidade), físicas (absorção d'água, porosidade e massa específica), na difusão de CO_2 e microestruturais (MEV e microtomografia de raios X) em concretos com ARM nos teores de substituição de 25, 50 75 e 100% em substituição parcial ao agregado natural e concreto de referência. As relações a/c foram 0,40, 0,50 e 0,60. Foram gerados modelos matemáticos para calcular o módulo de elasticidade a partir de uma f_{c28} e relação a/c desejada e o teor de ARM necessário. Etapa 2, o objetivo foi avaliar a eficiência da adição de cal hidratada dolomítica em concretos de cimento Portland, cinza volante (CV) e agregado reciclado (AR) como agregado graúdo, como forma de melhorar as propriedades mecânicas nas menores idades, bem como diminuir a profundidade de carbonatação. Para tal, foram produzidos concretos com 20% de CV em substituição parcial ao CP, adição de cal hidratada nas proporções de 5 e 10% do total de aglomerante em massa e relação água/aglomerante de 0,55. O ARM e agregado reciclado de concreto (ARC) foi na proporção de 50% de substituição por agregado graúdo natural. Para isso, foram realizados ensaios mecânicos (resistência à compressão axial, módulo de elasticidade), físicos (absorção d'água, porosidade e massa específica), na difusão de CO_2 e análise microestruturais (MEV e microtomografia de raios X). Os resultados da Etapa 1 mostraram que concretos com teor de ARM de 50% e relação a/c 0,50 apresentou queda na f_{c28} e E_{c28} de 18% e 54,9% respectivamente quando comparado ao concreto de referência. O aumento no volume de vazios foi de 33% quando comparado ao concreto de referência. Os resultados da Etapa 2 mostraram que a adição de 10% de cal hidratada em concretos com 80% de CP, 20% de CV e 50% de ARC apresentou resistência à compressão

aos 63 dias 12,47% maior quando comparado ao concreto sem cal hidratada. O E_{c28} melhorou 3,78% em comparação ao concreto sem cal hidratada. A espessura média da ITZ dos concretos com e sem 10% de cal hidratada foi de 3,61 µm e 6,28 µm respectivamente. A adição da cal hidratada em concretos de cimento Portland com CV e RA restabelece o teor remanescente de $Ca(OH)_2$ na matriz antecipando as reações pozolânicas em idades precoces.

Palavras-Chave: concreto; FA; ARM; ARC; cal hidratada.

ABSTRACT

DA SILVA, Sérgio Roberto. ***Use of construction and demolition waste (RCD), fly ash and hydrated lime for production of concrete applied in civil construction.*** *Porto Alegre. 2022*. PhD Thesis. Graduation Program in Materials Engineering and Technology, PONTIFICAL CATHOLIC UNIVERSITY OF RIO GRANDE DO SUL.

The research was developed in two stages: In stage 1, the objective was to evaluate the effect of mixed recycled aggregate (MRA) as coarse aggregate on the mechanical properties (compressive strength and elastic modulus), physical (water absorption, porosity, and bulk density), in the diffusion of CO_2 and microstructural (SEM and X-ray microtomography) in concretes with MRA in the substitution levels of 25, 50, 75 and 100% in partial substitution to the natural aggregate and reference concrete. The w/c ratios were 0.40, 0.50 and 0.60. Mathematical models were generated to calculate the elastic modulus from an f_{c28} and desired w/c ratio and the required MRA content. Stage 2, the objective was to evaluate the efficiency of adding hydrated dolomitic lime in Portland cement concrete, fly ash (CV), and recycled aggregate (RA) as coarse aggregate, as a way of improving the mechanical properties at the lowest ages, as well as reducing the depth of carbonation. For this, concretes were produced with 20% of CV in partial replacement of the CP, the addition of hydrated lime in the proportions of 5, and 10% of the total binder in mass and w/b ratio of 0.55. The MRA and recycled concrete aggregate (RCA) was 50% replaced by natural coarse aggregate. For this, mechanical (compressive strength, elastic modulus), physical (water absorption, porosity and bulk density), CO_2 diffusion and microstructural analysis (SEM and X-ray microtomography) tests were performed. The results of Stage 1 showed that concretes with MRA content of 50% and w/c ratio of 0.50 presented a decrease in f_{c28} and E_{c28} of 18% and 54.9%, respectively, when compared to the reference concrete. The increase in the volume of voids was 33% when compared to the reference concrete. The results of Stage 2 showed that the addition of 10% hydrated lime in concretes with 80% CP, 20% CV, and 50% ARC presented compressive strength at 63 days 12.47% higher when compared to concrete without lime hydrated. E_{c28} improved by 3.78% compared to concrete without hydrated lime. The average ITZ thickness of the concretes without and with 10% hydrated lime

was 3.61 µm and 6.28 µm, respectively. The addition of hydrated lime in Portland cement concretes with CV and RA restores the remaining $Ca(OH)_2$ content in the matrix, anticipating pozzolanic reactions at early ages.

Keywords: concrete; FA; MRA; RCA; hydrated lime.

LISTA DE FIGURAS

LISTA DE TABELAS

LISTA DE QUADROS

LISTA DE SÍMBOLOS

A	Absorção	mm
f_c	Resistência à compressão axial	MPa
E_c	Módulo de Elasticidade	GPa
f_{tD}	Resistência à tração por compressão diametral	MPa
K	Coeficiente de carbonatação	$mm/mês^{0,5}$
e_{CO_2}	Profundidade de carbonatação	mm
RCD	Resíduo de construção e demolição	
ARM	Agregado reciclado misto	
ARC	Agregado reciclado de concreto	
RA	Agregado reciclado	

SUMÁRIO

1. INTRODUÇÃO

Este capítulo apresenta a contextualização, justificava, hipótese, objetivo, delimitações bem como a estrutura da pesquisa.

1.1 CONTEXTUALIZAÇÃO

Ao longo dos anos, as infraestruturas tem sido construídas basicamente com concreto, aço e madeira, além do vidro, que são considerados os principais materiais utilizados na construção contemporânea (SEDDIK MEDDAH, 2017). A indústria da construção civil produz grande quantidade de resíduos sólidos proveniente de construção e demolição (RCD) (SOLÍS-GUZMÁN et al., 2009). No Brasil, em 2020, foram produzidos 47 milhões de toneladas de RCD que corresponde a 221,19 kg/hab/ano (ABRELPE, 2021). Um dos grandes desafios do uso do RCD como matéria-prima para a produção de novos concretos é variabilidade em sua composição bem como as impurezas e contaminantes que influenciam nas propriedades mecânicas e de durabilidade dos concretos (CUNHA, 2017). A extração de matérias-primas, o beneficiamento de materiais para a construção civil, as construções de edificações bem como reformas e demolições geram resíduos sólidos que, depositados de forma inadequada, podem trazer diversos problemas, tais como: proliferações de agentes transmissores de doenças, degradação das áreas de manancial e de proteção permanente, obstrução dos sistemas de drenagem, assoreamento de rios e córregos bem como ocupação de vias que degradam a paisagem urbana (SILVA; DE BRITO; DHIR, 2016).

O uso de resíduo de construção e demolição (RCD) em substituição parcial aos agregados naturais para a produção de concretos, em pequenas quantidades, apresentam resultados bastante promissores tanto nas propriedades mecânicas e de

durabilidade quanto no que tange ao ciclo de vida, como observado no estudo de Martínez-Lage et al. (2020). Entretanto, a variabilidade dos resíduos, com diferentes composições, propriedades físicas e mecânicas, para elevados teores de substituição, pode apresentar resultados negativos em função do aumento de porosidade, e absorção de água, que leva a um acréscimo da relação a/c, considerando uma mesma trabalhabilidade, tornando a pasta do cimento mais fraca e porosa (BRAVO et al., 2017;WANG; PARK, 2015;BRAVO et al., 2015a;CHOUSIDIS et al., 2016).

O setor da construção civil também tem participação na geração de dióxido de carbono (CO_2) (CAMPOS et al., 2020). Além disso, as emissões de CO_2 cresceram para 36,3 Gt em 2021, de acordo com Global Energy Review (INTERNATIONAL ENERGY AGENCY, 2022), e apenas o carvão foi responsável por mais de 40% do crescimento global das emissões de CO_2 em 2021 que foi de 15,3 Gt, superando o pico de 200 Mt de 2014. Meyer (2009) e Aprianti (2015) destacam que a redução da produção de cimento Portland seria uma das alternativas para diminuir o impacto ambiental. Uma das formas seria a utilização de subprodutos gerados por processos industriais como cinza volante (CV) em substituição parcial ao CP, e materiais reciclados proveniente de RCD como agregado graúdo e agregado miúdo em substituição parcial ao agregado natural. Acar e Atalay (2013) ressaltam que muitas usinas termoelétricas foram construídas em um período de 80 anos devido à crescente demanda para geração de energia elétrica. Os estados do Rio Grande do Sul, Maranhão e Ceará, considerados os maiores produtores de cinza volante no Brasil, produzem 2,66 milhões de toneladas/ano (CIRINO et al., 2021).

De modo geral, a adição de cinza volante em substituição parcial ao cimento Portland em massa apresenta uma influência positiva no que tange às propriedades mecânicas e relacionadas com a durabilidade em concretos com RCD, quando comparados com concretos com agregado reciclado e sem cinza volante nas maiores idades. Outro fator importante da adição de cinza volante em substituição parcial ao cimento Portland é o impacto ambiental positivo. O uso de cinza volante em concretos contribui para a redução da extração de reservas naturais de argila e calcário para a fabricação do cimento e, consequentemente, contribui para a redução do consumo energético para a produção do clínquer. Alguns estudos mostram que o uso de adições minerais tendem a diminuir o pH da solução dos poros em função do consumo

parcial ou total do hidróxido de cálcio (ANJOS et al., 2020; ZHAO et al., 2016). A diminuição do pH da solução dos poros tende a aumentar a porosidade e a absorção d'água (HUANG et al., 2021).

Pesquisas buscam potencializar o uso de cinza volante em concretos, pastas e argamassas com ativadores alcalinos. Os ativadores mais comuns utilizados nos estudos são hidróxido de sódio e sulfato de sódio (DE VARGAS et al., 2011;RODRIGUE et al., 2018). O emprego desses ativadores alcalinos vem apresentando resultados promissores, porém necessita de alto consumo de energia e tem efeitos negativos significativos na trabalhabilidade (RAKNGAN et al., 2018;RAKNGAN et al., 2018). A álcali-ativação da CV dependerá da sua composição química, do teor de silica reativa, da morfologia, da granulometria , do tipo de ativador empregado bem como sua concentração e do processo de cura (CIRINO et al., 2021; DE VARGAS et al., 2011). Quanto maior a área superficial da cinza volante maior será a sua reatividade pozolânica, ou seja, a finura da cinza volante tem influência no índice pozolânico (MYADRABOINA et al., 2017; GUNASEKARA et al., 2015) e consequentemente maior será a resistência mecânica do concreto (GUNASEKARA et al., 2015; KIATTIKOMOL et al., 2001). Segundo Blissett e Rowson (2012), a composição química das cinzas volantes é a base para avaliar a sua adequação para uso como material pozolânico.

A norma internacional ASTM C618:2012 classifica a cinza volante em "C" e "F", sendo classe "C" para as cinzas volantes que apresentam na soma dos principais óxidos ($SiO_2 + Al_2O_3 + Fe_2O_3$) teor inferior a 70% e classe "F" para os que apresentam teor maior ou igual a 70%. A Norma Brasileira NBR 12653 (ABNT 1992) classifica a cinza volante como classe "C" para as cinzas volantes que apresentam na soma dos principais óxidos teor superior a 70%. A estrutura cristalina no processo de hidratação também é outro fator inerente nas propriedades das cinzas volantes (DURDZIŃSKI et al., 2015). Grandes variações na quantidade de óxidos dentro de uma mesma classe de cinza volante estão associadas à sua origem e no processo de calcinação são observados em diferentes estudos (CHOUSIDIS et al., 2016; MYADRABOINA et al., 2017; HANUMANTHA RAO et al., 2016; TOSUN-FELEKOĞLU et al., 2017; WRIGHT et al., 2014; SHAFAATIAN et al., 2013).

A cura térmica de concretos com cinza volante álcali-ativada permite que o processo de policondensação seja acelerada resultando em ganho significativo da resistência em idades inicias (HEFNI; ZAHER; WAHAB, 2018; DING; DAI; SHI, 2016; HUSEIEN et al., 2019). Entretanto para cada ativador alcalino utilizado para o processo de ativação, existe uma temperatura adequada (DE VARGAS et al., 2011).

A adição da cal hidratada em concretos com cinza volante melhora a resistência mecânica entre 10 e 15% quando comparado aos concretos somente com cinza volante aos 28 dias de cura (BAGHABRA AL-AMOUDI et al., 2021). A presença de cinza volante com adição de cal hidratada na produção de concretos melhora as propriedades microestruturais e a penetração de íons cloreto (FILHO et al., 2013;FILHO, 2008a). A carência de informações referente ao efeito da cal hidratada em concretos de cimento Portland com CV e RA foi o carro chefe que instigou a desenvolver este estudo, com vista em agregar conhecimento científico sobre o tema. Nenhum estudo foi encontrado sobre adição de cal hidratada em concretos de cimento Portland, CV e RA.

1.2 JUSTIFICATIVA DA PESQUISA

As cinzas volantes, resíduos provenientes da queima de carvão geradas pelas usina termelétricas, são estocados em depósitos ao ar livre e apresentam potencial risco ao meio ambiente e aos ecossistemas circunvizinhos (CIRINO et al., 2021). A vantagem da adição de cinza volante em substituição parcial ao cimento Portland para a produção de concretos é a sua eficácia no que tange ao fator econômico e sustentável, e motiva a sua aplicação no mercado como componente de concretos estruturais (ALMEIDA; GOMES, 2021). Porém esta substituição resulta em um concreto com menor teor de clinquer e consequentemente o $Ca(OH)_2$ é reduzido na matriz do concreto. Para compensar a redução do $Ca(OH)_2$ alguns estudos sugerem a adição de cal hidratada (GUNASEKARA et al., 2020)(HURTADO-FIGUEROA; ECHAVARRIA-PAEZ; CÁRDENAS-GUTIÉRREZ, 2019)(VALCUENDE et al., 2020).

O ineditismo deste trabalho é a avaliação, de forma conjunta, do efeito da adição da cal hidratada em concretos com cimento Portland, cinza volante e agregado reciclado. Logo, a pesquisa desenvolvida neste trabalho justifica-se pelas seguintes razões:

a) pela necessidade de avaliar experimentalmente as propriedades físicas (absorção d'água, porosidade e massa específica), mecânicas (resistência à compressão e módulo de elasticidade), difusão de CO_2 e microestruturais dos concretos com cinza volante, cal hidratada e agregado reciclado;

b) pela importância de se analisar a distribuição dos poros em concreto de cimento Portland, com cinza volante, cal hidratada de agregado reciclado;

c) pela busca de encontrar alternativa para o emprego do resíduo sólido proveniente de construção e demolição como agregado reciclado e cinza volante em substituição parcial ao cimento Portland. Desta forma os benefícios seriam a redução do consumo dos recursos naturais e a diminuição das emissões de CO_2 no meio ambiente.

Considerando que o concreto é o material de construção civil mais utilizado no mundo, a contribuição para uma redução no impacto ambiental decorrente de seus processos produtivos é um desafio relevante para a sustentabilidade.

1.3 HIPÓTESES DA PESQUISA

A redução nas propriedades mecânicas e de durabilidade dos concretos quando o agregado natural é substituído parcialmente por RCD dependerá do teor de substituição de RCD, pois quanto maior o teor de substituição maior será os efeitos negativos nas propriedades físicas e mecânicas do concreto (DIMITRIOU; SAVVA; PETROU, 2018). Entretanto, muitos estudos vêm sendo desenvolvidos para encontrar um teor ótimo de cinza volante e agregado reciclado a fim de tornar possível o uso combinado destes materiais para a produção de novos concretos (ALI; GULZAR; RAZA, 2021; BISWAL; DINAKAR, 2021; VIEIRA et al., 2020).

Porém, alguns estudos mostram que a cinza volante com adição de cal hidratada na produção de concretos tem apresentado resultados positivos no que tange as propriedades mecânicas e de durabilidade dos concretos quando comparados com concretos com cinza volante sem adição da cal hidratada

(BAGHABRA AL-AMOUDI et al., 2021; ADESINA; OLUTOGE, 2019;FILHO et al., 2013).

Partindo desta premissa, a hipótese que se coloca nesta pesquisa é:

A adição de cal hidratada em concretos de cimento Portland, cinza volante e agregado reciclado proveniente de construção e demolição com agregado graúdo, tende a melhorar a resistência compressão, módulo de elasticidade, difusão de CO_2, bem como a morfologia da pasta de cimento.

1.4 OBJETIVO GERAL

O objetivo geral desta pesquisa é avaliar a potencialidade do emprego de resíduo da construção e demolição (RCD) como agregado graúdo reciclado e cinza volante com adição de cal hidratada na produção de concretos de cimento Portland.

1.5 OBJETIVOS ESPECÍFICOS

Como objetivos específicos, podem ser destacados:

a) Investigar o efeito do agregado reciclado misto em concretos de cimento Portland nas propriedades mecânicas (módulo de elasticidade, resistência a compressão e resistência à tração), nas propriedades físicas (absorção d'água, porosidade e massa específica), difusão de CO_2 e análises microestruturais (morfologia da pasta e porosidade).

b) Verificar as correlações entre as propriedades mecânicas (módulo de elasticidade, resistência à compressão e profundidade de carbonatação) considerando os concretos investigados;

c) Investigar o efeito da cal hidratada em concretos de cimento Portland com cinza volante e agregado reciclado graúdo de duas fontes (ARM e ARC) nas propriedades mecânicas (resistência à compressão e módulo de elasticidade), físicas (absorção d'água, porosidade e massa específica),

difusão de CO_2 e análises microestruturais (morfologia da pasta e porosidade).

d) Analisar as correlações das resistências à compressão aos 63 e 28 dias de cura dos concretos de cimento Portland, cinza volante, e dois diferentes tipos de agregado reciclado (ARM e ARC) como agregado graúdo, para avaliar o efeito da antecipação da reação pozolânica com a adição da cal hidratada;

1.6 DELIMITAÇÕES DA PESQUISA

Esta pesquisa limitou-se na produção de concretos com dois tipos de agregado reciclado (ARM e ARC) como agregado graúdo, cinza e de cal hidratada dolomítica. O período do desenvolvimento deste trabalho coincidiu com o período da pandemia que aconteceu no Brasil entre 2020 e 2021, que torna o prazo mais curto para realização dos ensaios mecânicos e de durabilidades dos concretos em idades superiores a 63 dias. Apesar das limitações, espera-se que este trabalho contribua para o avanço no conhecimento do efeito da adição da cal hidratada em concretos de cimento Portland, cinza volante e agregado reciclado.

1.7 ESTRUTURA DO TRABALHO

Este estudo foi desenvolvido em forma de artigo sendo composta por 5 capítulos, sendo que no primeiro capítulo está inserido a contextualização, justificativa, hipótese da pesquisa bem como o objetivo geral e objetivos específicos. No segundo capítulo está apresentada uma revisão bibliográfica que mostra as principais pesquisas relacionadas ao tema. No terceiro capítulo está inserida uma introdução do planejamento experimental que é dividido em duas etapas, método e o artigo da etapa 1 e o método e o artigo da etapa 2. No quarto capítulo estão apresentadas apresentado as conclusões finais e finalmente no quinto capítulo estão indicadas sugestões para a continuidade de pesquisas na área.

2. REVISÃO BIBLIOGRAFICA

Este capítulo apresenta as características físicas do agregado reciclado, análise comparativa entre concretos com agregado reciclado misto e agregado reciclado de concreto, uso da cinza volante em concretos com RCD, influência da adição da cal hidratada em concretos com cinza volante e RCD e análises microestruturas dos concretos com cimento Portland, cinza volante, cal hidratada e RCD

2.1 AGREGADO GRAÚDO RECICLADO PROVENIENTE DE RESÍDUO DE CONSTRUÇÃO E DEMOLIÇÃO (RCD)

O descarte de resíduos de construção e demolição é uma preocupação que as empresas que atuam na construção civil deveriam ter. O aproveitamento destes resíduos sólidos pode trazer benefícios econômicos, sociais e ambientais. Os RCD, em geral, são constituídos de agregado natural, argamassa aderida, tijolos de barro, gesso (MARTÍN-MORALES et al., 2011). Estes resíduos apresentam grande variabilidade, são mais porosos e apresentam maior capacidade de absorção d'água, o que leva a maiores relações a/c, e torna a pasta do cimento menos resistente mecanicamente e porosa (BRAVO et al., 2017;WANG; PARK, 2015;BRAVO et al., 2015a;CHOUSIDIS et al., 2016). A variabilidade dos RCD foi verificada por Bravo et al. (2015). O autor coletou RCD de cinco unidades de reciclagem de diferentes regiões (Valnor, Vimajas, Ambilei, Eutopontal e Retria) da Europa. A composição dos RCD coletados está apresentada no Figura 2.1.

Figura 2.1: Composição dos agregados reciclados graúdos coletados em diferentes regiões da Europa

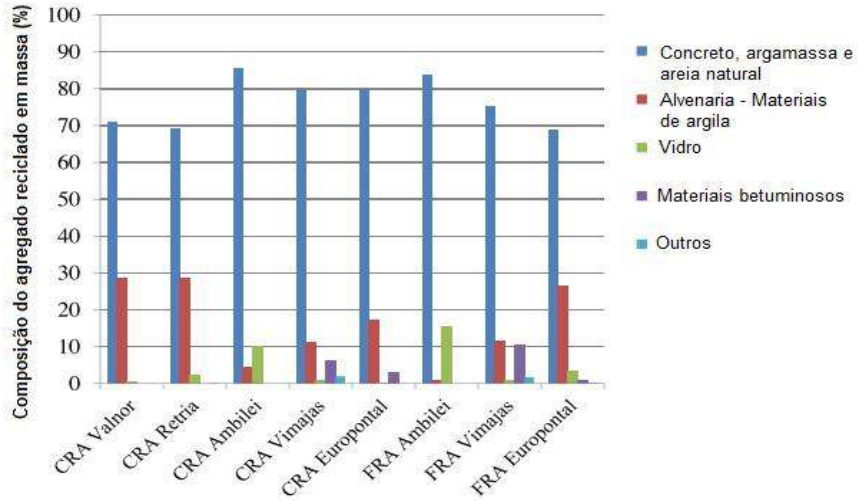

Fonte: Bravo et al. (2015).

De acordo com a composição do reciclado (CRA) de concreto como agregado graúdo em massa, a variabilidade dos matérias são bastante elevadas. Observa-se que em algumas origens os agregados reciclados contêm em sua composição materiais betuminosos em até 10%. A diferença nas propriedades físicas como densidade aparente, absorção d'água, índice de forma e densidade das partículas secas dos RCD de diferentes origens foram investigadas por Bravo et al. (2015) e está apresentada na Tabela 2.1.

Tabela 2.1 - Propriedades físicas do agregado natural e agregados reciclados de diferentes origens.

		Agregado reciclado graúdo				
Ensaios	**Agregado natural**	**Valnor**	**Retria**	**Ambilei**	**Vimajas**	**Europontal**
Densidade Aparente (kg/m³)	1350	1095	1236	1288	1261	1285
Absorção d'água (%)	1,5	8,6	8,4	9,9	6,4	5,5
Índice de forma (%)	17	24	24	14	25	21
Densidade partículas secas (kg/m³)	2609	2091	2137	1928	2243	2262

Fonte: Bravo et al. (2015).

A menor densidade e a maior capacidade de absorção d'água dos RCD estão relacionados com a porosidade intrínseca do material, que tende a diminuir a resistência mecânica dos concretos (CHOUSIDIS et al., 2016; WANG; PARK, 2015).

A capacidade de absorção d'água em agregado graúdo reciclado é superior quando comparado ao agregado graúdo natural. Segundo Martínez-lage et al. (2020) e Verian et al. (2018) a maior capacidade de absorção d'água em RCD se deve à porosidade da argamassa aderida, massa específica menor em comparação ao agregado natural, em função da presença da argamassa antiga ligada à sua superfície. Uma correlação entre a absorção d'água e a massa específica dos RCD foi verificada por Verian et al. (2018). De acordo com a análise realizada pelos autores (Figura 2.2), quanto maior for a absorção d'água, menor será sua massa específica.

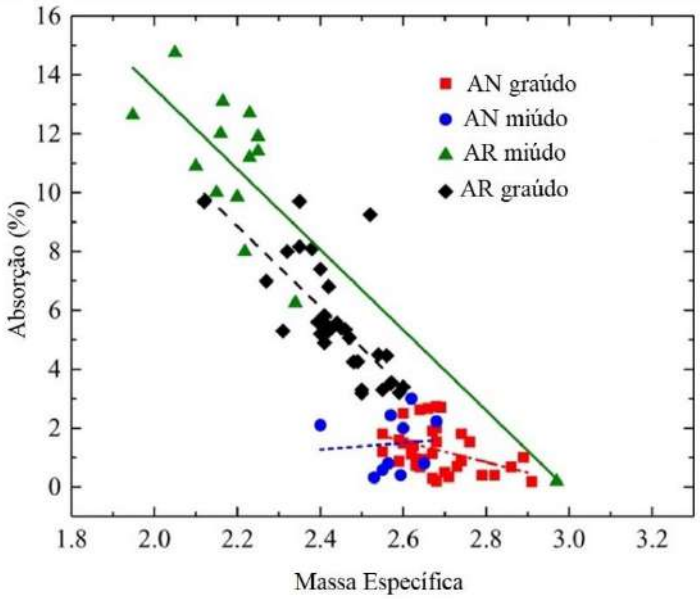

Figura 2.2: Massa específica e absorção d'água de agregado reciclado (RA) e agregado natural (na) em vários estudos (VERIAN et al., 2018)

Segundo alguns estudos o agregado reciclado é formado de duas Zonas de Transição Interfacial (ITZ), sendo uma localizada entre o agregado natural e a matriz de cimento antiga, e a outra localizada entre a matriz de cimento antiga e a nova matriz de cimento (POON; SHUI; LAM, 2004; XIAO et al., 2013; DUAN et al., 2013). Kisku et al. [59] fizeram um diagrama esquemático (Fig. 3.3) das Zonas de Transição Interfacial (ITZ) no agregado reciclado.

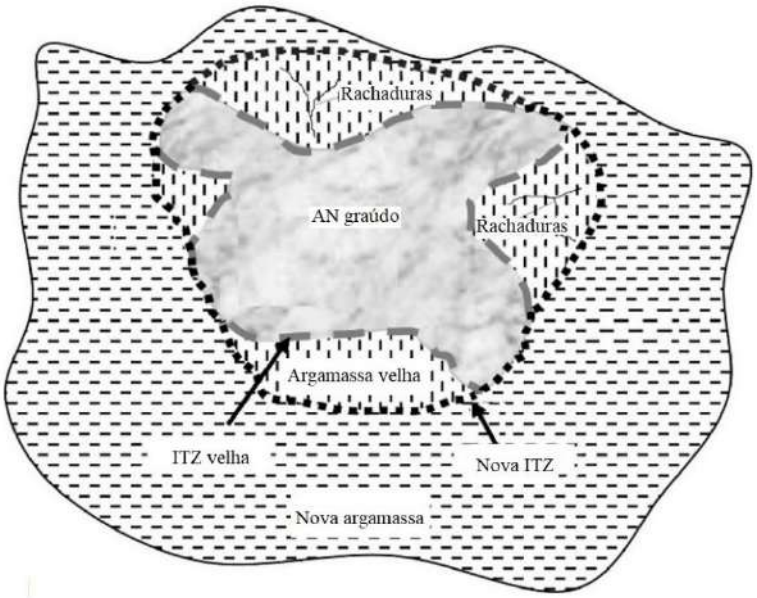

Figura 2.3: Diagrama esquemático da antiga e nova ITZ – adaptado de (KISKU et al., 2017).

Na perspectiva de Zhang et al. (2019), o agregado reciclado é constituído de três ITZ. A primeira ITZ está localizada entre o agregado novo e a nova argamassa de cimento, a segunda ITZ está localizada entre a argamassa velha e a nova e, por fim, a terceira ITZ está localizada entre a argamassa velha e o agregado velho. As três ITZ estão apresentadas na Figura 2.4.

Figura 2.4: Diagrama esquemático da microestrutura do agregado reciclado de concreto (ZHANG et al. 2019)

A zona de transição interfacial entre a argamassa e o agregado é a região mais frágil e influencia negativamente nas propriedades mecânicas e de durabilidade dos concretos (ZHAO; ZENG; ZHANG, 2017;BRAVO et al., 2015a). As características

físicas do agregado reciclado, como a presença de fissuras e maior porosidade, também influenciam negativamente nas propriedades mecânicas e durabilidade dos concretos (KOU; POON, 2012). De acordo com Kong et al. (2010), um dos métodos utilizado para melhorar a microestrutura do RCD é a adição de materiais pozolânicos na mistura do concreto. A seguir será apresentada uma análise comparativa entre o ARM e ARC e a existência de correlação entre propriedades mecânicas (resistência à compressão axial e módulo de elasticidade) e de durabilidade (absorção d'água e carbonatação).

2.2 ANÁLISE COMPARATIVA ENTRE CONCRETOS COM AGREGADO RECICLADO MISTO (ARM) E CONCRETO (ARC)

Martínez-Lage et al. (2020) realizaram uma análise comparativa de concretos produzidos com agregado reciclado misto (ARM) e agregado reciclado de concreto (ARC) em laboratório. Os autores realizaram ensaios de resistência à compressão, módulo de elasticidade, teste de penetração de água sob pressão. O cimento utilizado foi CEM II 42,5 (similar ao CP II-Z). A absorção de água do ARC variou entre 5,03 e 5,98%, enquanto que a absorção da água do ARM variou entre 7,59 e 8,79%. A massa específica do ARC variou entre 2290 e 2340 kg/m³, e do ARM variou entre 2120 e 2340 kg/m³. A relação a/c foi de 0,50 e os teores de substituição foram de 20 e 100% (C-20-C e C-100-C) para concretos com ARC e 20, 50 e 100% (C-20-M, C-50-M e C-100-M) para concretos com ARM. A água de amassamento foi ajustada para compensar o excesso ou a necessidade dos agregados reciclados. Os resultados estão representados nas Figuras 2.5 e 2.6.

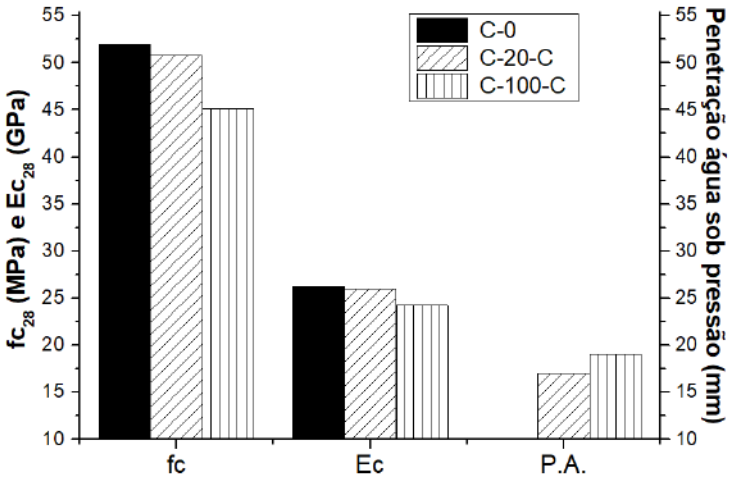

Figura 2.5: Resistência à compressão (28 dias), módulo de elasticidade (28 dias) e penetração de água sob pressão (p.A.) dos concretos com ARC – (MARTÍNEZ-LAGE et al., 2020)

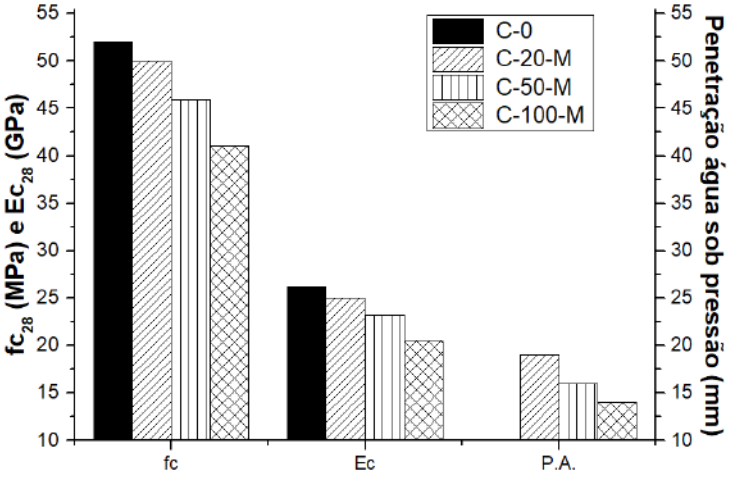

Figura 2.6: Resistência à compressão (28 dias), módulo de elasticidade (28 dias) e penetração de água sob pressão (P.A.) dos concretos com ARM - (MARTÍNEZ-LAGE et al., 2020)

Martínez-Lage et al. (2020) observou uma linearidade entre o teor de substituição de agregado natural por ARC na resistência à compressão bem como no módulo de elasticidade. Houve uma queda na resistência à compressão de 15 e 25% no concreto C-100-C e C-100-M, respectivamente, quando comparado ao concreto C-0. No módulo de elasticidade, o concreto C-100-C e C-100-M apresentaram queda de 7 e 22%, respectivamente, quando comparado ao concreto C-0. Segundo os autores, resultados similares foram encontrado por Bravo et al. (2015b) e Martínez-Lage et al.

(2012). Quanto à penetração de água sob pressão, na visão dos autores, todos os concretos atendem à norma EHE-08, que corresponde ao baixo nível de ataque químico para elementos de concreto submetido à água com pH entre 6,5 e 5,5. Para minimizar os efeitos negativos no que tange à grande variabilidade do RCD, muitos estudos vêm adicionando cinza volante em substituição parcial ao cimento Portland e serão apresentadas na subseção a seguir.

2.3 ADIÇÃO DE CINZA VOLANTE EM SUBSTITUIÇÃO PARCIAL AO CIMENTO PORTLAND EM CONCRETOS COM RCD

As cinzas volantes são materiais silicoaluminosos ou silicosos que, de acordo com a ABNT NBR 12653 (1992) possuem pouca propriedade cimentícia, porém na presença de umidade, a reação pozzolânica ocorre pela interação da fase vítrea da cinza volante com o $Ca(OH)_2$ formando assim os compostos com propriedades cimentantes (HOPPE FILHO, 2008a). A cinza volante é um pó heterogêneo que normalmente apresenta forma esférica, cujo diâmetro é menor que 45 μm e que pode ser altamente reativo (ABOUSTAIT et al., 2016; DAL MOLIN, 2011). A superfície específica das cinzas volantes varia entre 300 a 700 m^2/kg e sua massa específica variam entre 1900 e 2400 kg/m^3, enquanto que a massa específica do cimento Portland é de aproximadamente 3150 kg/m^3 (DAL MOLIN, 2011). Vários estudos mostram que o emprego de cinza volante como ligante em substituição parcial ao cimento Portland na produção de concretos com RCD melhora as propriedades mecânicas e de durabilidade, conforme apresentado na Quadro 2.1.

Quadro 2.1: Estudos sobre as propriedades mecânicas e de durabilidade de concretos produzidos com cinza volante e RCD

Propriedades	Tipo	Teores de substituição	Resultados	Autor
Resistência à compressão Axial	ARC	(AR 0% 50% 100%) (CV 0% 30% 60%)	Melhorou em maiores idades	Kurad et al. (2017)
	ARM	(AR 0% 25% 50% 75% 100%) (CV 0% 15% 20% 25% 30%)	Melhorou em maiores idades	da Silva e Andrade (2017)
	ARC	(AR 0% 25% 50%) (CV 0% 10%)	Melhorou aos 56 dias de cura.	Shaikh (2016)
Módulo de elasticidade	ARC	(AR 0% 100%) (CV 0% 20% 30%)	Redução não significativa	Sunayana e Barai (2017)
Coeficiente de carbonatação	ARC	(AR 0% 50% 100%) (CV 0% 25% 35% 55%)	Aumentou	Kou e Poon (2013)
	ARM	(AR 0% 25% 50% 75% 100%) (CV 0% 15% 20% 25% 30%)	Aumentou	da Silva e Andrade (2017)
Absorção d'água	ARM	(AR 0% 25% 50% 75% 100%) (CV 0% 15% 20% 25% 30%)	Melhorou	da Silva e Andrade (2017)
	ARC	(AR 0% 25% 50%) (CV 0% 10%)	Melhorou	Shaikh (2016)

ARC = Agregado Reciclado de Concreto; ARM = Agregado Reciclado Misto; AR = Agregado Reciclado; CV = Cinza Volante

A adição de cinza volante (CV) em substituição parcial ao cimento Portland tem relevância no desenvolvimento sustentável, pois contribui na redução das emissões de CO_2 e no consumo de energia (LIU; ZHANG, 2021). Segundo Gettu et al. (2019), a adição de 30% de CV em substituição parcial ao cimento Portland pode reduzir em aproximadamente 23% das emissões de CO_2 e a demanda de energia em torno de 21%. A melhora nas propriedades mecânica e de durabilidade dos concretos com a adição de CV pode estar atribuída à reação da cinza volante com o hidróxido de cálcio, que é um dos produtos da reação do cimento Portland, produzindo assim o silicato de cálcio hidratado (C-S-H secundário) que, por sua vez, preenche ainda mais os poros capilares e torna a microestrutura mais densa (GONZALEZ-COROMINAS; ETXEBERRIA; POON, 2016;GETTU et al., 2019).

A reação pozolânica da CV em comparação ao CP é mais lenta, e esta reação pozolânica ocorre através da interação da fase vítrea da pozolana com o $Ca(OH)_2$ que, em contato com a água, formam compostos com propriedades cimentantes

(MASSAZZA, 2003). Esta mistura resulta em rápida dissolução do $Ca(OH)_2$ provendo íons cálcio e hidroxila para a solução, conforme apresentado na Equação 1 e 2.

$$Ca(OH)_2 \longrightarrow Ca^{++} + 2(OH)^- \quad \text{Eq(1)}$$

$$Ca(OH)_2 \longrightarrow Ca(OH)^+ + (OH) \quad \text{Eq(2)}$$

Os Ca^{++} são absorvidos rapidamente pela superfície das partículas da cinzas volantes acarretando no processo de floculação destas partículas (MASSAZZA, 2003). Em seguida ocorre a dissolução destas partículas de cinza volante da seguinte forma (BROUWERS; EIJK, 2003) (Equação 3-6):

$$SiO_2 + 2OH^- \longrightarrow SiO_3^{2-} + H_2O \quad \text{Eq(3)}$$

$$Al_2O_3 + 1OH^- \longrightarrow 2AlO_2^- + H_2O \quad \text{Eq(4)}$$

$$CaO + H_2O \longrightarrow Ca^{2+} + 2OH^- \quad \text{Eq(5)}$$

$$Fe_2O_3 + 3H_2O \longrightarrow 2Fe^{3+} + 6OH^- \quad \text{Eq(6)}$$

Com o consumo de cálcio e a redução da solubilidade da cal hidratada, passa a formar-se C-S-H. Segundo Mehta (1987), isso ocorre porque os óxidos da CV ao reagirem com água e $Ca(OH)_2$ formam uma camada de C-S-H ao redor da partícula dificultando o acesso aos óxidos da parte mais interna. Com isso, o calor de hidratação da reação pozolânica é liberado mais lentamente tornando mais lento o desenvolvimento da resistência. Sendo assim, concretos com adição de CV em substituição parcial ao cimento Portland podem apresentar resistência mecânica inferior em comparação aos convencionais nas menores idades.

Segundo Kurad et al. (2017), o decréscimo real do efeito combinado de CV e ARC na resistência à compressão é menor do que a soma do efeito individual de CV e ARC, especialmente após 28 dias de cura. De acordo com os autores, um dos fatores que levam a esse comportamento é a reação pozolânica entre o dióxido de silício (SiO_2) da CV e o hidróxido de cálcio ($Ca(OH)_2$) do ARC. Com o aumento de $Ca(OH)_2$ em função da crescente razão de incorporação de agregado reciclado, o SiO_2 da CV terá mais Óxido de Cálcio (CaO) das partículas não hidratadas do cimento antigo para produzir mais C–S–H que é o principal contribuinte para o desenvolvimento da resistência do concreto.

Nesse contexto, segundo Filho (2008b), a adição de cinza volante em substituição parcial ao cimento Portland resulta em um concreto com menor teor de cimento. Logo, a disponibilidade de hidróxido de cálcio na matriz do concreto é diminuída e, consequentemente as propriedades mecânicas e de durabilidades tendem a ser menores nas idades iniciais (até 28 dias). A adição da cal hidratada em concretos com cinza volante visa estabelecer um aumento de $Ca(OH)_2$ na solução, por sua vez, a reação pozolânica é antecipada melhorando as propriedades nas menores idades. A seguir será apresentada a influência da adição da cal em concretos com cinza volante.

2.4 INFLUÊNCIA DA ADIÇÃO DE CAL HIDRATADA EM CONCRETOS COM CINZA VOLANTE

A influência da cal hidratada na reação da cinza volante está intimamente ligada à disponibilização imediata de hidróxido de cálcio que, junto com o $Ca(OH)_2$ proveniente da hidratação do cimento, permite maior grau de reação pozolânica. A soma do hidróxido de cálcio oriundo da cal hidratada e da reação do processo de hidratação do cimento resulta em maior concentração de $Ca(OH)_2$ (LORCA et al., 2014; BARBHUIYA et al., 2009) e, consequentemente antecipa o início da atividade pozolânica (KUMAR; SINGH; SINGH, 2012) .

Além da cal hidratada contribuir para o início da reação da cinza volante, a cal é um acelerador da cinética de hidratação do cimento Portland devido a supersaturação de íons cálcio em solução que ocorre em menos tempo e faz com que a aceleração das reações seja antecipada. (HOPPE FILHO, 2008a). A seguir serão apresentados alguns estudos do efeito da cal hidratada nas propriedades mecânicas e de durabilidade em concretos com adição de cinza volante com diferentes características físicas conforme apresentado no Quadro 2.2.

Quadro 2.2: Propriedades físicas da cinza volante, cal hidratada e o cimento Portland utilizado em cada estudo

Autores	Cimento Portland	Cinva Volante			Cal hidratada		
		Classe	Tamanho partículas (µm)	Massa Específica (g/dm³)	Tamanho partículas (µm)	Massa Específica (g/dm³)	Pureza (%)

Valcuende et al. (2020)	CEM I 52,5 R (CP I)	F	22,8	-	-	2,30	92
Gunasekara et al. (2020)	ASTM III (CP III)	F	45	-	-	-	91
Barbhuiya et al. (2009)	CEM 42,5N (CP II-Z)	F	-	2,30	-	1,90	-
Filho (2008)	CP V ARI	F	<75	2,48	58	2,26	-
Lorca et al. (2014)	CEM I 52,5 R (CP I)	F	23,7	2,50	48	2,30	87
Filho (2008b)	CP V – ARI	F	<75	2,38	47,27	2,26	91,3

O uso de cal hidratada nos concretos com cinza volante foram investigadas por Valcuende et al. (2020), Barbhuiva et al. (2009), Filho (2008) e Mira et al. (2002). A melhora nas propriedades mecânicas dos concretos variou de acordo com as propriedades químicas da cinza volante e o tipo de cimento empregado nos trabalhos.

2.4.1 RESISTÊNCIA À COMPRESSÃO AXIAL

Para analisar a influência da cal hidratada na resistência à compressão em concretos com 50% de adição de CV em substituição parcial ao cimento Portland, Valcuende et al. (2020) produziram o concreto de referência (C-0), concreto com 50% de CV em substituição ao cimento Portland (CFA-0L) e dois concretos com 50% de CV e diferentes teores de adição de cal hidratada (CFA-10L e CFA-20L) e relação a/agl. foi 0,50. Os ensaios foram realizados nas idades de 7, 28, 91 e 180 dias e duas amostras foram testadas em cada idade. Os corpos de prova foram curados em água (temperatura ambiente) até a data dos ensaios.

Com base nos resultados, Valcuende et al. (2020) observaram que, em idades maiores que 7 dias, a cal hidratada reage com a cinza volante dando origem a novos hidratos de silicato de cálcio (C-S-H), resultando em maiores resistências à compressão quando comparado aos concretos sem a adição da cal hidratada. A taxa da resistência à compressão é aumentada quando a cal é adicionada ao concreto em idades mais avançadas. Em um ano, segundo os autores, a resistência à compressão dos concretos C-FA10L e CFA-20L foi 11% e 18% maior do que o concreto CFA-0L, como mostra a Figura 2.7.

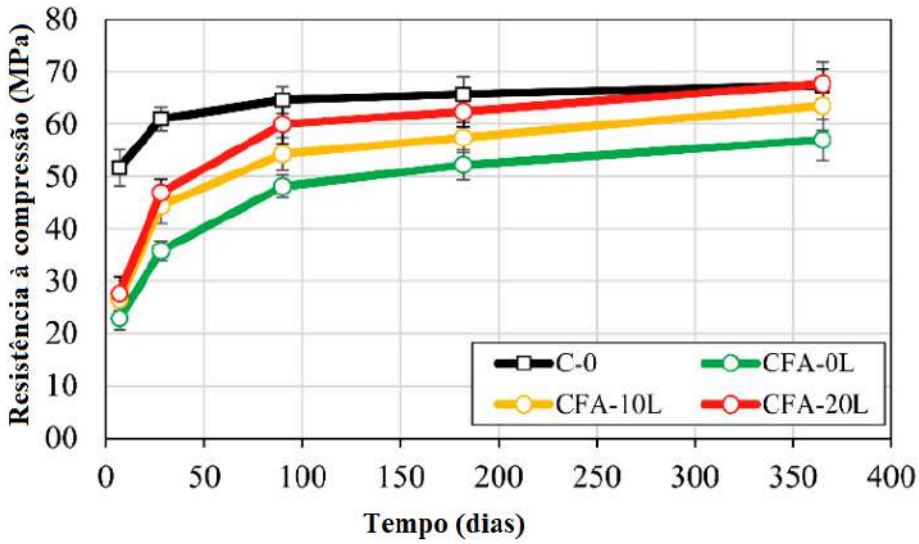

Figura 2.7: Evolução da resistência dos concretos (VALCUENDE et al., 2020).

A resistência à compressão do concreto CF-20L, CF-10L e CF-0L foi 5%, 14% e 26% menor quando comparado ao concreto CF-0 aos 180 dias. Resultados similares também foram observados por Lorca et al. (2014) e, conforme os autores, o ganho de resistência à compressão dos concretos com cinza volante e cal hidratada se deve a autoneutralização ácido-base da matriz por meio da reação pozolânica da cinza volante com o hidróxido de cálcio do cimento Portland e da cal hidratada.

Para avaliar o efeito da cal hidratada em concretos, Gunasekara et al. (2020), a relação água/aglomerante empregada foi igual a 0,3. As amostras de concretos foram curadas em tanques de água em temperatura ambiente até a data dos ensaios. Foram produzidos concretos de referência (100PC), concreto com 35% de cimento, 52% de CV e 13% de cal hidratada (HVFA-65) e concreto com 20% de cimento, 62% de CV e 18% de cal hidratada (HVFA-80), cujos resultados encontram-se apresentados na Figura 2.8.

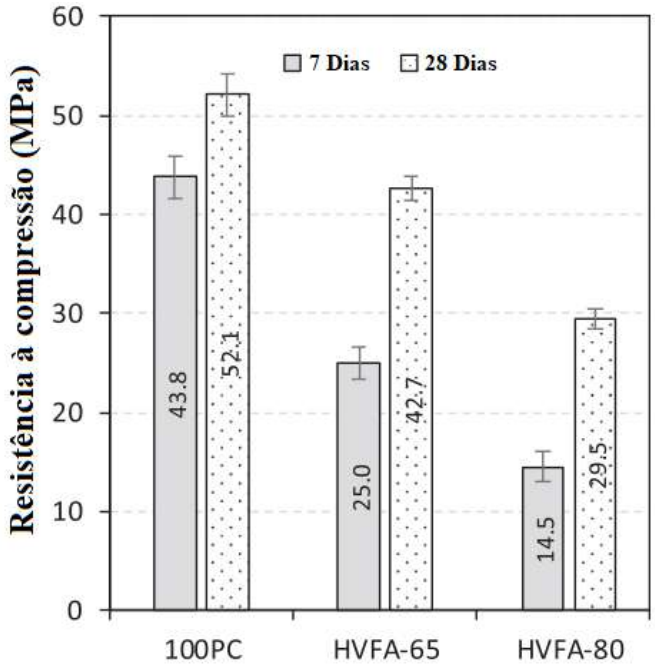

Figura 2.8: Desenvolvimento de resistência à compressão de diferentes concretos (GUNASEKARA et al., 2020) - Adaptado.

Os autores observaram que o ganho de resistência dos concretos entre as idades de 7 e 28 dias foi de 15,90% no concreto 100PC, 41,45% no concreto HVFA-65 e 50,85% no concreto HVFA-80. Segundo os autores, os concretos com cinza volante e cal hidratada apresentaram reação de hidratação contínua. A queda da resistência dos concretos HVFA-65 e HVFA-80 em comparação ao concreto 100PC aos 7 dias iniciais está relacionada a menor reação pozolânica devido à cinza volante adicionada, uma vez que a dissolução das camadas externas da cinza volante leva no mínimo 7 dias (GUNASEKARA et al., 2020).

O estudo realizado por Barbhuiya et al. (2009) mostrou que a adição de cal hidratada melhora a resistência à compressão axial dos concretos. Para a produção dos concretos dois teores de adição de cinza volante (30% e 50%) em substituição parcial ao cimento Portland foram usados neste estudo. A relação a/aglomerante para os concretos com 30% e 50% de cinza volante foi de 0,30 e 0,35, respectivamente. Foi adicionado 5% de cal hidratada em massa do conteúdo total de materiais cimentício em todos os concretos. Os concretos foram moldados em cubos de 150 mm e mantidos em ambiente interno (laboratório) à temperatura de 20ºC por 24 horas. Após a desmoldagem, as amostras foram curadas submersas em água até as idades

de ensaio de resistência à compressão (3, 7 e 28 dias). Os autores observaram melhoras na resistência à compressão em todos os concretos com cal hidratada, conforme apresentado nas Figuras 2.9 e 2.10.

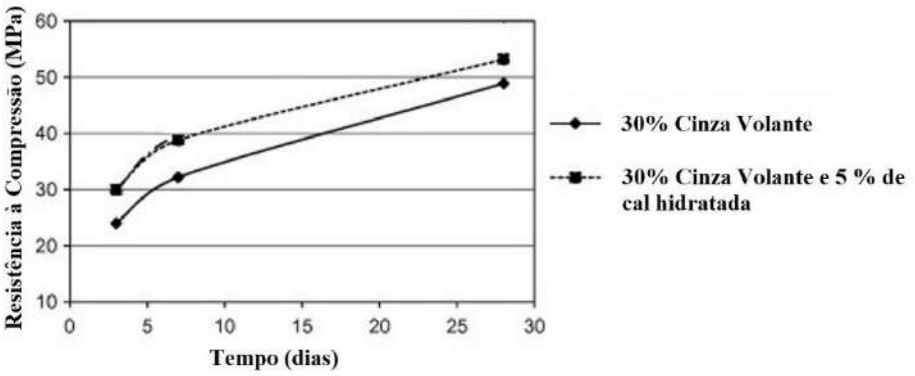

Figura 2.9: Resistência à compressão dos concretos com 30% de cinza volante e 5% de cal hidratada nas idades de 3, 7 e 28 dias (BARBHUIYA et al., 2009).

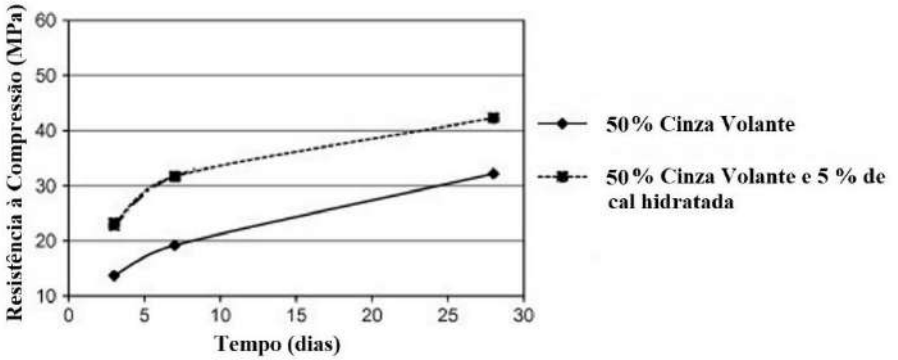

Figura 2.10: Resistência à compressão dos concretos com 50% de cinza volante e 5% de cal hidratada nas idades de 3, 7 e 28 dias (BARBHUIYA et al., 2009).

Segundo os autores, a melhora na resistência à compressão dos concretos com cinza volante e cal hidratada pode estar relacionada à quebra das partículas das cinzas volantes em função do alto teor de hidróxido de cálcio e a fase interna de silicato possibilitando mais produtos de hidratação (C-S-H adicional). Com base nos estudos realizados por Mira, Papadakis e Tsimas (2002) e Barbhuiva et al. (2009), é possível verificar que quanto menor for o teor de óxido de cálcio na cinza volante, maior será o efeito da cal hidratada nas propriedades mecânicas dos concretos com adição de cinzas volante.

Comportamento similar foi observado por Filho (2008) ao produzir concretos com 42% de cinza volante em substituição parcial ao cimento Portland e 16% de cal hidratada. Foram produzidos três diferentes tipos de concretos sendo: Concreto de

referência (100% cimento Portland), concreto com 50% de adição de cinza volante em substituição parcial ao cimento Portland em massa e concreto com 50% de cinza volante em substituição parcial ao cimento Portland em massa e adição de 20% de cal hidratada do total de aglomerante em massa. Foram empregados três teores de relação água/aglomerante (0,35, 0,50 e 0,65) e aditivo superplastificante de base éter carboxílico modificado (policarboxilato). O ensaio de resistência à compressão dos concretos foi realizado aos 28 e 91 dias de idade e os resultados estão apresentados no Figura 2.11.

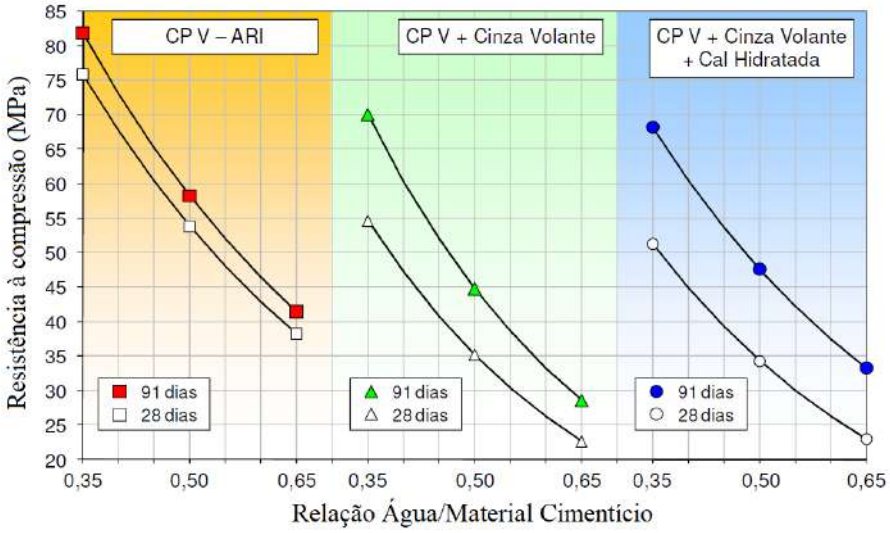

Figura 2.11: Resistência à compressão dos concretos aos 28 e 91 dias (FILHO, 2008)

Todos os concretos apresentaram resistências menores quando comparados ao concreto de referência. No entanto, o concreto com relação água/aglomerante 0,50, com 50% de cinza volante e adição de 5% de cal hidratada aos 91 dias de idade apresentou resistência à compressão axial 11,5% superior quando comparado ao concreto com 50% de cinza volante e sem cal hidratada. O autor observou que os concretos com cinza volante e cal hidratada aos 28 dias de cura apresentou um leve decréscimo na resistência quando comparado aos concretos com cinza volante e sem cal hidratada com a mesma idade de cura. Segundo o autor, ficou evidenciado que a contribuição da cal hidratada para a resistência à compressão axial requer maiores idades de hidratação.

2.4.2 Profundidade de carbonatação

Para analisar a profundidade de carbonatação em concretos com cinza volante e cal hidratada, Lorca et al. (2014) produziram corpos de prova com dimensões de 40 x 40 x 160 mm que foram expostos em ambiente de laboratório por um período de 360 dias a partir de 28 dias de cura. As amostras foram rompidas por flexão e uma solução de fenolftaleína a 1% foi aspergida na superfície fraturada. A profundidade de carbonatação foi testada no concreto de controle (C100), concreto com 50% de adição de cinza volante em substituição parcial ao cimento Portland (C50-1-0) e concreto com 50% de cinza volante e mais a adição de 20% de cal hidratada do total do aglomerante (C50-1-20), cujos resultados estão apresentados na Figura 2.12.

Figura 2.12: Aplicação da solução indicadora de fenolftaleína em uma superfície de fratura recente de concreto. Da esquerda para a direita C100, C50-1-0 E C50-1-20 (LORCA et al., 2014).

Segundo os autores, o concreto C100 não apresentou nenhuma frente de carbonatação e o concreto C50-1-20 apresentou uma pequena frente de carbonatação. O concreto C50-1-0 não apresentou frente de carbonatação. As manchas coloridas distribuídas aleatoriamente no concreto C50-1-0 são atribuídas à presença de algumas zonas da matriz em que a alcalinidade do C-S-H (hidratos de silicato de cálcio) era alta.

Para investigar a frente de carbonatação, Hoppe Filho (2008a) produziu concreto de referência, concreto com 50% de cinza volante em substituição parcial ao cimento Portland com e sem adição de 20% de cal hidratada do total de aglomerante em massa. As relações água/aglomerante foram 0,35, 0,50 e 0,65 e o tempo de cura

das amostras foi de 91 dias antes da exposição à carbonatação acelerada. A carbonatação foi realizada em câmara climatizada com controle de umidade relativa de 75 ± 2%, temperatura de 20°C e com 5% de anidrido carbônico (carbonatação acelerada) . Os resultados estão apresentados na Figura 2.13.

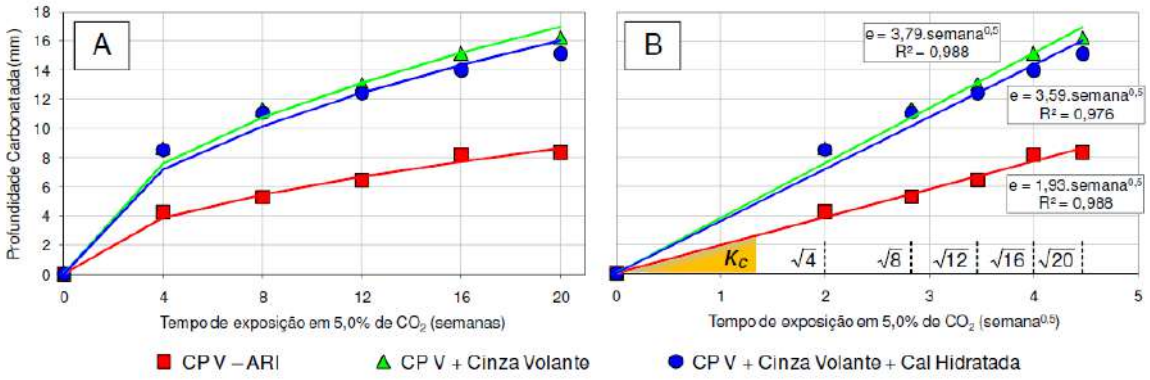

Figura 2.13: (A) Profundidade de carbonatação em função do tempo de exposição em ambiente com 5% de anidrido carbônico. (B) Coeficiente de carbonatação dos concretos ((HOPPE FILHO, 2008a)).

Segundo o autor, a profundidade de carbonatação do concreto com 50% de cinza volante foi o dobro quando comparado com o concreto de referência. A adição de 20% de cal hidratada em relação ao total de aglomerante em massa no concreto apresentou pouca eficiência na redução da espessura carbonatada em ensaio acelerado. O coeficiente de carbonatação do concreto de referência é 50% menor que o coeficiente de carbonatação do concreto com 50% de cinza volante. A adição de 20% de cinza volante apresentou uma pequena melhora no coeficiente de carbonatação de aproximadamente 5% em comparação ao concreto com apenas cinza volante. A evolução das reações de hidratação em ambiente natural é lenta e, com o passar dos anos, grande parte dos poros capilares são substituídos por mesoporos. Em maiores idades, o coeficiente de carbonatação pode diminuir a diferença em relação ao coeficiente de carbonatação do concreto de referência.

2.4.3 Análises microestruturais

A atividade pozolânica onde existe presença de cal hidratada e umidade é caracterizada pela alteração da microestrutura da pasta ao longo do tempo. Isto se deve ao refinamento do diâmetro dos poros que repercute diretamente sobre as

propriedades da pasta tais como permeabilidade, difusão, absorção capilar, entre outras (HOPPE FILHO, 2008b). Gunasekara et al. (2020) analisaram a microestrutura do concreto de referência (100PC), concreto com 35% de cimento, 52% de CV e 13% de cal hidratada (HVFA-65) e concreto com 20% de cimento, 62% de CV e 18% de cal hidratada (HVFA-80), cujos resultados estão apresentados na Figura 2.14.

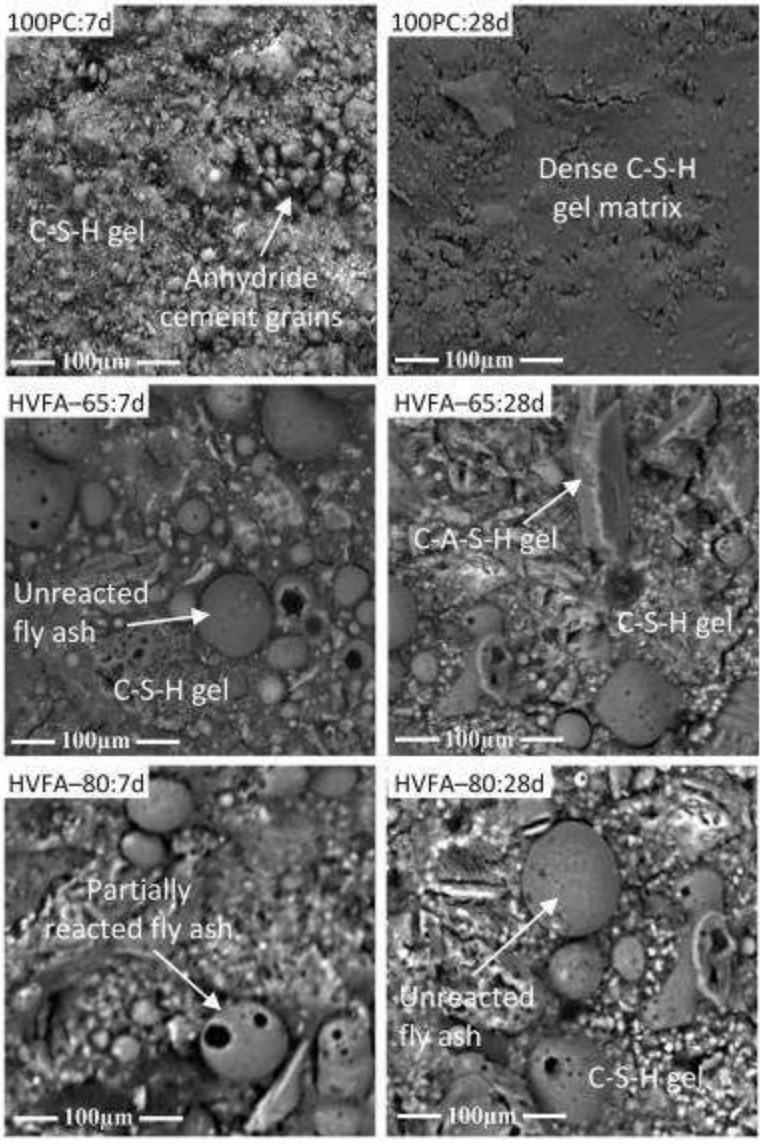

Figura 2.14: Desenvolvimento microestrutural do concreto HVFA-65 aos 7 e 28 dias e concreto HVFA-80 aos 7 e 28 dias (GUNASEKARA et al. 2020) - Adaptado.

O concreto 100PC, aos 7 dias, apresentou poucos grãos de cimento anidro na matriz, e aos 28 dias foi observada uma matriz de gel C-S-H mais densa e uniforme. Os concretos HVFA-65 e HVFA-80, aos 7 e 28 dias apresentaram uma microestrutura

mais heterogênea, com muitos grãos que não reagiram ou reagiram parcialmente. Segundo os autores, isso justifica a menor resistência à compressão em idades precoces. A adição da cal hidratada em concretos com cinza volante disponibiliza de forma imediata $Ca(OH)_2$ que permite a antecipação do início da reação pozolânica e aumenta o grau de reação da cinza volante nas idades inicias.

As análises microestruturais dos concretos analisados por Lorca et al. (2014) corroboram com o observado por Gunasekara et al. (2020). Os autores realizaram a análise microestrutural do concreto de referência (C100), concreto com 50% de cinza volante em substituição parcial ao cimento Portland (C50-1-0) e concreto com 50% de cinza volante e 20% de adição de cal hidratada no total de aglomerante em massa (C50-1-20). As imagens estão apresentadas nas Figuras 2.15, 2.16, 2.17.

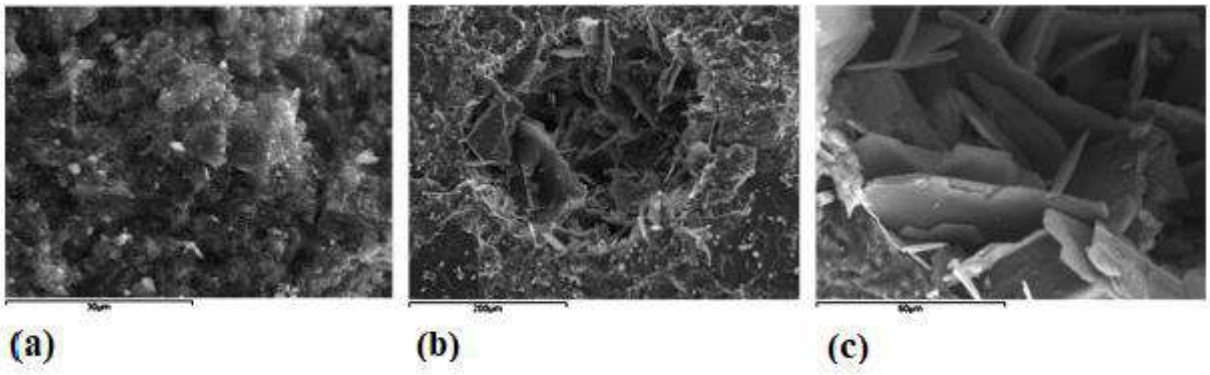

Figura 2.15 : Micrografias de microscopia eletrônica de varredura (MEV) DO concreto C100 (LORCA et al. 2014) - Adaptado.

De acordo com os autores, o concreto C100 (Figura 3.15-a) apresenta uma matriz densa e formação de produto de hidratação. Nas Figuras 3.15-b e 3.15-c são observadas presença de $Ca(OH)_2$. O concreto C50-1-0 apresenta partículas esféricas com superfícies lisas sem reagir (Figura 3.16-a).

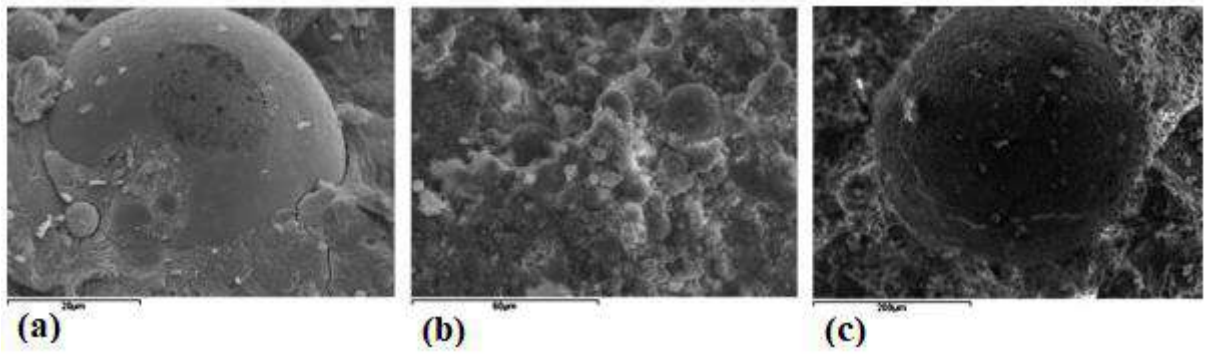

Figura 2.16: micrografias de microscopia eletrônica de varredura (MEV) DO concreto C50-1-0 (LORCA et al. 2014) - Adaptado.

Os autores sugerem que as cinzas volantes que ainda não reagiram, seja devido à insuficiência de produção de $Ca(OH)_2$ pelo cimento para uma reação completa (Figura 3.16-b). Os autores observaram macroporos que sugere a falta de formação de produtos de hidratação (Figura 3.16-c). Diferente do concreto C50-1-0, o concreto com cal hidratada (C50-1-20) apresentou uma estrutura densa conforme apresentado na Figura 2.17-a.

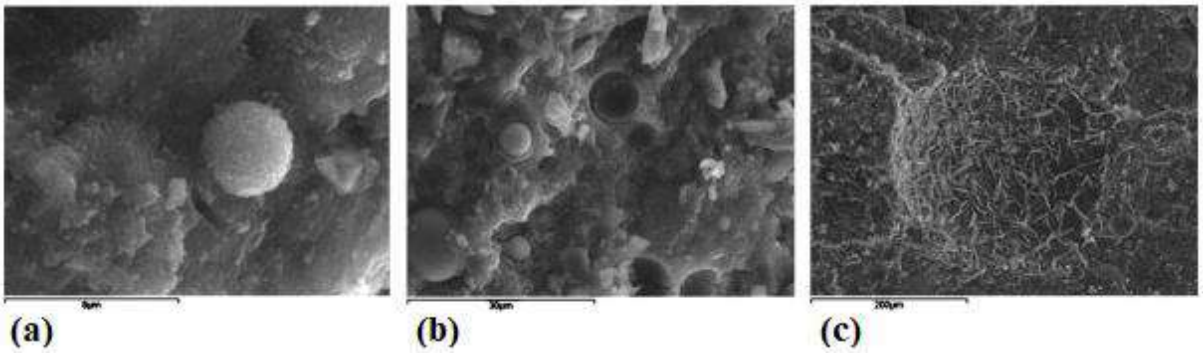

Figura 2.17 Micrografias de microscopia eletrônica de varredura (MEV) para argamassa C50-1-20.

As partículas de cinza volante do concreto C50-1-20 reagiram quase na sua totalidade (Figura 3.17-a). Existe maior presença inicial de $Ca(OH)_2$ (Figura 3.17-b) e formação de etringita que preenche o interior dos poros (Figura 3.17-c). Com base nas observações, os autores concluem que a natureza, a quantidade dos produtos de hidratação e a reação pozolânica são alteradas com a presença de cinza volante e cal hidratada.

2.5 CONSIDERAÇÕES FINAIS

A variabilidade da composição dos agregados reciclados proveniente de construção e demolição, bem como seus constituintes para produção de concretos estruturais preocupa autores como Leite e Monteiro (2016), Limbachiya, Meddah e Ouchagour (2012) e Silva, de Brito e Dhir (2014). Segundo os autores, a resistência à compressão, módulo de elasticidade, massa específica e profundidade de carbonatação desses concretos estão diretamente associadas à agregados reciclados. Como solução para esses problemas Silva, de Brito e Dhir (2014), sugerem uma classificação dos resíduos da construção por meio do processo demolição seletiva.

Estudos investigam a influência das cinzas volantes em concretos na hidratação no cimento bem como o processo de reação pozolânica. Segundo Mehta (1987), o calor de hidratação da reação pozolânica é liberado mais lentamente tornando mais lento o desenvolvimento da resistência. Assim, concretos com adição de cinzas volantes em substituição parcial ao cimento Portland podem apresentar resistência mecânica inferior em comparação aos convencionais nas menores idades. Com o objetivo de minimizar os efeitos negativos que os resíduos industriais causam em concretos como queda na resistência à compressão e módulo de elasticidade nas idades iniciais de cura, aumento na profundidade de carbonatação, entre outros (SUNAYANA; BARAI, 2017)(KURAD et al., 2017; DA SILVA; DE OLIVEIRA ANDRADE, 2017; SUPIT; SHAIKH; SARKER, 2014), muitos estudos buscam analisar efeitos combinados de outros produtos como a cal hidratada em concretos com cimento pozolânico. Segundo Filho (2008), o hidróxido de cálcio proveniente da cal hidratada e mais o hidróxido de cálcio oriundo do produto de hidratação do cimento resultam em maior concentração de $Ca(OH)_2$, que será consumida pela reação pozolânica em idade precoce. O efeito combinado de cinza volante e cal hidratada em sistemas cimentícios é bastante relevante e merece uma atenção especial para o desenvolvimento de mais pesquisas.

3. PLANEJAMENTO EXPERIMENTAL

3.1 INTRODUÇÃO

O planejamento experimental da pesquisa foi dividido em duas etapas, conforme observado na Figura 3.1. Na etapa 1 estudou-se as relações entre as propriedades mecânicas e carbonatação de concretos com agregado graúdo reciclado misto (ARM). Verificou-se a influência do ARM na resistência à compressão axial, módulo de elasticidade e profundidade de carbonatação do concreto estrutural, bem como suas correlações. Os teores de substituição de agregado graúdo natural por ARM foram de 0, 25, 50, 75 e 100% e relações a/c 0,40, 0,50 e 0,60. Foram realizadas análises das propriedades mecânicas (resistência à compressão, resistência à tração e módulo de elasticidade), físicas (porosidade e absorção d'água), análises microestruturais (microscopia eletrônica de varredura e microtomografia de raios-X) e de durabilidade (carbonatação acelerada nos concretos).

Como resultado foram observados decréscimos significativos nas propriedades mecânicas e de durabilidade dos concretos com ARM quando comparados com o concreto de referência. O ARM é composto por elevada proporção de materiais não estruturais que resulta em queda na resistência à compressão axial entre 20 e 50% quando utilizado taxa de substituição de 25 a 50% (ROBALO et al., 2021). Verificou-se na Etapa 1 que o módulo de elasticidade e a resistência à compressão axial diminui linearmente com o aumento do teor de substituição de agregado natural por ARM. A queda nas propriedades mecânicas e de durabilidade nos concretos com ARM quando comparado aos concretos de referência também foi observado por Juan-Valdés et al., (2018) e Martínez-Lage, Vásquez-Burgo e Velay-Lizancos, (2020). Para melhorar as propriedades dos concretos com ARM seria necessário o aumento no consumo do cimento para que a resistência à compressão axial se aproxime ao concreto de referência. Quanto maior o teor de ARM, maior será o consumo do cimento.

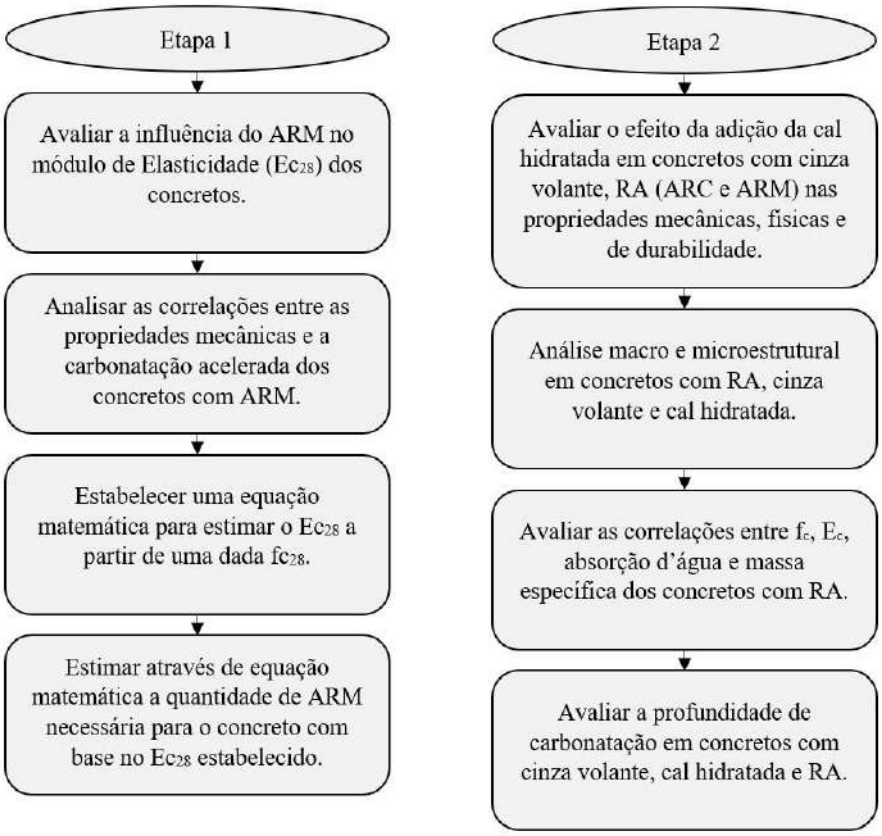

Figura 3.1: Diagrama-Resumo da Etapa 1 e Etapa 2 do programa experimental

Tendo em vista que as características físicas do agregado reciclado de concreto (ARC) são melhores quando comparados aos ARM (LOTFI et al., 2015), na Etapa 2 foi utilizado ARC, ARM, e cinza volante com cal hidratada foi utilizada com objetivo de reduzir os efeitos negativos que os agregados reciclados causam nas propriedades mecânicas, físicas e de durabilidade. Martínez-Lage et al. (2020) verificaram em seus estudos que o efeito negativo nas propriedades mecânicas dos concretos com ARM são maiores quando comparados aos concretos produzidos com ARC. Segundo Kou e Poon (2013), os melhores teores de substituição para um bom efeito combinado é entre 15 e 45% de cinza volante e 25 e 40% de agregado reciclado. De acordo com estudos realizados por Kurad et al. (2017), Shaikh (2016) e Kou e Poon (2013), a adição de cinza volante em substituição parcial ao cimento Portland tende a reduzir as propriedades mecânicas dos concretos nas primeiras idades. Esta redução se deve ao menor teor de cimento Portland, substituído pela cinza volante que diminui a quantidade de $Ca(OH)_2$ na matriz do concreto (HOPPE FILHO, 2008a).

A adição da cal hidratada tem como objetivo restabelecer o teor de $Ca(OH)_2$ na matriz do concreto (BARBHUIYA et al., 2009).

Na etapa 2 foram avaliadas as propriedades mecânicas (resistência à compressão axial e módulo de elasticidade), físicas (massa específica, porosidade e absorção d'agua) e de durabilidade (profundidade de carbonatação) em concretos com ARM, ARC, cinza volante e cal hidratada. No item a seguir será apresentado o planejamento do experimento da etapa 1.

3.2 ETAPA 1 – RELATIONSHIP BETWEEN THE MECHANICAL PROPERTIES AND CARBONATION OF CONCRETES WITH CONSTRUCTION AND DEMOLITION WASTE

A metodologia empregada visou avaliar as correlações entre as propriedades mecânicas (Resistência à Compressão, Módulo de Elasticidade) e profundidade de carbonatação. Procedimento experimental, métodos, resultados e discussão são apresentados neste capítulo em forma de artigo, o qual foi publicado na revista Qualis Eng. II A2: *Case Studies in Construction Materials*, v.16, (2022) e00860.

Link: https://www.sciencedirect.com/science/article/pii/S2214509521003752

Case Studies in Construction Materials 16 (2022) e00860

Contents lists available at ScienceDirect

Case Studies in Construction Materials

journal homepage: www.elsevier.com/locate/cscm

Case study

Relationship between the mechanical properties and carbonation of concretes with construction and demolition waste

Sérgio Roberto da Silva [a], Felipe Nunes Cimadon [b], Pietra Moraes Borges [a], Jessica Zamboni Schiavon [a], Edna Possan [c], Jairo José de Oliveira Andrade [d,*,1]

[a] Graduate Program of Materials Engineering and Technology, Pontifical Catholic University of Rio Grande do Sul (PGETEMA/PUCRS), Brazil
[b] Civil engineering, Pontifical Catholic University of Rio Grande do Sul (PUCRS), Brazil
[c] Engineering Department, Federal University of Latin American Integration (UNILA), Brazil
[d] Graduate Program of Materials Engineering and Technology, Pontifical Catholic University of Rio Grande do Sul (PGETEMA/PUCRS), Brazil

ARTICLE INFO

Keywords:
Construction and demolition waste
Coarse recycled aggregate
Physical-mechanical properties
Microstructural analysis

ABSTRACT

The use of construction and demolition waste in the construction industry has been a constant issue for several years due to the amount of waste generated as well as the need to reduce the consumption of natural aggregates. This study has the aim of optimizing recycled aggregate from construction and demolition to verify its influence on the elastic modulus in structural concrete. For this, the substitution of coarse natural aggregate by coarse recycled aggregate was evaluated at replacement percentages of 0%, 25%, 50%, 75%, and 100% for concrete with different water/cement ratios (0.40, 0.50, and 0.60). With these criteria, macrostructural tests (compressive strength, splitting strength, porosity and water absorption), microstructural tests (scanning electron microscopy and X-ray microtomography), and accelerated carbonation were employed. The results showed that the mechanical and durability properties in relation to CO_2 diffusion decreased as the substitution content of natural aggregate for recycled aggregate increased. The lower the a/c ratio, the denser the concrete and, consequently, the concrete properties are improved. Results showed that there are correlations between the mechanical properties and the carbonation of concrete with recycled aggregate. Through the proposed equations, it is possible to estimate elastic modulus from a given compressive strength at 28 days and with a w/c ratio ranging from 0.4 to 0.6. Based on the compressive strength and w/c ratio, it is possible to estimate the amount of substitution of natural aggregate needed in concretes for an expected elastic modulus.

1. Introduction

Construction and demolition waste (CDW) consists mainly of concrete blocks, mortar, bricks, plain and reinforced concrete, and asphalt, as well as ceramics, plaster, and wood [1]. The use of this recycled aggregate in the construction industry can generate financial and environmental benefits, reducing the amount of natural resources used and the amount of waste that would be deposited

* Correspondence to: PUCRS, Av. Ipiranga, 6681, Building 30/D Office 228., Porto Alegre, RS, Brazil.
E-mail addresses: sergio.roberto@acad.pucrs.br (S.R. da Silva), felipe.cimadon@acad.pucrs.br (F.N. Cimadon), pietra.borges@acad.pucrs.br (P.M. Borges), jessica.schiavon@acad.pucrs.br (J.Z. Schiavon), edna.possan@gmail.com (E. Possan), jairo.andrade@pucrs.br (J.J.O. Andrade).
[1] ORCID: 0000-0003-2073-6763.

https://doi.org/10.1016/j.cscm.2021.e00860
Received 6 September 2021; Received in revised form 21 December 2021; Accepted 23 December 2021
Available online 24 December 2021

in landfills [2]. Due to the current economic and environmental crisis, the demand for more sustainable development in the construction industry requires a different approach using concrete technology [3]. Replacing 100% natural coarse aggregate with recycled concrete aggregate can save more than 35% of waste generation and 50% of abiotic depletion [4]. There are two kinds of recycled aggregates (RA) that can be used in concrete after separation, crushing, and sieving: recycled concrete aggregate (RCA) and mixed recycled aggregate (MRA). The main difference between these materials is related to their origin: while RCA comes from the demolition of concrete, MRA is composed mainly of old concrete, bricks, and masonry, which leads to a higher variability. The determination of a mean value for the physical-mechanical and durability properties of concrete made with RA is therefore a challenge considering the possibility of application of this material on a large scale.

According to Lotfi et al. [5], the use of RA in concrete can result in better mechanical properties and durability, provided that a lower water/cement (w/c) ratio is adopted. In this way, the use of more than 50% of recycled aggregate can be achieved by limiting use of the concrete to applications with moderate exposure conditions. According to the author, recycled aggregate is more porous than natural aggregate, as the mortar adhered to recycled aggregate has a weak and porous structure. The greater the replacement content of natural aggregate by recycled aggregate in the production of concrete, the more significant will be the reduction in mechanical properties and durability of these concretes. According to Lotfi et al. [5], for the production of concrete with high levels of replacement of natural aggregate by recycled aggregate, a technology consisting of a combination of smart demolition, autogenous grinding and a new technology for dry separation of recycled aggregate is needed. However, according to the authors, the replacement of content above 50% should be done with more care, and its applications should be limited. According to Guo et al. [6], compared to concrete using NA, the durability of RCA is lower because of the old bonded mortar adhering to the RC particles [7]. The mixing procedure proposed by Fathifazl et al. [8], called the equivalent mortar volume (EMV) method, considers this residual hydration potential in the proportion of concrete to RCA, maintaining the same performance conditions as the mixture without recycled aggregate.

The use of 100% RA content may cause up to twice the carbonation depth of the corresponding reference mixtures [9]. Carbonation is related to concrete porosity, and the incorporation of recycled aggregate creates a more permeable concrete and therefore greater carbonation depth [9]. The sustainability evaluation of concrete with MRA is based on a holistic approach. Bravo et al. [10] evaluated the mechanical and durability properties of recycled aggregate concrete with and without superplasticizer, where carbonation was the property most affected by the porosity of these materials.

Andal et al. [11] verified that the use of RA and classified as of good quality, presented mechanical properties similar to those of the reference concrete for a partial replacement content of 30%. However, when all natural coarse aggregates are replaced by mixed recycled aggregates, the tendency is that the compressive strength (f_c) decreases by between 25% and 45%, while the elastic modulus (E_c) decreases by between 28% and 36% [4]. Kumar [12] evaluated the use of recycled concrete aggregates and the f_c and flexural strength of RCA were lower than those of natural aggregate concrete. Thus, as the amount of RA used as a partial replacement increases, the strength of the concrete mixture decreases [13]. According to Nepomuceno et al. [14], when using masonry aggregate, there is a 11.1% decrease in f_c for concrete with a replacement level of 75%, when compared to the reference concrete. The flexural strength shows a linear decrease as the replacement increases, with a reduction of approximately 6%. The research carried out by Duarte et al. [15] showed a drop in f_c values of up to 30% at 7, 28 and 56 days with 100% use of recycled aggregate.

The microstructure of concrete with recycled concrete aggregate is less dense than that of the reference concrete [16]. Under these conditions, concrete demonstrates greater porosity and weakening of the aggregate–paste interface [9]. The water excess generates porosity in the calcium silicate hydrate (C-S-H) gel formed by spaces between its layers. The presence of ettringite within the pores suggests that this porosity is due to pores of the paste being bound to the recycled aggregate [17]. Djerbi [18] suggested that RCA can be influenced by pre-saturating the RA with water, which can be released in the new paste, damaging the microstructure, forming a new interfacial transition zone (ITZ). Pradhan et al. [19] observed that the mortar adhering to the recycled aggregate and the presence of microcracks resulted in greater water absorption. The authors found that the thickness of the ITZ in natural aggregate concrete was 40–60 μm, while in recycled aggregate concrete it increased to approximately 60–80 μm.

Of the mechanical properties influenced by the use of RA, the elastic modulus (E_c) is the most significant, as this characteristic is fundamental to the design of reinforced concrete structures when considering the overall stability of the structure from the service limit state [20]. However, owing to the variation in mixtures, the existing formulae used to calculate E_c for natural aggregate concrete cannot be used for recycled aggregate concrete [21]. According to Silva et al. [22], the water compensation method during mixing provides recycled aggregate concrete with smaller decreases in E_c owing to the improved interfacial transition zone between the aggregate and the new cement paste. E_c showed a reduction of 30.83% compared to the reference concrete, which is associated with the higher deformability of the recycled aggregate. According to Wang et al. [23], the E_c of recycled aggregate concrete decreased by between 18.9% and 23.6% with 100% aggregate replacement. The E_c value of the concrete with 50% aggregate replacement decreased by between 6.8% and 16.0%. According to the author, these results indicate the possibility of applying recycled aggregate for structural use, if the replacement content of natural aggregate by recycled aggregate is less than 50%. Adessina et al. [24] obtained similar results when the total substitution of natural aggregate by recycled aggregate reduced the E_c of the concrete by up to 20%.

Some studies have examined the performance level of concrete containing recycled aggregate in terms of the use of the material for structural concrete. Brito et al. [20] concluded that studies should focus not only on the mechanical properties, but also on the durability and the verification of the structural performance of recycled aggregate concrete. The use of RA as a building material is still regarded with caution by builders because recycled aggregate is often considered to be a material with high variability in its properties and has unpredictable behavior.

There are many new studies on carbonation depth analysis in concrete with recycled aggregate. A study by Mi et al. [25] concluded that the greater the strength of recycled concrete, the lower the carbonation depth. Another study carried out by the same authors was an analysis of the inhomogeneity of concrete with recycled aggregate under the effect of loading [26]. Another developmental study by

Mi et al. [27] was an evaluation of the degree of carbonation of the recycled aggregate concrete based on the width of the carbonation zone. According to the authors, this method can help engineers to assess the service life of a structure with greater precision based on the width of the carbonation zone from the carbonation depth. Mi et al. [28] developed a carbonation model that, according to the authors, can provide very reasonable results. For the construction of the model, the authors used Fick's second law and the law of conservation of mass and also took into account the influence of the transition zone of the interfaces of the aggregates.

The carbonation process of concrete must be given special attention, as according to Shen et al. [29], structural concrete exposed in areas with a high concentration of CO_2, such as industrial areas, can cause the deterioration of the reinforcement. This is because the carbonation front, upon reaching the armature, will be placed in an environment of low alkalinity. According to Mi et al. [26] concretes with recycled aggregate after the load effect are more heterogeneous than control concretes regarding carbonation depth distributions, and this can be attributed to the fact that concrete with recycled aggregate presents old mortar and new mortar. Furthermore, according to the authors, the microstructure of the mortar and the width of the corrosion zone have a very significant impact when submitted to loading. The diffusion capacity of CO_2 in these two mortars are different. To differentiate the old mortar from the new mortar, the authors Mi et al. [27] used red iron oxide to color the old mortar during the preparation of the concrete. In this way it was possible to identify the different mortars (old and new) at all depths. This technique allowed to invest the carbonation depth of concretes with greater precision in the zones of traction, compression and in the load-free zones.

In this way, the present investigation has a main goal investigate the synergic effect of important aspects such as durability, microstructure and mechanical properties. An important comparison of values obtained from E_c based on the FIB model code, Eurocode and Brazilian standards was performed. In addition, the influence of the parameters of the increase in recycled aggregate content in the variation of the water/cement ratio of the concrete in this property was investigated. Through analysis of the results obtained in this study, it is possible to verify the relationship between the mechanical properties (f_c and E_c) and durability (void volume and depth of carbonation) in concretes with RA with substitution levels varying between 0% and 100%. In this way, it is possible to establish equations that allow the estimation the E_c of concretes with RA at 28 days from the characteristic strength of the concrete at 28 days (f_{ck}) and the w/c ratio. The novelty of this work is a general proposal that allows the estimation of the elastic modulus of a given compressive strength, having as dependent variable the ratio w/c (between 0.4 and 0.6) and f_{c28} (MPa). Based on the analysis of the results, the equation can be used in a situation where the engineer has the f_{c28} parameters and the concrete w/c ratio that would be used in a real case.

2. Experimental procedure

2.1. Materials

Concrete samples were prepared using Brazilian early age Portland cement, similar to ASTM C 150 III, with a specific surface of 3.05 g/cm^3, bulk density of 0.98 g/cm^3, particle mean diameter of 14.16 μm, and mean compressive strength at 28 days of 54.1 MPa. The natural aggregate (NA) used has basaltic origin, and the coarse recycled aggregate (RA) was prepared from CDW, which was collected from a building site located in the city of Porto Alegre, Brazil, and classified using a mechanical crusher. The gravimetric composition of the CDW consisted of 43% concrete, 26% ceramics, 9% natural aggregate, and 22% of different materials such as paper, wood, plastic, metal. The semi-quantitative chemical analysis of the X-ray fluorescence of cement and RA is presented in Table 1.

The coarse and fine aggregates, natural and recycled, were evaluated according to the bulk density [30], fineness modulus and maximum size [31], apparent specific gravity and water absorption for fine aggregate [32] and coarse aggregate [33]. The physical properties of the natural and recycled aggregates are presented in Table 2.

The variation in the physical properties of RA can be explained primarily due to its origin and the availability of materials in different regions. Can be observed that values of specific gravity varying between 2.54 and 2.67 kg/dm^3 and the water absorption between 3.1% and 8.6% according to similar research [10,32–34], mainly due to the differences observed in RA composition. The particle size distribution of the sand, NA and RA are presented in Fig. 1, measured according to NBR NM 248 [31].

X-ray diffraction (XRD) was performed using a Shimadzu model XRD 7000. The results showed the presence of quartz, calcite, albite, and magnetite as crystalline phases in the entire RA sample (Fig. 2).

2.2. Mix proportioning

The concrete mixtures were proportioned for a workability equal to 90 ± 10 mm with a mortar content of 53%, with w/c ratios of 0.40, 0.50, and 0.60 (Table 4), without the use of superplasticizers. Four replacement levels of NA by RA (0, 25, 50 75% and 100%), in mass were used. Due to the difference in the specific mass between the NA and RA, the volume compensation method suggested by Lovato et al. [34] was used based on Eq. (1).

Table 1
X-Ray fluorescence for materials used.

Materials	SiO_2	Al_2O_3	CaO	MgO	K_2O	SO_3	Na_2O	LOI
Portland cement	16.9	3.5	64.4	2.7	1.2	4.2	0.1	3.89
RA	52.4	11.6	15.6	2.3	1.1	0.6	0.2	11.37

Table 2
Natural and recycled aggregates properties.

Properties	Fine natural aggregate	Coarse aggregate	
		NA	RA
Maximum size aggregate (mm)	4.75	19	19
Fineness modulus	2.57	7.1	6.98
Specific gravity (kg/dm^3)	2.61	2.92	2.23
Bulk density (kg/dm^3)	1.50	1.54	1.24
Water absorption rate (%)	0.8	0.4	5.8

Where: NA = natural aggregate; RA = recycled aggregate.

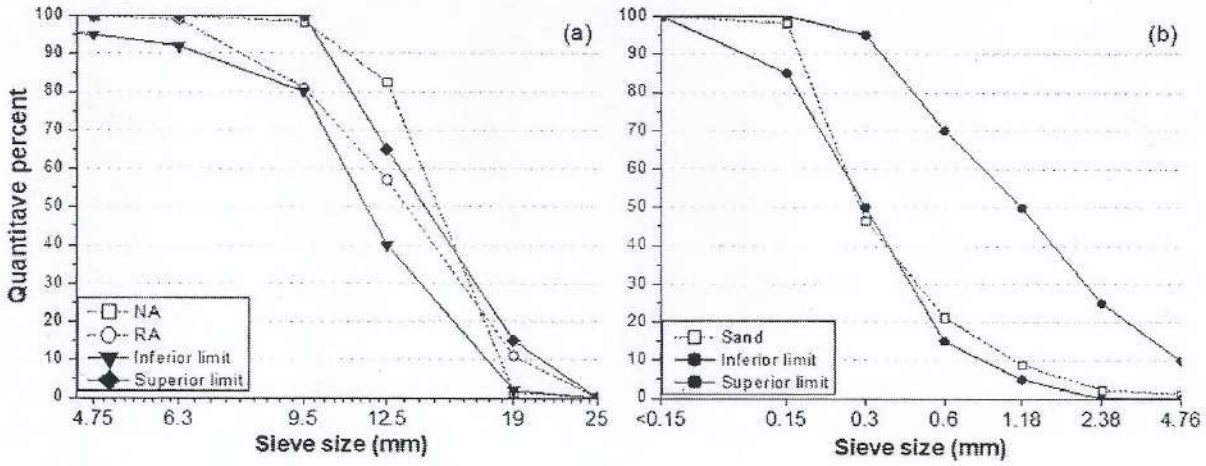

Fig. 1. Particle size distribution: (a) NA and RA; (b) Sand.

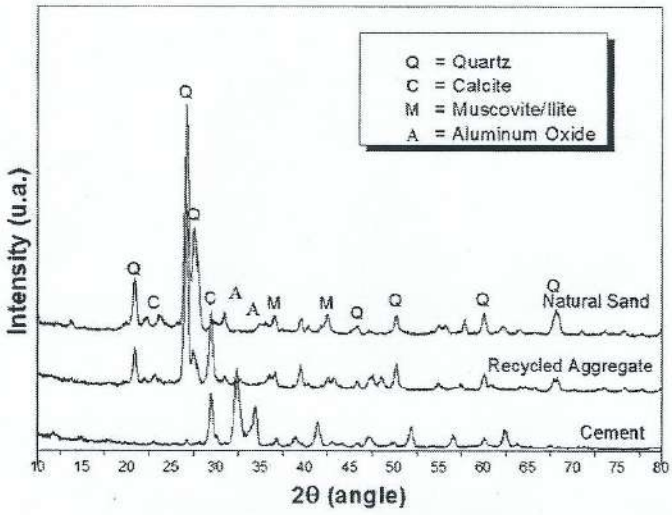

Fig. 2. XRD standard of materials used.

$$M_{RA} = M_{NA} \times \frac{\gamma_{RA}}{\gamma_{NA}} \quad (1)$$

where M_{RA} = recycled aggregate mass, in kg; M_{NA} = natural aggregate mass, in kg; γ_{RA} = recycled aggregate bulk density, in kg/dm^3; γ_{NA} = natural aggregate bulk density, in kg/dm^3.

Due to the porosity of the RA, it was pre-moistened for 24 h, as recommended by da Silva and Andrade [35]. The mixtures obtained are presented in Table 3.

Table 3
Mix proportioning of concretes.

Mix design	Proportioning[a]	Aggregates (kg/m³)			C (kg/m³)
		Fine	NA	RA	
0.40-R0	1:1.37:2.10:0	692.92	1062.31	0	505
0.40-R25	1:1.37:1.58:0.53	675.08	776.22	198.96	492
0.40-R50	1:1.37:1.05:1.05	657.25	503.81	387.41	479
0.40-R75	1:1.37:0.53:1.58	640.78	245.59	566.56	467
0.40-R100	1:1.37:0:2.10	624.32	0	736	455
0.50-R0	1:2.08:2.73:0	810.17	1063.41	0	389
0.50-R25	1:2.08:2.05:0.68	789.34	777.06	199.18	379
0.50-R50	1:2.8:1.37:1.37	768.51	504.37	387.84	369
0.50-R75	1:2.08:0.68:2.05	749.77	246.03	567.57	360
0.50-R100	1:2.08:0:2.73	731.02	0	737.85	351
0.60-R0	1:2.79:3.36:0	885.46	106.34	0	317
0.60-R25	1:2.79:2.52:0.84	860.33	77.05	199.17	308
0.60-R50	1:2.79:1.68:1.68	837.98	50.58	388	300
0.60-R75	1:2.79:0.84:2.52	815.63	24.56	566.48	292
0.60-R100	1:2.79:0:3.36	796.08	0	73.2	285

[a] Cement: sand: RA: NA.

2.3. Properties evaluated

The mechanical and physical tests were carried out in accordance with current Brazilian standards (Table 4), after curing in a humid chamber.

There are several equations that can be used to estimate the E_c of concrete from f_c. The Brazilian standard NBR 6118 [40] suggests the Eq. (2) to determine the E_{ci} at 28 curing days for an f_{ck} between 20 and 50 MPa.

$$E_{ci} = \alpha_E \times 5600\sqrt{f_{ck}} \tag{2}$$

where E_{ci} is the initial tangent concrete deformation module; α_E is a parameter that depends on the nature of the aggregate and influences the E_{ci}; f_{ck} is the characteristic strength at 28 days.

The Fédération Internationale du Béton [41] suggests that the concrete initial tangent E_{ci} (Eq. (3)) can be estimated by considering the concrete equivalent factor whose factor is equivalent to that presented in Table 2 for an f_{ck} between 12 and 80 MPa.

$$E_{ci} = 21.5 \times 10^3 \alpha_E \times \sqrt{\frac{(f_{ck}+8)^{\frac{1}{3}}}{10}} \tag{3}$$

The COMITE EURO-INTERNATIONAL DU BETON [42] also considers the aggregate nature. The secant E_c is calculated based on the formula represented by Eq. (4).

$$E_{ci} = 22 \times \alpha_E \times \left(\frac{fcm}{10}\right)^{0.3} \rightarrow f_{cm} \quad in \quad MPa \tag{4}$$

Where: f_{cm} is the average f_c of concrete at 28 days.

2.4. Accelerated carbonation

For accelerated carbonation testing, an open circuit chamber with 3% CO_2 concentration was used, with humidity between 65% and 75%. Before the test, the samples were submerged in water for 28 days followed by 24 h of exposure to air in a laboratory environment for drying. A phenolphthalein solution (1%) dissolved in a mixture of 70% ethyl alcohol and 30% distilled water was used

Table 4
Mechanical and physical test methods.

Properties	Brazilian Standard	Dimensions	Amount	Age (days)
Water absorption by immersion (A) Porosity (P) Bulk density (B)	NBR 9778 [36]	Cylinders (100 × 200 mm)	3	28
Compressive strength (f_c)	NBR 5739 [37]	Cylinders (100 × 200 mm)	6	7, 28 and 63
Splitting strength	NBR 7222 [38]	Cylinders(100 × 200 mm)	6	7, 28 and 63
Elastic modulus	NBR 8522 [39]	Cylinders (100 × 200 mm)	3	28
Accelerated carbonation	Procedure adopted by da Silva and de Andrade [35]	Prismatic (100 × 100 × 300 mm)	2	45–150 days
X-Ray microtomography	Specific procedure	Cubes (a–2.5 mm)	–	28
Scanning electron microscopy	Specific procedure	Pieces (2–5 mm)	–	28

to determine the carbonation depth with a caliper, according to RILEM [43] recommendation. Measurements were taken at 45, 60, 75, 90, 105, 120, 135, and 150 CO_2 exposure days in a four-point slice of a fractured sample (Fig. 3).

The concrete carbonation front when exposed to CO_2 tends to stabilize over time. To analyze this behavior, Fick's second law was used [44], being function of the square root of time (t). According to Khunthongkeaw et al. [45] the carbonation coefficient (K) is inversely proportional to the concrete carbonation resistance, as expressed in Eq. (5).

$$X_c = K\sqrt{t} \tag{5}$$

where X_c is the carbonation depth (mm), t is the exposure duration time (months), and K is the corresponding carbonation coefficient ($mm/month^{0.5}$).

2.5. Scanning Electron Microscopy (SEM)

In order to analyze the interface transition zone (ITZ) between aggregate and paste and perform the chemical characterization of concrete samples produced with RA, Scanning Electron Microscopy (SEM) was used. The equipment used energy levels of between 0.3 and 30 kV and a point resolution of 1.2 nm. The cracked sample test was coated with carbon, after wet curing for 28 days before the analysis.

2.6. X-ray microtomography

The X-ray microtomography test was performed using a Bruker SkyScan 1173 model, with an operating energy of 50 kV, electric current of 0.3 mA, and resolution of 10 μm. The test was conducted on cubic samples of size 1 cm, extracted from the specimens after 28 days of curing. The same technique was used by Lu et al. [46] to study the structure and connectivity of concrete pores. Gallucci et al. [47] used this technique to quantify the anhydrous cement content and the tortuosity of the pore network in cement paste. Saha et al. [48] carried out a study of X-ray microtomography images in concrete and concluded that it is an effective method to analyze the voids in a concrete sample.

2.7. Statistical modeling and analysis

Experimental planning was carried out using two-way analysis of variance (ANOVA) in order to observe the effect of different NA substitution contents for mixed RA. Subsequently, mathematical models were generated with the respective statistical significance analysis, with a confidence interval of 95%.

3. Results and discussion

With the results obtained in experimental program, mathematical models were developed for mechanical properties and durability parameters of concretes, being expressed by Eqs. (6)–(12).

$$f_c = 92.4032 - 34.3604 \times e^{\frac{w}{c}} - 0.1116 \times RA - 32.6673 \times \frac{1}{Age} \tag{6}$$

$$f_{ci,sp} = 1.84832 - 1.95644 \times log\left(\frac{w}{c}\right) - 0.00910 \times RA - 0.08315 \times Age^{0.5} \times log\left(\frac{w}{c}\right) \tag{7}$$

$$E_c = 35.42662 - 5.37947 \times log\left(\frac{w}{c}\right) - 0.30860 \times RA + 0.00129 \times RA^2 \tag{8}$$

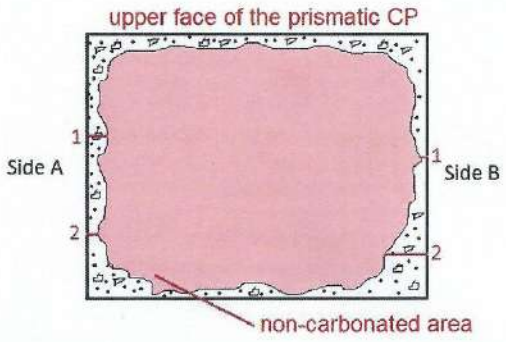

Fig. 3. Representation of carbonation depth measurements.

$$P = 2.299 + 3.307696 \times \frac{w}{c} + 0.102096 \times RA - 0.000431 \times RA^2 - 0.012198 \times \frac{w}{c} \times RA \quad (9)$$

$$A = 2.253095 + e^{(3.625328 \times \frac{w}{c})} + 0.100582 \times RA \quad (10)$$

$$D = 2.57 - 1.00 \times \frac{w}{c} - 1117.66 \times \frac{w}{c} \times RA - 1.28 \times \frac{w^2}{c} + 0.00003 \times RA^2 \quad (11)$$

$$e_{CO2} = -4.90395 + 2.74207 \times \frac{w}{c} + 0.00436 \times RA + 0.20438 \times Age^2 \quad (12)$$

where f_c = compressive strength (MPa); $f_{ct,sp}$ = splitting strength (MPa); E_c = elastic modulus (GPa); P = porosity (%); A = water absorption (%); D = bulk density (kg/dm^3); e_{CO2} = carbonation depth (mm); RA = recycled aggregate replacement (%); age = age of concretes (days); w/c = water/cement ratio.

The analysis of variance (ANOVA) for the response variables are presented in Table 5. All the effects of the isolated variables and their interactions were statistically significant.

3.1. Elastic modulus (E_c)

It was observed in this study that the E_c was reduced as the substitution content of RA increased (Fig. 4). It was also observed that the replacement of the natural aggregate by recycled aggregate had a greater influence on E_c than the increase in the w/c ratio.

The 0.40-R50 and 0.40-R100 concrete mixtures (Fig. 4-a) have E_c values that were 30.3% and 44.6% smaller than that of SI-R0 concrete, respectively. The decrease in the concrete E_c values for 0.60-R50 and 0.60-R100 (Fig. 4-c) are more significant, being 32% and 47.2% smaller, respectively, compared to R0. In addition to the w/c ratio and aggregate size, the E_c of the aggregate and the porosity are factors that influence E_c [49]. The porosity of the transition zone (ITZ) between the cement paste, aggregates, capillary voids, microcracks, and $Ca(OH)_2$, found in the ITZ, are also factors that influence E_c behavior [50]. It can be seen in Fig. 5 that there is a correlation between E_c and f_c in all concrete mixtures.

According to Barbudo et al. [51], the reason for the difference in correlation between the mixtures may be a function of the amount of mortar adhered to the particles, which is related to the amount of RA. Despite the good relationship between E_c and f_c, according to Wang et al. [23], the recycled aggregate influences f_c because of the increase in the ITZ between particles and paste and the w/c ratio, while E_c is influenced by the decrease in aggregate stiffness. The current Brazilian standard NBR 6118 [40] assigned a factor (α_E) for each type of natural aggregate in order to estimate E_c from the equations. For basalt and diabase, granite and gneiss, limestone, and

Table 5
ANOVA for developed models.

Response	Source	SS	DF	MS	F test	p-value
f_c	Model	49,408.28	4.00000	12,352.07	4509.169	0.000000
	Residual	161.62	59.00000	2.74		
	Total	49,569.90	63.00000			
	$R^2 = 0.939$					
$f_{ct,sp}$	Model	530.72	4.0	132.68	2136.99	0.000000
	Residual	3.35	54.0	0.0621		
	Total	534.069	58.0			
	$R^2 = 0.815$					
E_c	Model	38,795.36	4.00000	9698.840	7485.646	0.000000
	Residual	53.12	41.00000	1.296		
	Total	38,848.48	45.00000			
	$R^2 = 0.973$					
A	Model	1395.809	4.00000	348.9524	408.8680	0.000000
	Residual	24.750	29.00000	0.8535		
	Total	1420.560	33.00000			
	$R^2 = 0.828$					
P	Model	6914.300	3.00000	2304.767	716.6837	0.000000
	Residual	93.260	29.00000	3.216		
	Total	7007.560	32.00000			
	$R^2 = 0.849$					
D	Model	51.35376	6.0	8.558960	16,196.10	0.000000
	Residual	0.00264	5.0	0.000538		
	Total	51.35640	11.0			
	$R^2 = 0.987$					
e_{co2}	Model	120.1349	4.0000	30.03371	460.3145	0.000000
	Residual	9.2649	142.0000	0.06525		
	Total	129.3998	146.0000			
	$R^2 = 0.834$					

SS = Sum of squares, DF = degrees of freedom, MS = Mean square.

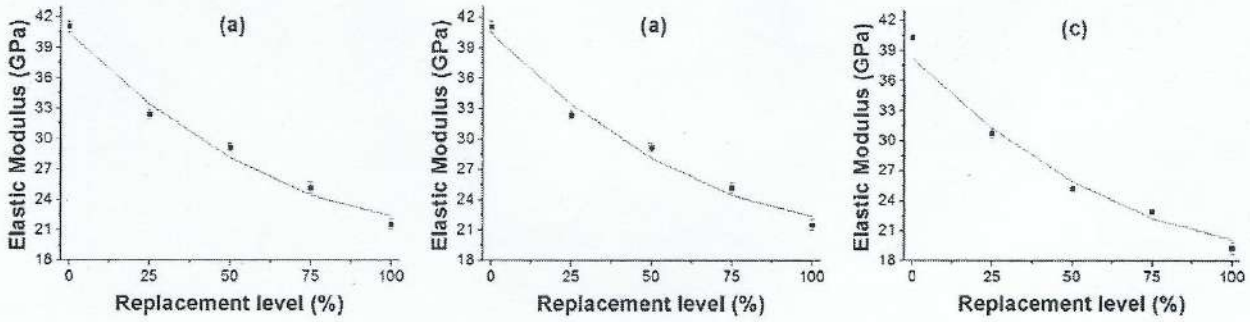

Fig. 4. Elastic modulus at 28 days: w/b ratio (a) 0.40, (b) 0.50 e (c) 0.60.

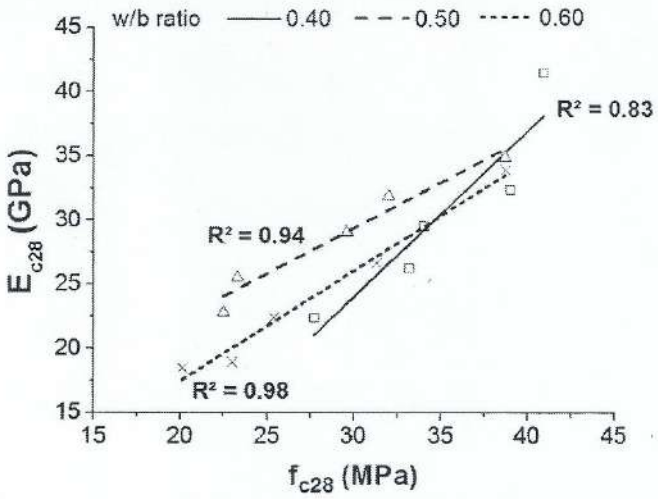

Fig. 5. Relationship between elastic modulus and f_c of concrete.

sandstone aggregates, α_E values of 1.2, 1.0, 0.9, and 0.7 are assigned, respectively. The elastic properties of constituent materials as well as the interface area between the aggregate and the paste has a strong influence on the concrete elastic properties [52]. Uysal [53] states that the effect of using coarse aggregate has a stronger influence on E_c than on f_c.

Based on the results obtained in the study of E_c of concrete using RA and adopting an f_{ck} of 50 MPa, a value of α_E was estimated for each mixture tested based on Brazilian and international standards. The results of α_E are presented in Table 6.

It was found that the normative values of α_E based on the COMITE EURO-INTERNATIONAL DU BETON [42] standard are very similar to those found in the Brazilian standard NBR 6118 [40]. Based on these results, it can be concluded that a concrete with up to

Table 6
Equivalent α_E factor for concretes evaluated.

Mixture	Elastic Modulus (GPa)	α_E estimated		
		NBR 6118 [40]	FIB Model [41]	EUROCODE 2 [42]
0.40-R0	41.05	0.86	0.77	0.96
0.40-R25	33.4	0.70	0.63	0.78
0.40-R50	28.43	0.60	0.54	0.66
0.40-R75	24.74	0.52	0.47	0.58
0.40-R100	22.48	0.47	0.42	0.53
0.50-R0	40.03	0.84	0.75	0.94
0.50-R25	32.14	0.68	0.61	0.75
0.50-R50	27.01	0.57	0.51	0.63
0.50-R75	23.32	0.49	0.44	0.55
0.50-R100	21.07	0.44	0.40	0.49
0.60-R0	39.60	0.83	0.75	0.93
0.60-R25	30.99	0.65	0.58	0.72
0.60-R50	25.86	0.54	0.49	0.6
0.60-R75	22.17	0.47	0.42	0.52
0.60-R100	19.91	0.42	0.38	0.47

50% of NA replacement by RA has an α_E of approximately 0.60, as in the case of 0.40-R50. Considering a replacement level equal to 25%, the values approximate the results for the limestone aggregate.

In addition to the correlation between E_c and f_c, the relationship between E_c and the bulk density (D) was also examined for all the concrete mixtures, as presented in Fig. 6.

The concrete bulk densities for 0.40-R25, 0.40-R50, 0.40-R75, and 0.40-R100 showed a decrease of 4.65%, 7.84%, 9.61%, and 9.91%, respectively, when compared to concrete 0.40-R0. Cantero et al. [54] observed that concrete (w/c = 0.45 and 28 days curing) with 20%, 25%, and 50% RA content presented a bulk density reduction of approximately 3.1%, while concrete with 75% and 100% RA content showed a reduction of 4.2% compared to the reference concrete.

3.2. Compressive strength (f_c)

To analyze the f_c (Fig. 7), the regression model (Eq. (6)) was used for all replacement content considering the w/c ratios investigated.

The concrete 0.50-R25, at 28 days curing, presented f_c values that was 8.7% lower than the reference. At 63 days curing the concrete 0.60-R100 had a 61.60% lower value of f_c compared to 0.60-R0. The concrete 0.60-R25 with 28 days curing had the closest value of f_c to 0.60-R0, at 7.37% lower. Cantero et al. [54] did not observe a decrease in f_c with up to 50% RA and observed a decrease of 7% in the concrete with 100% RA content when compared to the reference concrete. The RA used in that study presents approximately 87.82% of old concrete and stone products and 10.93% masonry materials in their composition, which explains the low reduction in f_{c28}.

The variability of RA has a direct influence on the mechanical and durability properties of RA concretes. The recycled aggregate used by Zieliński et al. [55] for the production of concretes consisted of 25% concrete, 25% mortar and 50% ceramic. The water absorption of recycled aggregate was 3.5 times higher compared to natural aggregate. The authors observed that the drop in compressive strength of concretes with recycled aggregate compared to control concretes, in general, is greater than 20%. Cantero et al. [54] used mixed recycled aggregate to produce concrete. The mixed recycled aggregate consisted of 43.98% concrete, a concrete and mortar product, 43.84 natural stone, 10.93% masonry, 0.02% floating particles and 0.02% other materials such as glass and plaster. The w/c ratio was constant in all mixtures (0.45). In this study, with recycled aggregate, the authors observed that concretes with 20%, 25% and 50% similar axial compressive strengths compared to control concrete. Concretes with 75% and 100% recycled aggregate drop by 3% and 7% respectively. According to Xiao et al. [56], the old mortar from the recycled aggregate have porosity and cracks that allow an increase in water consumption. In this way, the transition zone regions of the recycled aggregate take less water for hydration and consequently influence the concrete properties. According to the authors, in general, the increase in replacement level tends to decrease the compressive strength of concrete, however, if the content of recycled aggregate is lower than 30%, the decrease in compressive strength in comparison to control concrete will not be significant. Already Etxeberria et al. [57] observed in their studies that concretes with 25% recycled aggregate can present axial compressive strength very close to the reference concrete. However, concretes with more than 50% recycled aggregate need to have between 4% and 10% less w/c and 5–10% more cement than control concrete to achieve the same axial compressive strength at 28 days.

Seddik Meddah [58] reported that the negative effect of RA in f_c values depends not only on the concrete properties but also on the method used for the production of concretes with RA. According to Pedro et al. [59] the decrease in f_c with RA when compared to reference concrete is due to the presence of adhered old mortar, which results in a higher effective w/c ratio and a transition zone between the matrix and the weaker aggregate.

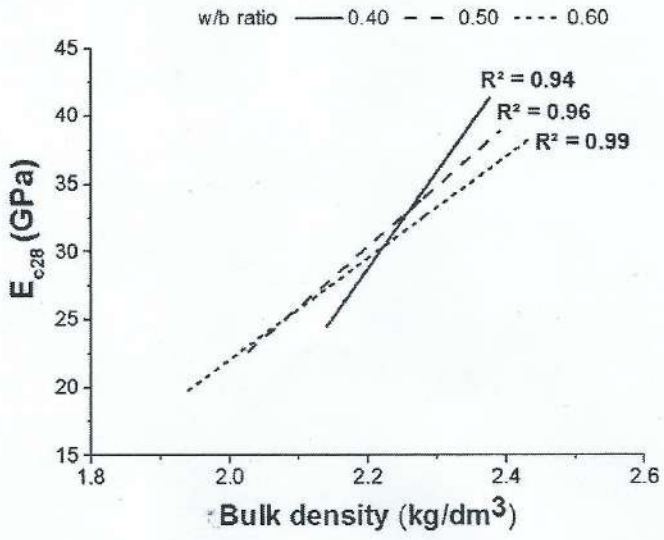

Fig. 6. Correlation between concrete elastic modulus and bulk density.

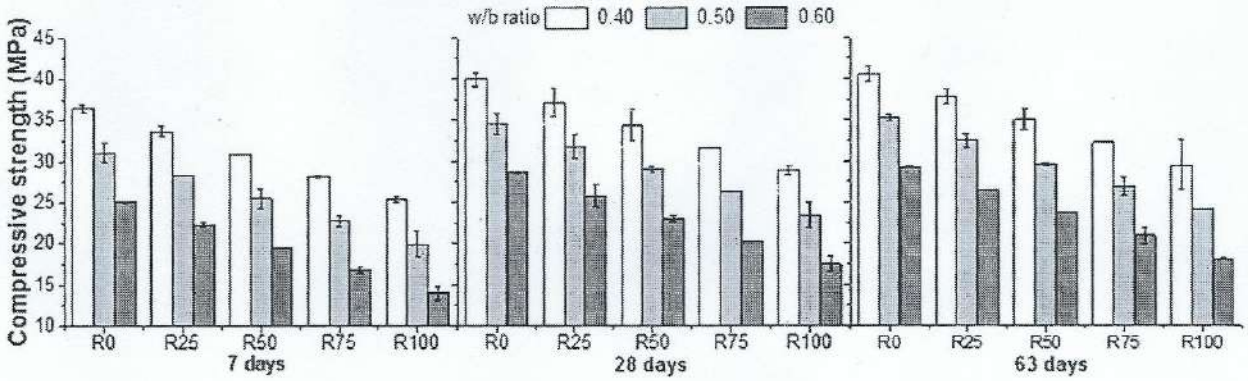

Fig. 7. RA influence on compressive strength of concretes.

Based on the results for f_c of concretes after 28 and 63 days of curing, it is possible to verify the growth rate as a function of the w/c ratio (Fig. 8). It was observed that the highest growth rate of f_c over time was for concrete 0.60-R100 for a w/c ratio of 0.6.

The higher the w/c ratio, the higher the f_c growth rate with age (Fig. 8). The concrete strength growth rates of 0.40-R25, 0.40-R75, and 0.40-R100 compared to 0.40-R0 are 0.12% 0.42% and 0.62%, respectively, while concrete with a w/c ratio of 0.6 showed a resistance increase of 0.23%, 0.91%, and 1.41%, respectively. According to Eckert and Oliveira [60], this behavior may be related to the lower stiffness of the RA, resulting in a lower degree of restriction between the particles as well as the internal curing of the RA that attenuates the shrinkage stress by reducing microcracks. Another possibility is that the greater the amount of RA in concrete, the greater the number of aggregates with water excess in the capillary pores [60], and this water is released according to Juan-Valdés et al. [61].

3.3. Splitting strength ($f_{ct,sp}$)

As observed in the f_c behavior, $f_{ct,sp}$ decreases with the substitution of natural aggregate by recycled ones (Fig. 9).

When analyzing the effect of the w/c ratio on concrete with RA, it can be seen that the mixtures 0.40-R50, 0.50-R50, and 0.60-R50 showed a decrease in $f_{ct,sp}$ at 28 days of 10%, 11.4%, and 16.1%, respectively, when compared to the reference concrete (0.40-R0, 0.50-R0, and 0.60-R0). The RA effect in the concrete was seen in the mixtures 0.50-R25, 0.50-R50, and a decrease in the $f_{ct,sp}$, at 28 days, is 5.7% and 11.4%, respectively, when compared to the reference concrete (0.50-R0). Other smaller values were found by Cantero et al. [54] in the concrete, with 3% for 75% RA and 4% for 100% RA at 28 days and a w/c ratio of 0.45. This may be related to the amount of fragile material in the RA, as according to Lovato et al. [34], cracks tend to propagate in the most fragile aggregates, thus reducing the $f_{ct,sp}$. Zieliński et al. [55] observed that concretes obtained with recycled aggregate do not present differences in tensile strength when compared to control concrete. On the other hand, Oner et al. [62] observed in their studies that the tensile strength tends to decrease between 25% and 30% when compared to control concrete.

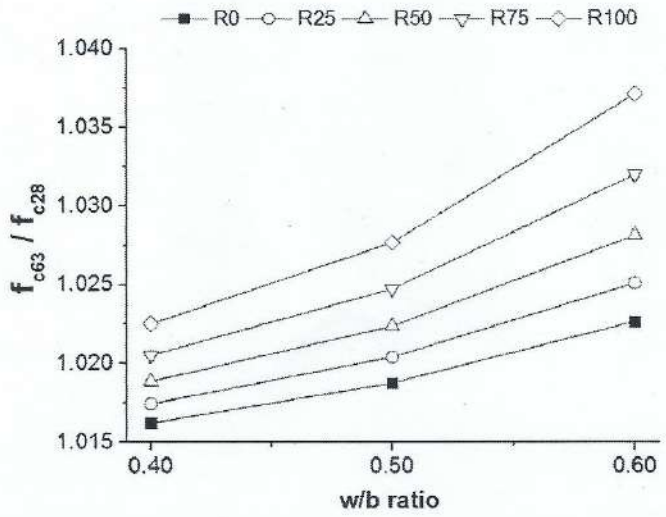

Fig. 8. Influence of w/b ratio in the compressive strength growth rate of concrete with RA and w/b 0.4, 0.5 and 0.6.

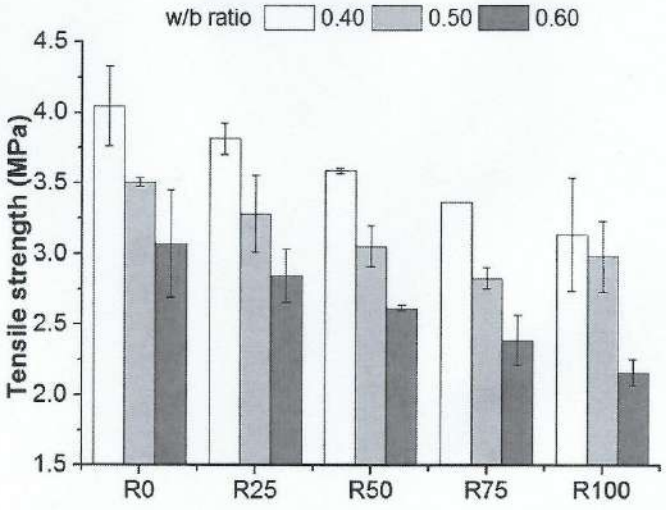

Fig. 9. RA influence on concrete in splitting strength at 28 days.

3.4. Carbonation depth

To measure the carbonation depth, the greatest and smallest depths measured from the sides of the prismatic specimen were considered and the average of each side represents the carbonation depth. The base and top were not considered and the average of the sides represented the carbonation depth of the sample. This method was suggested by Pauletti [63] and Kulakowski [64]. The use of accelerated carbonation techniques to evaluate the carbonation resistance of concrete with RA are shown in Figs. 10 and 11. The 0.60-R25 concrete had a greater carbonation depth (e_{co2}) when compared to the 0.60-R0 concrete.

Carbonation resistance is higher in concrete with lower w/c ratios and lower percentage of NA replacement by recycled aggregate (Fig. 12).

The concrete 0.60-R100 showed carbonation depths (e_{co2}) at 45 and 120 days that were greater by 29.80% and 18.70%, respectively, when compared to 0.60-R0. The concrete 0.40-R50 showed e_{co2} at 45 and 120 days that were greater by 14.90% and 9.35%, respectively, when compared to 0.40-R0. Similar behavior was observed by Debieb et al. [65], Zhao et al. [66], Kou and Poon [67] and Silva et al. [9] Studies have observed that natural aggregate replacement levels by recycled aggregate increases carbonation depth by up to 100%. According to Kisku et al. [68], the increase in carbonation depth is closely linked to factors such as water/binder ratio, natural aggregate replacement content by recycled aggregate, binder content, additives as well as curing conditions. Buyle-Bodin and Zaharieva [69] report in their studies that the carbonation depth almost doubles when the specimes are cured in water and, according to the authors, this behavior is related to high internal moisture of concrete with recycled aggregate.

The increase in e_{co2} is directly related to the increase in the w/c ratio rather than the increase in the RA content. According to Silva et al. [22], the carbonation depth is associated with the more porous structure of RA and the presence of old pre-carbonated mortar. It can be seen that the greater the age, the lower is the rate of increase of carbonation depth. This is because layers of insoluble salts such as $CaCO_3$ are formed in the capillary pores over time, reducing the penetration capacity of CO_2 in these pores [70].

Fig. 13 presents the correlation between K as a function of time for concrete mixtures 0.40-R0, 0.40-R25, and 0.40-R100. According to the results observed, the carbonation coefficient tends to decrease as the time of exposure to CO_2 increases.

In 2 months of exposure to CO_2 the concrete 0.40-R0 showed a carbonation coefficient of 4.13 mm/month$^{0.5}$ while the 0.40-R25

a) b) c) d)

Fig. 10. Carbonation of concrete R0 with w/c = 0.60: (a) 60 days; (b) 75 days; (c) 105 days; (d) 120 days.

Fig. 11. Carbonation of concrete R25 with w/c = 0.60: (a) 60 days; (b) 75 days; (c) 105 days; (d) 120 days.

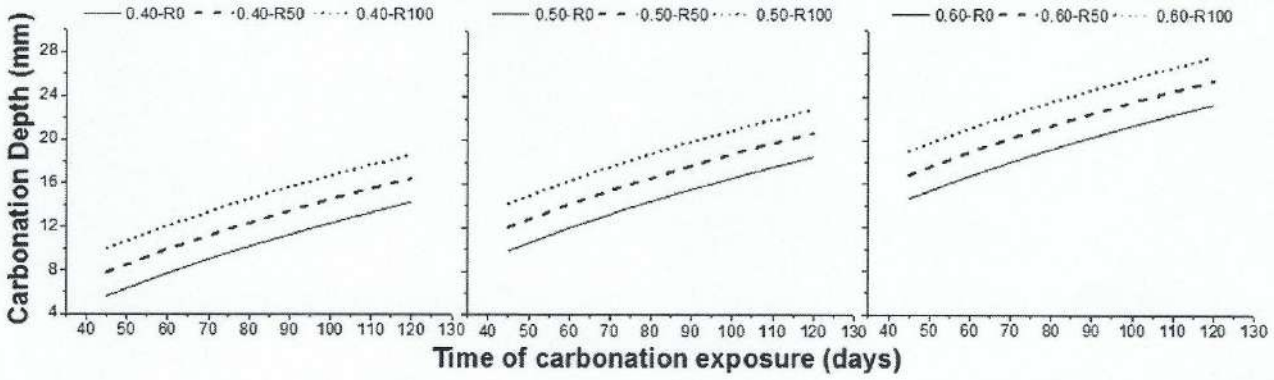

Fig. 12. Carbonation depth in concretes over time for w/c ratio 0.4, 0.5 and 0.6.

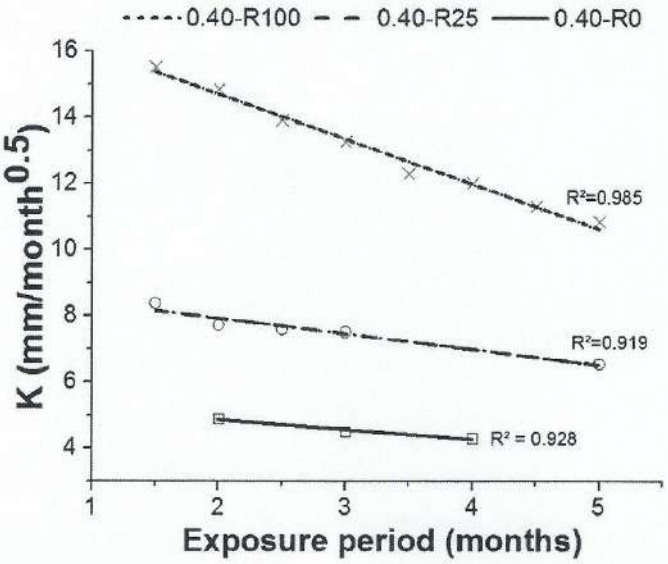

Fig. 13. Correlation between K (mm/month$^{0.5}$) and t (months).

and 0.40-R100 mixtures showed values of 7.22 and 12.34 mm/month$^{0.5}$, respectively. Limbachiya et al. [71] observed the same carbonation coefficient tendency in concrete with recycled aggregate, where the replacement percentages were 0%, 50%, and 100% and the w/c ratio was 0.50, with 3.5% CO_2 concentration. The reference concrete showed a carbonation coefficient in 20 weeks of CO_2 exposure of about 2.54 mm/week$^{0.5}$ and the concrete with 50% and 100% recycled aggregate content showed values of 2.85 and 2.98 mm/week$^{0.5}$ [71]. Bosque et al. [72] carried out accelerated carbonation tests at 1% concentration of CO_2 in concrete with 25%

and 50% recycled aggregate content with a w/c ratio of 0.45. This study observed a carbonation coefficient of 1.05 and 1.19 mm/year$^{0.5}$ greater compared to the reference concrete, corroborating with the results obtained in this study.

3.5. SEM with EDS and X-ray microtomography

The reference concrete (Fig. 14 (a)) showed that the calcium silicate hydrates (C-S-H) appeared uniform, although it contained pores between the characteristic layers of the C-S-H gel. In the EDS results (Fig. 14 (b)), a large amount of Si and small peaks of Ca and O can be observed. Fig. 15 (a) shows the sample concrete with 50% replacement of RA. The C-S-H microstructure appears less dense, with the presence of needle-shaped ettringite. Based on Fig. 15 (b), a large amount of Si and small peaks of Ca and O can be observed.

Fig. 16 shows a concrete sample with RA. It is known that the recycled aggregate contains old adhered paste and consequently an old interfacial transition zone. Therefore, the new cement paste is more compact and denser than the old paste involved in recycled aggregate, according to Thomas et al. [73]. Fig. 17 shows the recycled aggregate interface with the old paste (a) and the new paste (b). In contrast, Fig. 18 shows the microstructure of the 100% replacement concrete and the presence of some ettringite and $Ca(OH)_2$ crystals. This behavior was identified by Li et al. [74], who showed that in the interfacial transition zone (ITZ), there is a significantly weak microstructure with large porosity and $Ca(OH)_2$ crystals.

As an old paste adhered to the aggregate is very similar to a new paste of new concrete, two criterions were adopted to identify it as two pastes. The first criterion was visually analyzed the sample and verifying the difference in porosity between the two pastes, as presented in Fig. 16. The second criterion was the slight difference in color that exists between the old paste and the new paste. In this study, it was observed that an old paste had a slightly darker color than a new paste. According to Gracioli et al. [75] with the use of recycled aggregate, the microstructure demonstrates ettringite needles and the structure of the C-S-H is less evident. The same behavior was identified by Guedes et al. [76]. Xiao et al. [77] presented a microstructure with voids and $Ca(OH)_2$ crystals near the ITZ. Compared to the old ITZ, there are more C-S-H gels in the new ITZ.

Figs. 19–21 show the porosity of concrete using the X-ray microtomography technique. The dark gray composition represents the paste, and the light gray part corresponds to the natural or recycled aggregate.

The results indicate that the concrete porosity increases with the addition of RA. For 0.50-R0 (Fig. 20), the reduced void volume occurs in spaces where there is no aggregate present. In Fig. 21, the difference in porosity between natural and recycled aggregates becomes clear. The space occupied by natural aggregate has no apparent voids, while the volume filled by RA shows a higher concentration of voids. In Fig. 21, with 100% RA, the void volume is predominant in all regions of the sample. The increase in void volume can be explained by the high absorption rate of the RA, which is the only difference between the tested traits, since the w/c is set at 0.50. In concrete and cement paste, porosity significantly impairs strength, may increase its permeability, and compromises material densification [78]. The presence of voids within the RA justifies the method of pre-wetting the aggregate adopted in the molding of the specimens. In this way, the aggregate does not absorb water intended for cement hydration. In research conducted by Leite and Monteiro [79], microtomography images showed that mixtures with recycled aggregate developed interconnected macropores around the material. To reduce the large pores, resulting in improved behavior, the use of recycled aggregate should be reduced to less than 50%.

From the results of water absorption and porosity for concrete in the hardened state, it was found that these properties are associated with natural aggregate substitution by recycled aggregate and with the w/c ratio (Fig. 22), and the results obtained in the microtomography were corroborated.

Based on the results, it was observed that as the substitution content of NA by RA is increased for the same w/c ratio, there is an increase in the water absorption due to the increase in the number of voids and consequently the specific mass reduction of the analyzed concrete. However, it is observed that the lower the w/c ratio, the smaller the effect is on these properties. The 0.40-R50 concrete showed an increase of 70% and 56% in the water absorption and porosity, respectively, when compared to the reference concrete 0.40-R0. The RA used in this study contains a large amount of material with an angular shape and rough surface. According to El-Hassan et al. [80], more air is retained the concrete capillary pores, making them more porous and consequently lighter. Bravo et al. [81] analyzed water absorption in concrete produced with RA from different recycling plants and found variations in the order of 7.1–28.6% for 100% replacement with RA.

3.6. Relations between mechanical properties and durability

The comparison presented in Fig. 23 illustrates all changes in the properties of concrete in relation to the addition of RA. An increase of less than 1% in the quantity of voids per total volume generates a resistance decrease of 17.2% from 0.50-R0 to 0.50-R50, rising to 34.5% between R2-S0 and 0.50-R100. Also important is the enhancement in water absorption that accompanies the increase in void volume. In all analyzed mixtures, the relationship between the variables remained at an average of 33.5%. Similar results were found by Pacheco et al. [82], where mixtures with lower f_c showed larger voids in microtomography analysis.

Fig. 24 showed that the values of E_c for concrete 0.50-R50 and 0.50-R100 are lower than the concrete 0.50-R0, according to Zhou and Chen [83]. This can be attributed to the decrease in the stiffness of the recycled aggregate as well as the decrease in the apparent density.

It can be seen in Fig. 24 that there is a direct correlation between E_c and the mechanical properties (f_c and $f_{ct,sp}$). As the RA substitution content increases, E_c, f_c, and $f_{ct,sp}$ all decrease. Silva et al. [84] carried out an in-depth study of the correlation between E_c and f_c where different types of recycled aggregates are used. The authors observed that the increase in the recycled aggregate content as well as its quality had a significant influence on the value of E_c of the concrete. Bravo et al. [81] found that the recycled aggregate

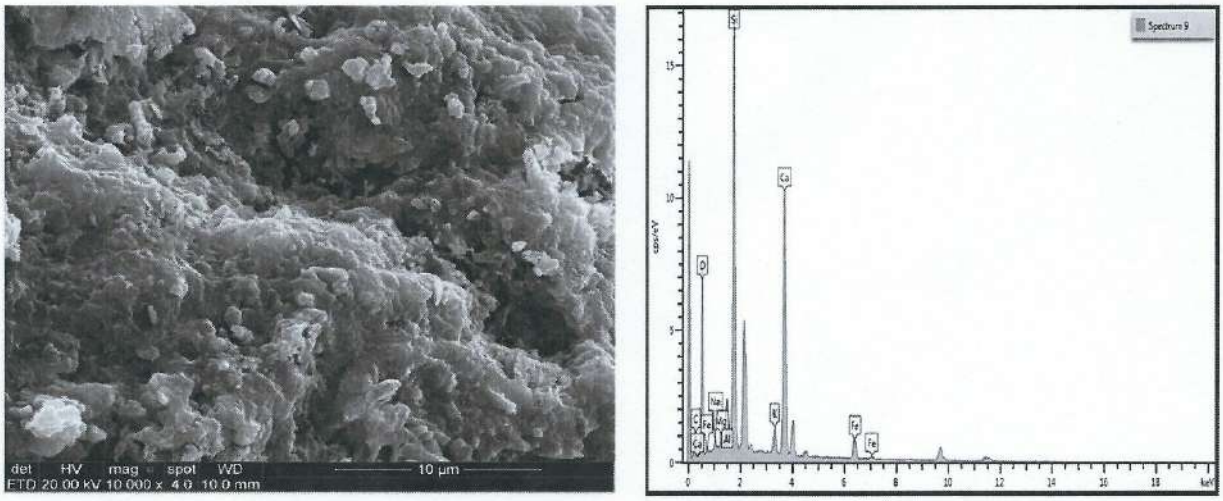

(a) (b)

Fig. 14. SEM for reference concrete with w/c = 0.5 (a), EDS of highlight area (b).

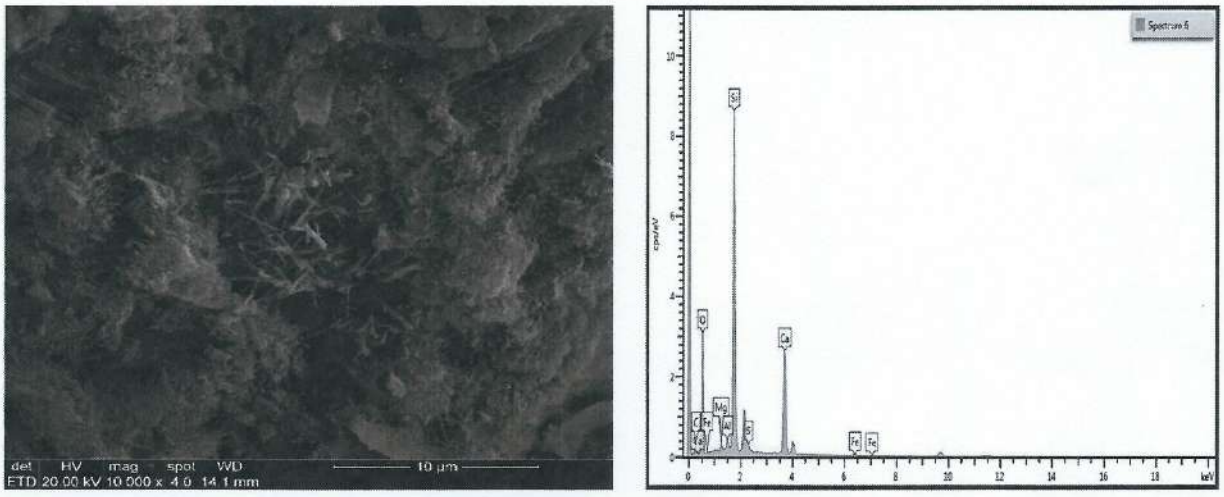

(a) (b)

Fig. 15. SEM concrete with 50% RA and w/c = 0.5 (a), EDS of highlight area (b).

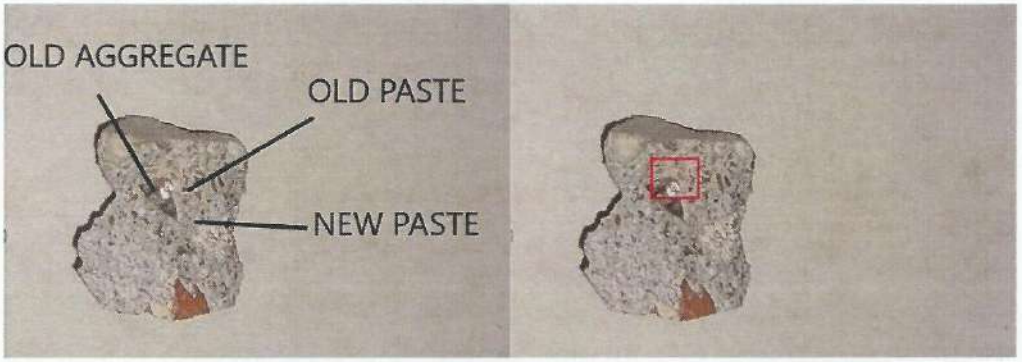

Fig. 16. Concrete sample containing only recycled aggregate (0.50-R100).

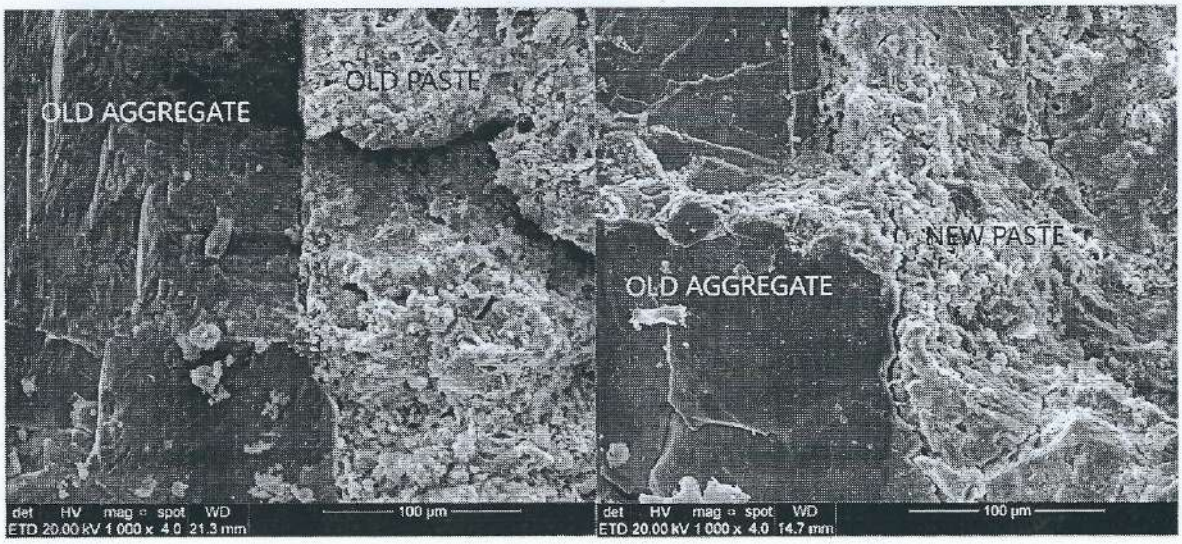

Fig. 17. SEM concrete containing 100% recycled aggregate and old paste (a), 100% recycled aggregate and new paste (b).

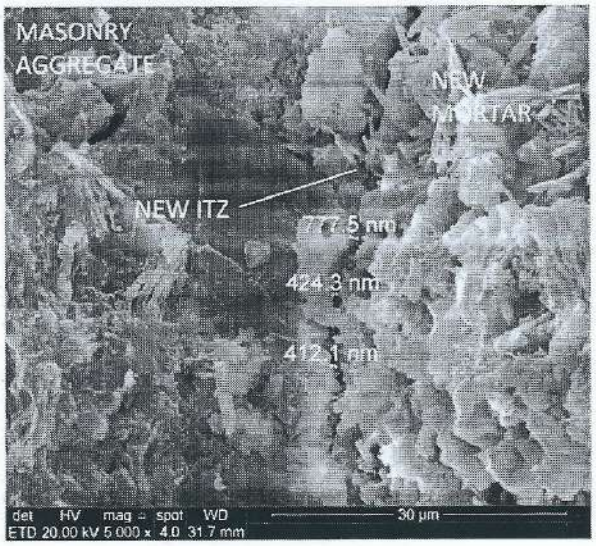

Fig. 18. SEM for reference concrete and w/c = 0.5 (0.50-R100).

concrete from eight different recycling plants showed a varied reduction in E_c when compared to reference concrete. According to the authors, the composition of recycled aggregate is the factor that most influenced the E_c results.

The relationship between E_c, f_c, carbonation depth, and cement content for concrete with a w/c ratio of 0.50 is presented in Fig. 25. The determination coefficient of the proposed equations varied between 0.996 and 0.999. An R^2 value close to 1 was expected because the correlation was based on the sample data from the models presented in Eqs. (6)–(12).

As shown in Fig. 25, as the E_c of concrete decreases due to the increase in the RA replacement content, f_c also decreases. Consequently, the void volume and carbonation depth increase. For the concrete 0.50-R50, compared to 0.50-R0, there was a reduction in the f_{c28} of 16.13% and E_{c28} of 31.2%. The e_{c45} and void volume increased by 22.07% and 17.2%, respectively.

3.7. Proposed method for design concretes with RA

Based on the analyses in the previous sections, it is possible to evaluate the ability to use the RA in this study in concrete for a given compressive strength (f_{C28}) and a certain w/c ratio. Based on the correlations discussed previously, it was possible to determine a method (Fig. 26) using only two equations.

The values of a, b and c of the equations will depend on the variability of the recycled aggregate, type of cement used, particle size

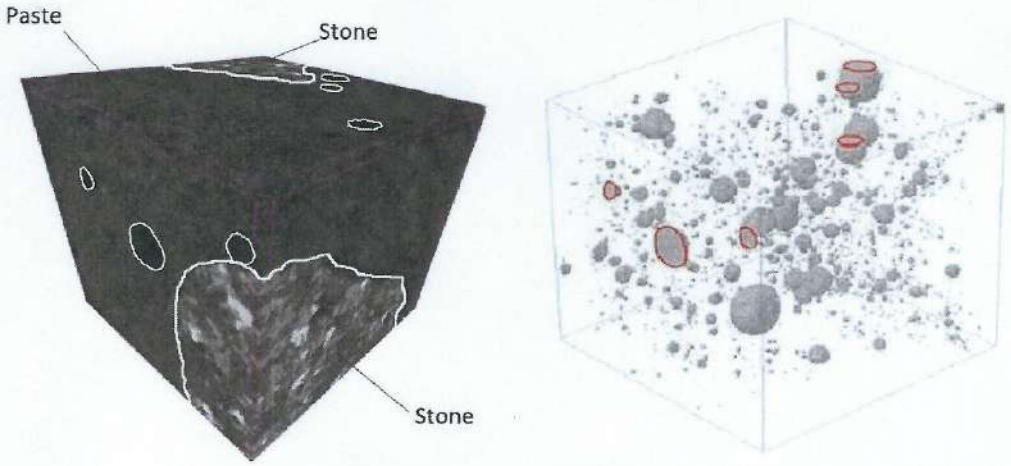

Fig. 19. Reconstructed image and pores of reference concrete (0.50-R0).

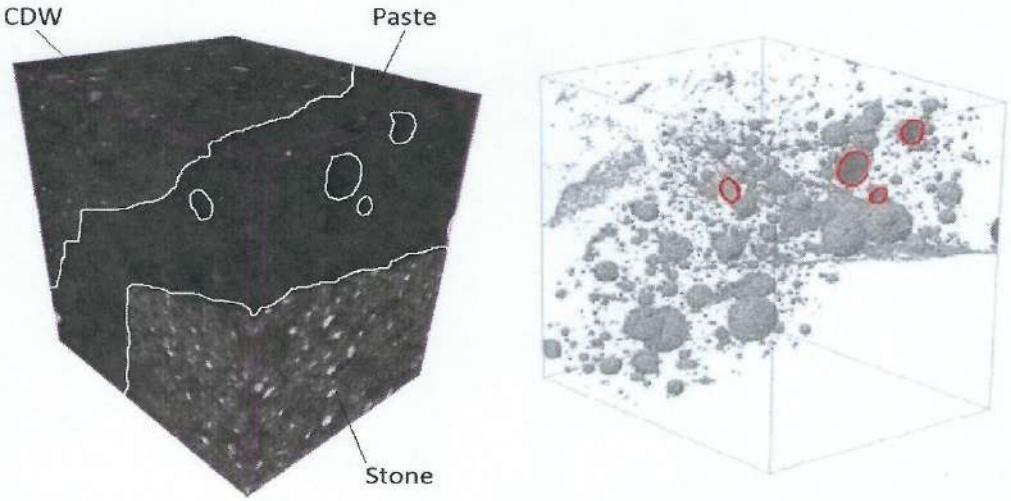

Fig. 20. Reconstructed image and pores of concrete (0.50-R50).

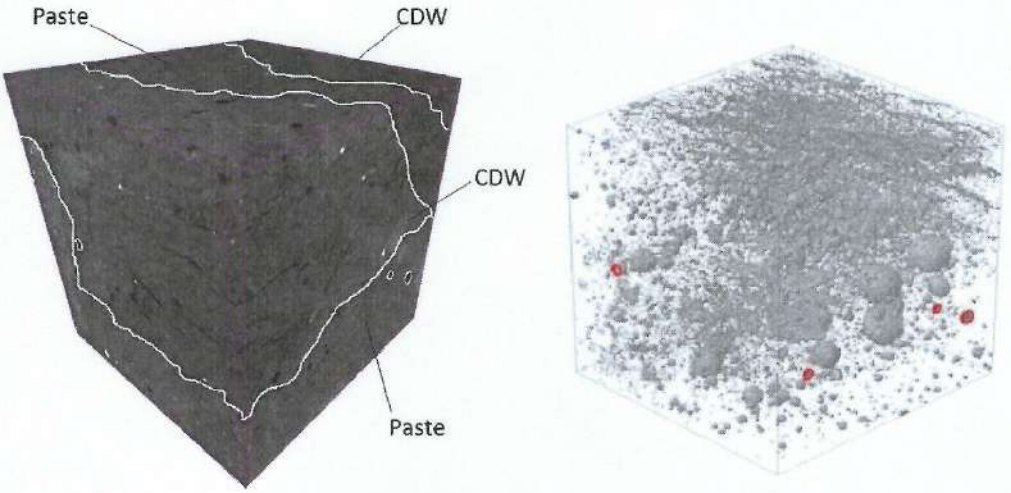

Fig. 21. Reconstructed image and pores of concrete (0.50-R100).

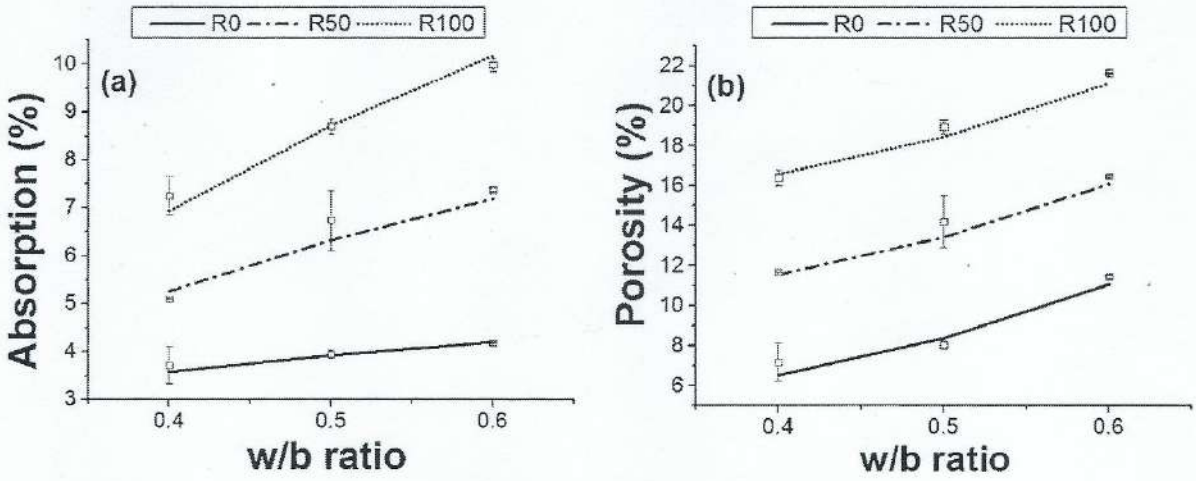

Fig. 22. Concrete investigated at 28 days (a) Absorption, (b) Porosity.

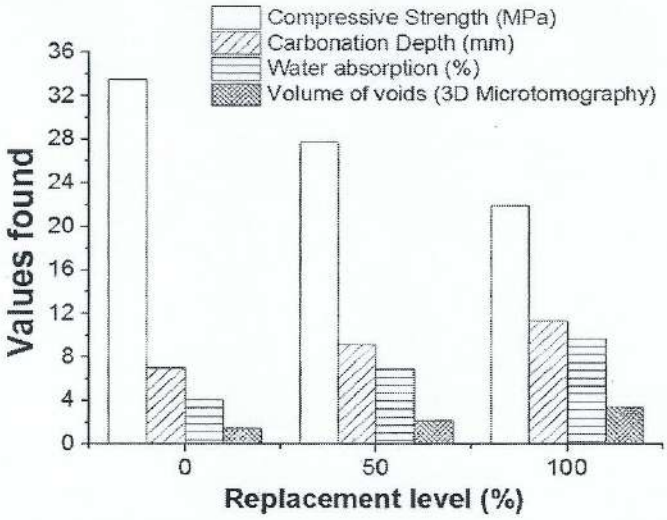

Fig. 23. Comparative analysis of the studied variables for concrete with w/c = 0.50 and 28 days.

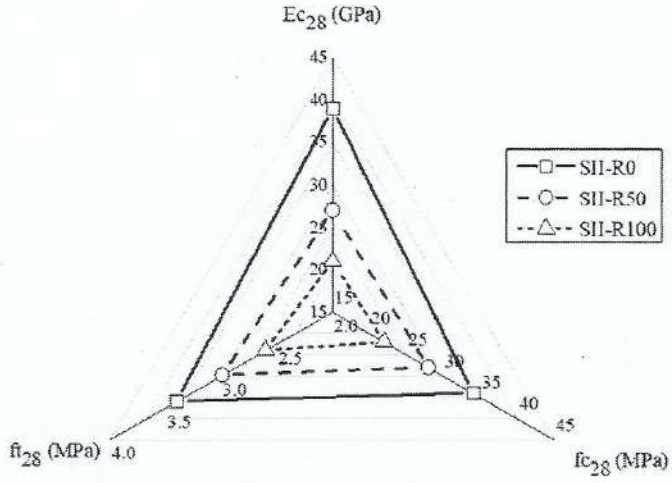

Fig. 24. Correlation between the mechanical properties f_{c28} (MPa), f_{t28} (MPa) and E_{c28} (GPa).

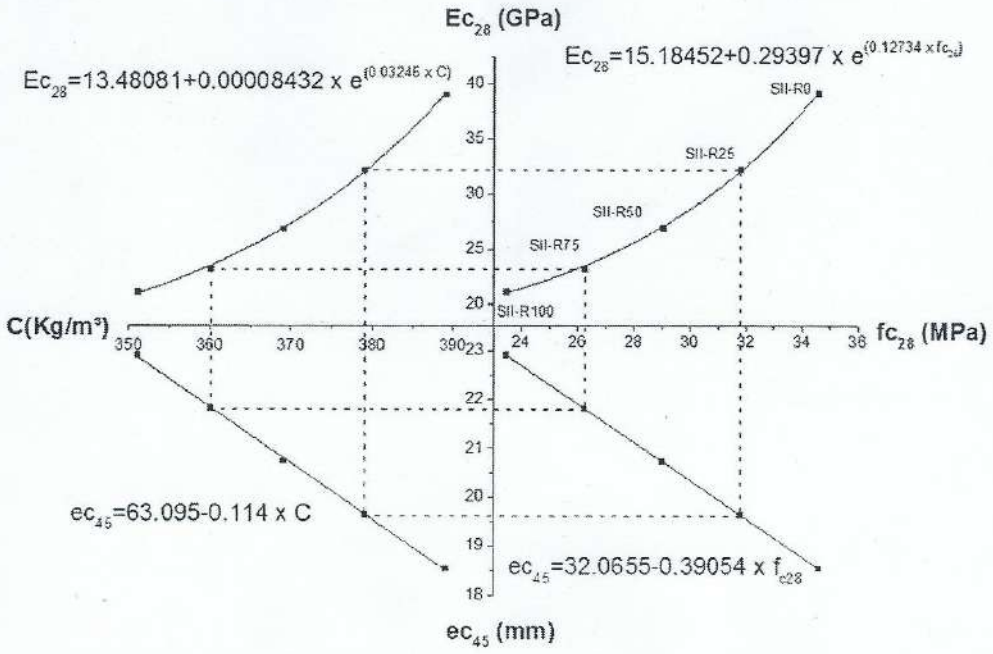

Fig. 25. Relationship between E_{c28} (GPa), f_{c28} (MPa), ec45 (mm) and C(kg/m^3) for concrete with w/c(= 0.50.

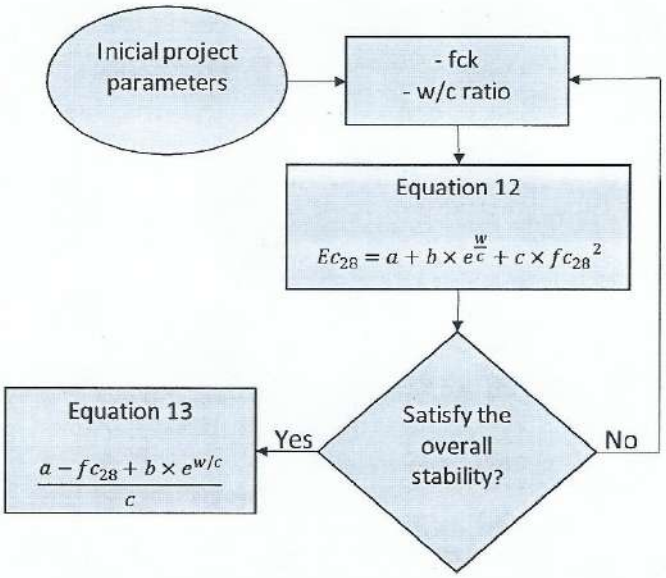

Fig. 26. Application of the proposed equations.

of the recycled aggregate, concrete curing method, as well as the compressive strength and modulus of elasticity test method. This equation, with the values a, b and c corresponding to the recycled aggregate used, can be used in a situation where the engineer has the fc_{28} parameters and the w/c relation of the concrete that would be used in a real case. Once these parameters are defined in the design phase, the engineer can determine the Ec_{28} value for the concrete. Based on the aggregate used in this study, it was possible to obtain Eq. (13). The modulus of elasticity is important in the design because it can be used to calculate general structural stability.

Table 7
ANOVA of the elastic modulus for concrete.

Beta in	Partial Correlation	Semi partial Correlation	Tolerance	F-test	R-square	P-level
w/c ratio	1.001135	0.952063	0.649299	0.420634	0.579366	0.000000

Declaration of Competing Interest

The authors declare that they have no known competing financial interests or personal relationships that could have appeared to influence the work reported in this paper.

Acknowledgment

This study was financed in part by the Coordenação de Aperfeiçoamento de Pessoal de Nível Superior – Brasil (CAPES) – Finance Code 001 to the first author. The authors are thankful to Professor Giselle Spindler from FASEG-UFRGS, undergraduate student Vinícius Susin Bocchese and laboratory technicians José Eduardo Cruz, and Douglas T. Rodrighiero.

References

[1] A. Ossa, J.L. García, E. Botero, Use of recycled construction and demolition waste (CDW) aggregates: a sustainable alternative for the pavement construction industry, J. Clean. Prod. 135 (2016) 379–386, https://doi.org/10.1016/j.jclepro.2016.06.088.
[2] P. Sormunen, T. Kärki, Recycled construction and demolition waste as a possible source of materials for composite manufacturing, J. Build. Eng. 24 (2019), 100742, https://doi.org/10.1016/j.jobe.2019.100742.
[3] S. Santos, P.R. da Silva, J. de Brito, Self-compacting concrete with recycled aggregates – a literature review, J. Build. Eng. 22 (2019) 349–371, https://doi.org/10.1016/j.jobe.2019.01.001.
[4] I. Martínez-Lage, P. Vázquez-Burgo, M. Velay-Lizancos, Sustainability evaluation of concretes with mixed recycled aggregate based on holistic approach: technical, economic and environmental analysis, Waste Manag. 104 (2020) 9–19, https://doi.org/10.1016/j.wasman.2019.12.044.
[5] S. Lotfi, M. Eggimann, E. Wagner, R. Mróz, J. Deja, Performance of recycled aggregate concrete based on a new concrete recycling technology, Constr. Build. Mater. 95 (2015) 243–256, https://doi.org/10.1016/j.conbuildmat.2015.07.021.
[6] H. Guo, C. Shi, X. Guan, J. Zhu, Y. Ding, T.C. Ling, H. Zhang, Y. Wang, Durability of recycled aggregate concrete – a review, Cem. Concr. Compos. 89 (2018) 251–259, https://doi.org/10.1016/j.cemconcomp.2018.03.008.
[7] M. Zhang, Pore-scale modelling of relative permeability of cementitious materials using X-ray computed microtomography images, Cem. Concr. Res. 95 (2017) 18–29, https://doi.org/10.1016/j.cemconres.2017.02.005.
[8] G. Fathifazl, G. Razaqpur, O. Isgor, A. Abbas, B. Fournier, S. Foo, Fresh and hardened properties of recycled aggregate concrete proportioned by the equivalent mortar volume (EMV) method. Proc. 2nd Can. Conf. Eff. Des. Struct, McMaster Univ., 2008.
[9] R.V. Silva, R. Neves, J. De Brito, R.K. Dhir, Carbonation behaviour of recycled aggregate concrete, Cem. Concr. Compos. 62 (2015) 22–32, https://doi.org/10.1016/j.cemconcomp.2015.04.017.
[10] M. Bravo, J. de Brito, L. Evangelista, J. Pacheco, Durability and shrinkage of concrete with CDW as recycled aggregates: benefits from superplasticizer's incorporation and influence of CDW composition, Constr. Build. Mater. 168 (2018) 818–830, https://doi.org/10.1016/j.conbuildmat.2018.02.176.
[11] J. Andal, M. Shehata, P. Zacarias, Properties of concrete containing recycled concrete aggregate of preserved quality, Constr. Build. Mater. 125 (2016) 842–855, https://doi.org/10.1016/j.conbuildmat.2016.08.110.
[12] R. Kumar, Influence of recycled coarse aggregate derived from construction and demolition waste (CDW) on abrasion resistance of pavement concrete, Constr. Build. Mater. 142 (2017) 248–255, https://doi.org/10.1016/j.conbuildmat.2017.03.077.
[13] S. Ghorbani, S. Sharifi, S. Ghorbani, V.W. Tam, J. de Brito, R. Kurda, Effect of crushed concrete waste's maximum size as partial replacement of natural coarse aggregate on the mechanical and durability properties of concrete, Resour. Conserv. Recycl. 149 (2019) 664–673, https://doi.org/10.1016/j.resconrec.2019.06.030.
[14] M.C.S. Nepomuceno, R.A.S. Isidoro, J.P.G. Catarino, Mechanical performance evaluation of concrete made with recycled ceramic coarse aggregates from industrial brick waste, Constr. Build. Mater. 165 (2018) 284–294, https://doi.org/10.1016/j.conbuildmat.2018.01.052.
[15] G. Duarte, M. Bravo, J. de Brito, J. Nobre, Mechanical performance of shotcrete produced with recycled coarse aggregates from concrete, Constr. Build. Mater. 210 (2019) 696–708, https://doi.org/10.1016/j.conbuildmat.2019.03.156.
[16] C.S. Poon, Z.H. Shui, L. Lam, Effect of microstructure of ITZ on compressive strength of concrete prepared with recycled aggregates, Constr. Build. Mater. 18 (2004) 461–468, https://doi.org/10.1016/j.conbuildmat.2004.03.005.
[17] C. Thomas, J. Setién, J.A. Polanco, A.I. Cimentada, C. Medina, Influence of curing conditions on recycled aggregate concrete, Constr. Build. Mater. 172 (2018) 618–625, https://doi.org/10.1016/j.conbuildmat.2018.04.009.
[18] A. Djerbi, Effect of recycled coarse aggregate on the new interfacial transition zone concrete, Constr. Build. Mater. 190 (2018) 1023–1033, https://doi.org/10.1016/j.conbuildmat.2018.09.180.
[19] S. Pradhan, S. Kumar, S.V. Barai, Multi-scale characterisation of recycled aggregate concrete and prediction of its performance, Cem. Concr. Compos. 106 (2020), 103480, https://doi.org/10.1016/j.cemconcomp.2019.103480.
[20] J. De Brito, J. Ferreira, J. Pacheco, D. Soares, M. Guerreiro, Structural, material, mechanical and durability properties and behaviour of recycled aggregates concrete, J. Build. Eng. 6 (2016) 1–16, https://doi.org/10.1016/j.jobe.2016.02.003.
[21] E.M. Golafshani, A. Behnood, Automatic regression methods for formulation of elastic modulus of recycled aggregate concrete, Appl. Soft Comput. J. 64 (2018) 377–400, https://doi.org/10.1016/j.asoc.2017.12.030.
[22] R.V. Silva, J. De Brito, R.K. Dhir, Establishing a relationship between modulus of elasticity and compressive strength of recycled aggregate concrete, J. Clean. Prod. 112 (2016) 2171–2186, https://doi.org/10.1016/j.jclepro.2015.10.064.
[23] Y. Wang, H. Zhang, Y. Geng, Q. Wang, S. Zhang, Prediction of the elastic modulus and the splitting tensile strength of concrete incorporating both fine and coarse recycled aggregate, Constr. Build. Mater. 215 (2019) 332–346, https://doi.org/10.1016/j.conbuildmat.2019.04.212.
[24] A. Adessina, A. Ben, J. Barthélémy, C. Chateau, Experimental and micromechanical investigation on the mechanical and durability properties of recycled aggregate concretes, Cem. Concr. Res. 126 (2019), 105900, https://doi.org/10.1016/j.cemconres.2019.105900.
[25] R. Mi, G. Pan, K.M. Liew, T. Kuang, Utilizing recycled aggregate concrete in sustainable construction for a required compressive strength ratio, J. Clean. Prod. 276 (2020), 124249, https://doi.org/10.1016/j.jclepro.2020.124249.
[26] R. Mi, K.M. Liew, G. Pan, T. Kuang, Carbonation resistance study and inhomogeneity evolution of recycled aggregate concretes under loading effects, Cem. Concr. Compos. 118 (2021), 103916, https://doi.org/10.1016/j.cemconcomp.2020.103916.
[27] R. Mi, G. Pan, Y. Li, T. Kuang, Carbonation degree evaluation of recycled aggregate concrete using carbonation zone widths, J. CO2 Util. 43 (2021), 101366, https://doi.org/10.1016/j.jcou.2020.101366.
[28] R. Mi, G. Pan, Q. Shen, Carbonation modelling for cement-based materials considering influences of aggregate and interfacial transition zone, Constr. Build. Mater. 229 (2019), 116925, https://doi.org/10.1016/j.conbuildmat.2019.116925.
[29] X. Han Shen, W. Qiang Jiang, D. Hou, Z. Hu, J. Yang, Q. Feng Liu, Numerical study of carbonation and its effect on chloride binding in concrete, Cem. Concr. Compos. 104 (2019), 103402, https://doi.org/10.1016/j.cemconcomp.2019.103402.
[30] A.B.D.N.T. ABNT, NBR-NM 45-2006 - Agregados - determinação da massa unitária e do volume de vazios.pdf, Abnt Nbr Nm 45 (2006) 8.
[31] ABNT - Associação Brasileira de Normas Técnicas, NBR NM 248: Agregados-Determinação da composição granulométrica, Rio Janeiro, 2003.
[32] A.-A.B. de, N. Técnicas, N.B.R. NM, 52: Agregado miúdo - determinação da massa específica e massa específica aparente, Rio Jan. (2003) 6.
[33] A.B.D.N.T. ABNT, NBR MN 53: Agregado graúdo - determinação de massa específica, massa específica aparente e absorção de água, Abnt Nbr Nm 53 (2009) 8.

[34] P.S. Lovato, E. Possan, D.C.C.D. Molin, Â.B. Masuero, J.L.D. Ribeiro, Modeling of mechanical properties and durability of recycled aggregate concretes, Constr. Build. Mater. 26 (2012) 437–447, https://doi.org/10.1016/j.conbuildmat.2011.06.043.
[35] S.R. da Silva, J.J. de Oliveira Andrade, Investigation of mechanical properties and carbonation of concretes with construction and demolition waste and fly ash, Constr. Build. Mater. 153 (2017) 704–715, https://doi.org/10.1016/j.conbuildmat.2017.07.143.
[36] A.B.D.N.T. ABNT, Argamassa e concreto endurecidos - Determinação da absorção de água, índice de vazios e massa específica, ABNT NBR 9778, 2005, p. 4.
[37] A.B.D.N.T. ABNT, Ensaios de compressão de corpos de prova cilíndricos., ABNT NBR 5739, 2007, p. 9.
[38] A.B.D.N.T. ABNT, Concreto e argamassa — Determinação da resistência à tração por compressão diametral de corpos de prova cilíndricos, ABNT NBR 7222, 2011, p. 5.
[39] A.B.D.N.T. ABNT, ABNT NBR 8522: Concreto: determinação dos módulos estáticos de elasticidade e de deformação à compressão, Rio Jan. (2017) 20.
[40] NBR, 6118:2014 Projeto de estruturas de concreto - Procedimento, Assoc. Bras. Normas Técnicas. (2014) 256, https://doi.org/01.080.10; 13.220.99.
[41] Fédération Internationale du Béton (fib), Fib Model Code for Concrete Structures 2010, 2013., n.d.
[42] COMITE EURO-INTERNATIONAL DU BETON, Design of concrete structures - Part 1-1: general rules and rules for buildings, EUROCODE 2 (2010) 225.
[43] Mater Struct, RILEM CPC 18, Measurement of hardened concrete carbonation depth, 1988.
[44] K. Tuutti, Corrosion of Steel in Concrete., in: Proceedings of EUROCOR '77, Eur Congr Met Corros, 92nd Event Eur Fed Corros., 1977, pp. 655–661.
[45] J. Khunthongkeaw, S. Tangtermsirikul, T. Leelawat, A study on carbonation depth prediction for fly ash concrete, Constr. Build. Mater. 20 (2006) 744–753, https://doi.org/10.1016/j.conbuildmat.2005.01.052.
[46] S. Lu, E.N. Landis, D.T. Keane, X-ray microtomographic studies of pore structure and permeability in Portland cement concrete, Mater. Struct. Constr. 39 (2006) 611–620, https://doi.org/10.1617/s11527-006-9099-7.
[47] E. Gallucci, K. Scrivener, A. Groso, M. Stampanoni, G. Margaritondo, 3D experimental investigation of the microstructure of cement pastes using synchrotron X-ray microtomography (μCT), Cem. Concr. Res. 37 (2007) 360–368, https://doi.org/10.1016/j.cemconres.2006.10.012.
[48] S.K. Saha, S. Pradhan, S.V. Barai, Use of machine learning based technique to X-ray microtomographic images of concrete for phase segmentation at meso-scale, Constr. Build. Mater. 249 (2020), 118744, https://doi.org/10.1016/j.conbuildmat.2020.118744.
[49] J. de Brito, R. Robles, Recycled aggregate concrete (RAC) methodology for estimating its long-term properties, Indian J. Eng. Mater. Sci. 17 (2010) 449–462.
[50] J.M.P. MEHTA, P. Kumar. MONTEIRO, Concreto: microestrutura, propriedades e materiais, 2 ed., IBRACON, São, 2014.
[51] A. Barbudo, F. Agrela, M.G. Beltrán, J.R. Jiménez, A.P. Galvín, Effect of cement addition on the properties of recycled concretes to reach control concretes strengths, J. Clean. Prod. 79 (2014) 124–133, https://doi.org/10.1016/j.jclepro.2014.05.053.
[52] M.G.A , T.I. Milne, Influence of Cement Blend and Aggregate Type on the Stress-Strain Behavior and Elastic Modulus of Concrete, ACI Mater. J. 92 (n.d.). (https://doi.org/10.14359/1114).
[53] M. Uysal, The influence of coarse aggregate type on mechanical properties of fly ash additive self-compacting concrete, Constr. Build. Mater. 37 (2012) 533–540, https://doi.org/10.1016/j.conbuildmat.2012.07.085.
[54] B. Cantero, I.F. Sáez del Bosque, A. Matías, C. Medina, Statistically significant effects of mixed recycled aggregate on the physical-mechanical properties of structural concretes, Constr. Build. Mater. 185 (2018) 93–101, https://doi.org/10.1016/j.conbuildmat.2018.07.060.
[55] K. Zieliński, Impact of recycled aggregates on selected physical and mechanical characteristics of cement concrete, Procedia Eng. 172 (2017) 1291–1296, https://doi.org/10.1016/j.proeng.2017.02.157.
[56] J. Xiao, W. Li, Y. Fan, X. Huang, An overview of study on recycled aggregate concrete in China (1996-2011), Constr. Build. Mater. 31 (2012) 364–383, https://doi.org/10.1016/j.conbuildmat.2011.12.074.
[57] M. Etxeberria, E. Vázquez, A. Marí, M. Barra, Influence of amount of recycled coarse aggregates and production process on properties of recycled aggregate concrete, Cem. Concr. Res. 37 (2007) 735–742, https://doi.org/10.1016/j.cemconres.2007.02.002.
[58] M. Seddik Meddah, Recycled aggregates in concrete production: engineering properties and environmental impact, MATEC Web Conf. 101 (2017) 05021, https://doi.org/10.1051/matecconf/201710105021.
[59] D. Pedro, J. de Brito, L. Evangelista, Evaluation of high-performance concrete with recycled aggregates: Use of densified silica fume as cement replacement, Constr. Build. Mater. 147 (2017) 803–814, https://doi.org/10.1016/j.conbuildmat.2017.05.007.
[60] M. Eckert, M. Oliveira, Mitigation of the negative effects of recycled aggregate water absorption in concrete technology, Constr. Build. Mater. 133 (2017) 416–424, https://doi.org/10.1016/j.conbuildmat.2016.12.132.
[61] A. Juan-Valdés, D. Rodríguez-Robles, J. García-González, M.I. Guerra-Romero, J.M. Morán-del Pozo, Mechanical and microstructural characterization of non-structural precast concrete made with recycled mixed ceramic aggregates from construction and demolition wastes, J. Clean. Prod. 180 (2018) 482–493, https://doi.org/10.1016/j.jclepro.2018.01.191.
[62] A. Oner, S. Akyuz, R. Yildiz, An experimental study on strength development of concrete containing fly ash and optimum usage of fly ash in concrete, Cem. Concr. Res. 35 (2005) 1165–1171, https://doi.org/10.1016/j.cemconres.2004.09.031.
[63] C. Pauletti, Estimativa da carbonatação natural de materiais cimentícios a partir de ensaios acelerados e de modelos de predição, Universidade Federal do Rio Grande do Sul - UFRGS, 2009. (http://hdl.handle.net/10183/30120).
[64] M.P. Kulakowski, Contribuição ao estudo da carbonatação em concretos e argamassas compostos com adição de sílica ativa, Universidade Federal do Rio Grande do Sul - UFRGS, 2002. (http://hdl.handle.net/10183/3594).
[65] F. Debieb, L. Courard, S. Kenai, R. Degeimbre, Roller compacted concrete with contaminated recycled aggregates, Constr. Build. Mater. 23 (2009) 3382–3387, https://doi.org/10.1016/j.conbuildmat.2009.06.031.
[66] H. Zhao, W. Sun, X. Wu, B. Gao, The properties of the self-compacting concrete with fly ash and ground granulated blast furnace slag mineral admixtures, J. Clean. Prod. 95 (2015) 66–74, https://doi.org/10.1016/j.jclepro.2015.02.050.
[67] S.C. Kou, C.S. Poon, Enhancing the durability properties of concrete prepared with coarse recycled aggregate, Constr. Build. Mater. 35 (2012) 69–76, https://doi.org/10.1016/j.conbuildmat.2012.02.032.
[68] N. Kisku, H. Joshi, M. Ansari, S.K. Panda, S. Nayak, S.C. Dutta, A critical review and assessment for usage of recycled aggregate as sustainable construction material, Constr. Build. Mater. 131 (2017) 721–740, https://doi.org/10.1016/j.conbuildmat.2016.11.029.
[69] F. Buyle-Bodin, R. Zaharieva, Influence of industrially produced recycled aggregates on flow properties of concrete, Mater. Struct. 35 (2002) 504–509, https://doi.org/10.1007/BF02483138.
[70] V. Carević, I. Ignjatović, J. Dragaš, Model for practical carbonation depth prediction for high volume fly ash concrete and recycled aggregate concrete, Constr. Build. Mater. 213 (2019) 194–208, https://doi.org/10.1016/j.conbuildmat.2019.03.267.
[71] M. Limbachiya, M.S. Meddah, Y. Ouchagour, Use of recycled concrete aggregate in fly-ash concrete, Constr. Build. Mater. 27 (2012) 439–449, https://doi.org/10.1016/j.conbuildmat.2011.07.023.
[72] I.F.S. Bosque, P.V. Heede, N. Belie, M.I.S. Rojas, C. Medina, Carbonation of concrete with construction and demolition waste based recycled aggregates and cement with recycled content, Constr. Build. Mater. 234 (2020), 117336, https://doi.org/10.1016/j.conbuildmat.2019.117336.
[73] C. Thomas, J. Setién, J.A. Polanco, P. Alaejos, M. Sánchez De Juan, Durability of recycled aggregate concrete, Constr. Build. Mater. 40 (2013) 1054–1065, https://doi.org/10.1016/j.conbuildmat.2012.11.106.
[74] W. Li, J. Xiao, Z. Sun, S. Kawashima, S.P. Shah, Interfacial transition zones in recycled aggregate concrete with different mixing approaches, Constr. Build. Mater. 35 (2012) 1045–1055, https://doi.org/10.1016/j.conbuildmat.2012.06.022.
[75] B. Gracioli, M.V.F. Varela, C.S. Beutler, A. Frare, C.A. da Luz, J.I. Pereira Filho, Considerations on the mechanical behavior and hydration process supersulfated cement (CSS) formulated with phosphogypsum, Rev. Mater. 22 (2017), https://doi.org/10.1590/s1517-707620170001.0107.
[76] M. Guedes, L. Evangelista, J. De Brito, A.C. Ferro, Microstructural characterization of concrete prepared with recycled aggregates, Microsc. Microanal. 19 (2013) 1222–1230, https://doi.org/10.1017/S1431927613001463.
[77] J. Xiao, W. Li, Z. Sun, D.A. Lange, S.P. Shah, Properties of interfacial transition zones in recycled aggregate concrete tested by nanoindentation, Cem. Concr. Compos. 37 (2013) 276–292, https://doi.org/10.1016/j.cemconcomp.2013.01.006.

[78] Í.B. da Silva, X-ray Computed Microtomography technique applied for cementitious materials: a review, Micron 107 (2018) 1–8, https://doi.org/10.1016/j.micron.2018.01.006.
[79] M.B. Leite, P.J.M. Monteiro, Microstructural analysis of recycled concrete using X-ray microtomography, Cem. Concr. Res. 81 (2016) 38–48, https://doi.org/10.1016/j.cemconres.2015.11.010.
[80] H. El-Hassan, P. Kianmehr, S. Zouaoui, Properties of pervious concrete incorporating recycled concrete aggregates and slag, Constr. Build. Mater. 212 (2019) 164–175, https://doi.org/10.1016/j.conbuildmat.2019.03.325.
[81] M. Bravo, J. De Brito, J. Pontes, L. Evangelista, Durability performance of concrete with recycled aggregates from construction and demolition waste plants, Constr. Build. Mater. 77 (2015) 357–369, https://doi.org/10.1016/j.conbuildmat.2014.12.103.
[82] F. Pacheco, R.P. de Souza, R. Christ, C.A. Rocha, L. Silva, B. Tutikian, Determination of volume and distribution of pores of concretes according to different exposure classes through 3D microtomography and mercury intrusion porosimetry, Struct. Concr. 19 (2018) 1419–1427, https://doi.org/10.1002/suco.201800075.
[83] C. Zhou, Z. Chen, Mechanical properties of recycled concrete made with different types of coarse aggregate, Constr. Build. Mater. 134 (2017) 497–506, https://doi.org/10.1016/j.conbuildmat.2016.12.163.
[84] R.V. Silva, J. De Brito, R.K. Dhir, Properties and composition of recycled aggregates from construction and demolition waste suitable for concrete production, Constr. Build. Mater. 65 (2014) 201–217, https://doi.org/10.1016/j.conbuildmat.2014.04.117.

3.3 ETAPA 2 – SYNERGIC EFFECT OF RECYCLED AGGREGATES, FLY ASH, AND HYDRATED LIME FOR PRODUCTION OF ECO-FRIENDLY CONCRETE

Procedimento experimental, resultados e discussão estão apresentados neste capítulo em forma de artigo, o qual está em avaliação desde 24/08/2022 pela revista *Construction and Building Materials*, conforme anexo A.

SYNERGIC EFFECT OF RECYCLED AGGREGATES, FLY ASH, AND HYDRATED LIME FOR PRODUCTION OF ECO-FRIENDLY CONCRETE

Sérgio Roberto da Silva* (1), Jairo José de Oliveira Andrade (2)

(1) Graduate Program of Materials Engineering and Technology, Pontifical Catholic University of Rio Grande do Sul (PGETEMA/PUCRS), Orcid: 0000-0002-9843-002X e-mail: sergio.roberto@acad.pucrs.br

(2) Professor, Graduate Program of Materials Engineering and Technology, Pontifical Catholic University of Rio Grande do Sul (PGETEMA/PUCRS), Orcid: 0000-0003-2073-6763
e-mail: *jairo.andrade@pucrs.brbr*

PUCRS – Av. Ipiranga, 6681, Building 30/D Office 228. Porto Alegre – RS, Brazil.

HIGHLIGHTS

1. Two types of CDW (mixed recycled aggregate and recycled concrete aggregate) were used with one level of recycled aggregate replacement (50%), fly ash replacement (20%) by Portland cement, and two levels of hydrated lime addition (5 and 10 %) were investigated.
2. The addition of hydrated lime in concrete with fly ash and recycled aggregate anticipated the dissolution of fly ash particles for the pozzolanic reaction.
3. The effect of the addition of hydrated lime in concretes with fly ash and recycled aggregate altered the microstructure of the paste as a function of the refinement of the pore diameter.
4. Carbonation depth was reduced with the addition of hydrated lime in fly ash and recycled aggregate concretes when compared to concrete without hydrated lime.

ABSTRACT

The use of construction and demolition waste (CDW) as recycled aggregate (RA) and fly ash (FA) in the composition of cementitious material makes the new concrete more sustainable. However, RA is more heterogeneous, porous, and less dense materials than natural aggregates (NA), influencing mechanical resistance. On the other hand, the reaction of FA with hydration products of Portland cement is slow, delaying the resistance development at an early age. An alternative to increase the concrete strength with FA at an early age is the use of hydrated lime (HL). This research aims to evaluate the efficiency of adding hydrated lime (HL) in concrete with RA and FA. In this way, this research has two stages. In the first stage, produced concretes only with mixed concrete aggregates (MRA) and concrete recycled aggregates (CRA). From the mix proportioning diagram, a w/c ratio of 0.55 and an RA content of 50% were fixed, considering similar compressive strengths. In the second stage, produced concretes with 20% in partial replacement of Portland cement (PC) and addition of HL in proportions of 5% and 10% (by mass) of the total content of cementitious material and water/binder ratio of 0.55. Performed mechanical tests (compressive strength, elastic modulus), durability (water absorption, carbonation depth), and microstructural analysis (SEM and X-ray microtomography) in concretes. The results showed that the addition of 10% HL in concretes with 80% Portland cement and 20% FA improves compressive strength, elastic modulus, water absorption, porosity, and apparent density of concretes when compared to concretes without HL from 28 days old, considering the concretes with 20% FA. The reduction in carbonation rate was observed when HL was added to all concretes evaluated. The microstructural analysis shows that adding HL tends to increase the concrete homogeneity. Results show that adding hydrated lime influences the mechanical properties and durability of concrete with FA and RA and that including these residual materials in concrete mixtures would positively contribute to the environmental impact.

Keywords: Construction and demolition waste; Coarse recycled aggregate; fly ash; hydrated lime; Physical-mechanical properties; Microstructural analysis.

1 Introduction

Society depends on natural resources for experience and socioeconomic development, but the need to explore these natural resources also increases due to population growth. Concrete plays a key role in the socioeconomic development of a country, but it also has a very significant adverse effect on the environment and the depletion of natural resources. The construction industry produces large amounts of solid waste from construction and demolition activities [1]. In 2020, 47 million tons of construction and demolition waste (CDW) were produced in Brazil, corresponding to 221.19 kg/inhabitant/year [2]. The materials extraction, as well as their processing for use in civil construction, generate large amounts of solid waste that, improperly deposited, can bring various problems to the environment, such as the proliferation of disease-transmitting agents, degradation of the large areas, obstruction of drainage systems, silting up rivers and streams as well as the occupation of roads that degrade the urban landscape [3]. Besides, carbon hydroxide (CO_2) emissions grew to 36.3 Gt in 2021, according to the Global Energy Review [4], this is a record high, and only coal accounted for more than 40% of the global growth of CO_2 emissions in 2021 which was 15.3 Gt, surpassing the 2014 peak of 200 Mt. In Brazil, according to Cirilo [5], around 2.5% of the total CO_2 is emitted on a global scale. Considering this scenario, it is necessary to investigate the construction sector's contribution to find alternatives to reduce the consumption of natural resources and greenhouse gas emissions. One alternative is the reuse of CDW as a by-product (sand, coarse aggregate) in the production of new concretes, which has been studied by several researchers [6][7][8][9][10][11]. Nevertheless, one of the significant challenges of using recycled aggregate (RA) from CDW as raw material for producing new concrete is the variability in its composition, as well as impurities and contaminants that influence the mechanical and durability properties of concrete [12].

After processing the CDW, the concrete recycled aggregate (CRA) and mixed concrete aggregate

(MRA), which is the most significant part of the RA, are obtained [11]. MRA and CRA have very different physical characteristics. In general, the MRA is a more porous material when compared to CRA [13]. According to Chen et al. [13], the average CRA and MRA densities are 2325 kg/m³ and 2169 kg/m³, respectively. The water absorption of CRA and MRA vary between 4.9% and 7.4%, respectively [14] [15]. Another factor that should be taken into account, according to Sáez del Borque [16], is the elastic modulus of the interfacial transition zone (ITZ) between the RA and the cement paste that varies with the type of constituent material in the MRA, as this impacts in concrete properties. However, some undesired characteristics of RA feasibility studies of the use of RA in the substitution of natural aggregates (NA) for concrete production in small quantities present promising results both in the mechanical and durability properties, as observed in the literature [17][18][19][20].

Concerning the contribution of the construction industry to reducing CO_2 emissions in the environment, one alternative would be, according to Meyer [21] and Aprianti [22], the optimization of the production process of Portland cement (PC). One of the ways would be using by-products generated by industrial processes, agricultural waste, and recycled materials such as rice husk ash, palm oil fuel ash, bagasse ash, wood waste ash, and corn cob ash. Mineral additions in partial replacement to PC present advantages such as reduced energy consumption, CO_2 emissions, and a reduction in concrete production cost. The slag and FA partially replace PC by up to 90%, reducing CO_2 emissions by 81%, reducing 58% of energy consumption, decreasing 5% of its cost, and increasing the average durability index by 34% [23]. The combined use of RA and FA for the new concrete production is one of the ways to obtain concrete focused on sustainability. Studies show that the addition of FA in partial replacement to PC tends to delay the development of concrete resistance because, according to Mehta [24], the FA keep in an induction period due to a waterproof film that is formed around its surface when the FA oxides come into contact with $Ca(OH)_2$ and water, making it difficult to access the innermost oxides. However, studies also show that there is an interaction between FA and RA in concretes, where silicon dioxide (SiO_2) from FA reacts with existing particles of CA (OH_2) from CRA [25] and, according to Corinaldesi and Moriconi [26], the FA also benefits from the calcium oxide (CaO) unhydrated from the old CRA paste to produce more C-S-H, which is the main contributor to the development of concrete strength. Sunayana and Barai [27] made concrete with 50% CRA, two levels of FA (20% and 30%), and a w/b 0.50 ratio. The compressive strength at 28 days of RC was 43 MPa, and the concretes with 20% and 30% of FA presented 41 and 42 MPa, respectively. Similar behavior was also observed by da Silva and de Oliveira Andrade [28], considering the interaction between MRA and FA. According to the authors, the mechanical properties are similar to the reference concrete at higher ages [29].

Studies have shown that FA in concrete with RA tends to reduce carbonation resistance and, according to Geng e Sun [30], this behavior is associated with a reduction in the amount of PC due to the addition of FA causes the alkalinity of the pore solution to decrease and consequently tends to increase the carbonation depth. The increase in the carbonation rate is also associated with the reduction of CaO in the cement matrix, which leads to a decrease in the pH of the concrete [31]. However, in older ages, the pore's pozzolanic reaction of the FA in the pores contributes to reducing the carbonation speed [28]. However, the addition of hydrated lime (HL) in cement paste with FA (residue used in this study) increases the effect on cement hydration kinetics and the degree of reaction of this residue, which, in turn, alters the microstructure of the hydrated matrix [32]. The influence of HL on the reaction of the FA is closely linked to the immediate availability of $Ca(OH)_2$ for the reaction with the HL. The HL contributes to increasing the concentration of $Ca(OH)_2$ in concrete [33][34], and prospects anticipate the start of pozzolanic activity [35]. The HL contributes to the beginning of the reaction of the FA, and HL is an accelerator of the hydration kinetics of PC due to the supersaturation of calcium ions in a solution that occurs in less time and causes the fraction of inert material existing in the composition of HL acts physically in the hydration of cement as a nucleating agent due to high fineness and specific area of these particles [32].

Valcuende et al. [36] observed that, at ages greater than 7 days, HL reacts with the FA giving rise to new calcium silicate hydrates (C-S-H), resulting in higher compressive strengths when compared to the reference concrete (RC). At 180 days, the concretes 50%FA+20%HL, 50%FA+10%HL and 50%FA+0%HL presented compressive strength 5%, 14%, and 26% lower when compared to the RC. However, the compressive strength of the concretes 50%FA+10%HL and 50%FA+20%HL was 11% and 18% higher when compared to the concrete 50%FA+0%HL at 360 days. Similar results were also observed by Lorca et al. [33] and, according to the authors, the increase of compressive strength of the concretes with FA and HL is due to the acid-base self-neutralization of the matrix using the pozzolanic reaction of the FA with the $Ca(OH)_2$ of PC and HL.

Gunasekara et al. [37] produced concrete with 35% PC, 52% FA, and 13% HL and concrete with 20% CP, 62% FA, and 18% of HL. The authors observed an increase in compressive strength, between 7 and 28 days, in the RC of 15.90%, in the concrete 30%CP+52%FA+13%H of 41.45%, and the concrete 20%CP +62%FA+18% LH of 50.85%. According to the authors, the concretes with FA and HL presented a continuous hydration reaction. The pozzolanic activity where HL exists is characterized by the alteration of the microstructure of the paste over time due to the refinement of the pore diameter that directly affects the properties of the paste, such as permeability, diffusion, and capillary absorption, among others [32]. Gunasekara et al. [37] analyzed the RC microstructure, concrete 35%CP+52%FA+13%HL, and concrete 20%CP+62%FA+18%HL. The RC, at 7 days, presented a few grains of anhydrous cement in the matrix, and at 28 days, a denser and uniform C-S-H gel matrix was observed. The concretes 35%CP+52%FA+13%HL and 20%CP+62%FA+18%HL, at 7 and 28 days, presented a more heterogeneous microstructure, with many particles that did not react or partially reacted. According to the authors, this justifies the lower compressive strength early. Adding HL in concrete should accelerate the dissolution of the FA particles, providing extra nucleation locations. The microstructural of the concretes analyzed by Lorca et al. [33] is what is observed by Gunasekara et al. [37]. The authors performed the RC microstructural analysis, concrete 50%FA+0%HL, and concrete 50%FA+20%HL. According to the authors, the RC presented a dense matrix and formation of hydration product. The concrete 50%FA+0%HL presented spherical particles with smooth surfaces without reacting. The authors suggest that the FA that has not yet reacted is either due to the insufficiency of portlandite production by cement for a complete reaction, and the macropores observed are due to the lack of formation of hydration products. The concrete 50%FA+20%HL presented a denser dense structure when compared to the concrete 50%FA+0%HL. The combined effect of FA and HL in cementitious systems is quite relevant and deserves special attention for the development of more research.

Considering the carbonation process, Lorca et al. [33] observed that the RC and the concrete with 50% FA replacement, after 360 days of exposure in a natural environment in the laboratory, did not present any carbonation front. Concrete with 50% FA and 20% HL presented an approximately 3 millimeters carbonation front. The same levels of FA and HL were used by Hoppe Filho [38] to analyze the carbonation depth over 20 weeks. According to the author, the carbonation depth of the concrete with 50% FA was twice more significant than the RC. The addition of 20% of HL in the concrete with 50% of FA in partial replacement of PC showed little efficiency in reducing the thickness of carbonates under accelerated conditions. The carbonation coefficient of the RC is 50% lower than the carbonation coefficient of the concrete with 50% of FA. The addition of 20% FA showed a slight improvement in the carbonation coefficient of approximately 5% compared to concrete with only FA. According to the author, concrete with high ash content fly ash requires caution. The evolution of hydration reactions in a natural environment is slow; over the years, many capillary pores have been replaced by mesopores. At older ages, the carbonation coefficient can reduce the difference in about carbonation coefficient of the RC. The objective of this study is to evaluate the effect of the addition of HL at different levels (5% and 10%) on the mechanical (f_c and E_c), physical (water absorption, bulk density and porosity) and durability (carbonation depth) properties of Portland cement concretes with 20% of FA and 50%

of RA. To analyze the microstructure of concrete mortar with HL compared to concrete without HL in order to compare microcrack, porosity and morphology between mortars.

The sustainability of civil construction encourages the incorporation of FA, hydrated lime to produce new Portland cement concrete. Although few up-to-date investigations on these mixtures are available in the literature [39][40][36][32][41], studies on the addition of HL to concrete with FA and RA have not been reported. This study aims to investigate the possible application of HL in concretes with FA and RA, since the reuse of these residues will allow a deceleration in the exploitation of natural resources and a reduction in the emissions of harmful gases to the environment. The addition of HL in the production of concrete with FA tends to improve the properties of these concretes, leading to results close to the reference concretes.

2 Experimental Program

2.1 Materials

2.1.1 Cement, fly ash, and hydrated lime

Concrete was prepared using Brazilian early-age Portland cement, similar to ASTM C 150 III, with a mean compressive strength at 28 days of 54.1 MPa. The FA (Class F - ASTM C 618) used in this experiment comes from a thermoelectric plant located in the city of Candiota (Brazil). Before the FA mixture was sieved in sieve no. 200 as recommended by Chindaprasirt [42]. According to the author, FA with a greater surface area is more reactive, and there is also less water due to its spherical shape with a smooth surface. The other positive factor is the ability to fill the voids leading to an increase in density. The HL used in this study was obtained commercially. The determination of the specific mass (g/cm³) of the binders was obtained through the Brazilian standard NBR 16605 [43]. The physical characteristics of the materials are presented in Table 1.

Table 1: Particle size distribution of binders used

Binder	$Ø_{10}$ (µm)	$Ø_{50}$ (µm)	$Ø_{90}$ (µm)	$Ø_{medium}$ (µm)	Specific surface (g/cm³)	bulk density (g/cm³)
Cement	2.60	11.34	29.84	14.16	3.07	1.03
Fly ash	6.40	34.94	97.77	44.85	2.09	0.83
Hydrated lime	1.92	7.06	19.31	47.09	2.43	0.63

The semiquantitative chemical analysis of Portland cement, FA, and HL was obtained with the X-ray Fluorescence Spectrometer, PANalytical model Axios Max. The results are presented in Table 2.

Table 2: X-ray Fluorescence for materials used (% by mass)

	SiO_2	Al_2O_3	CaO	MgO	K_2O	SO_3	Na_2O	L.O.I
Cement	19.45	4.86	64.44	0.62	0.7	2.94	0.2	0.78
Fly Ash	61.3	19.3	6.00	1.2	2	0.4	0.2	0.99
Hydrated lime	4.25	0.15	42.38	26.51	-	-	-	27.52

LOI = Loss of ignition

The results of X-ray diffraction (XRD) showed that the FA shows the presence of a significant quartz crystalline phase, as well as other authors [28][44][42]. $Ca(OH)_2$ content was the highest according to the XRD analysis results observed by Hoppe Filho [38]. In the area located between 18 and 28° 2Θ, it is possible to observe an amorphous halo (Figure 1).

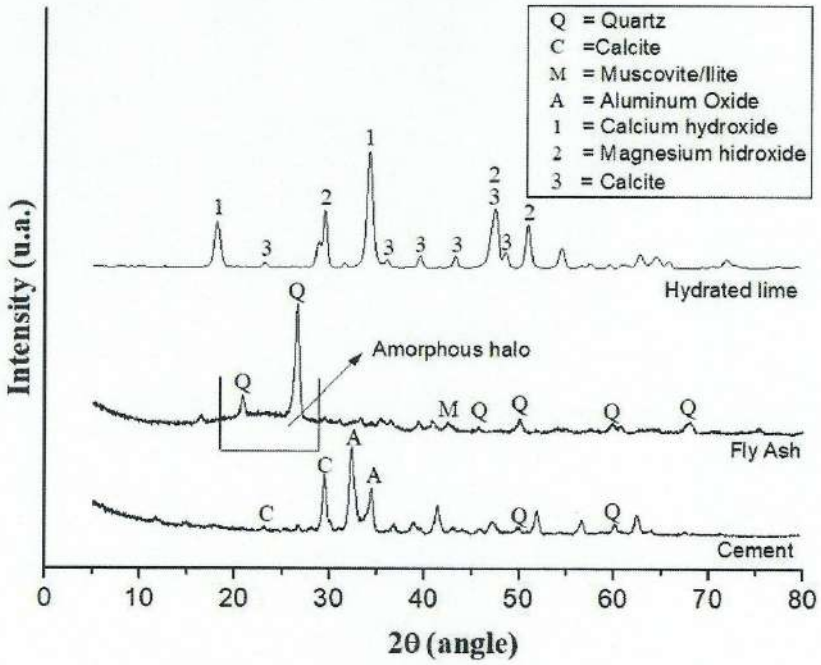

Figure 1: X-ray diffraction (XRD) from PC, FA, and HL samples

2.1.2 Aggregates

The natural coarse aggregate is of basaltic origin, and the sand used presents siliceous compounds. The CRA was obtained from the crushing of concrete specimens, and the MRA comes from a recycling plant located in the municipality of Porto Alegre (Brazil). The results of the physical characterization of the aggregates were obtained based on Brazilian standards, as shown in Table 3.

Table 3: Characterization of the aggregates

Aggregate type	Specific gravity (g/cm^3) NBR NM 52:53/2009	bulk density (g/cm^3) NBR NM 45/2006	Fineness modulus NBR NM 248/2003	Maximum size (mm) NBR NM 248/2003	Water absorption (%) NBR NM 30/2001
Sand	2.3	1.61	2.76	4.75	0.98
NA	2.81	1.42	6.96	19	0.82
MRA	2.51	1.25	6.84	19	5.23
CRA	2.57	1.04	6.87	19	2.42

Where NBR = Brazilian technical standard; NA = Natural coarse aggregate; MRA = Mixed recycled aggregate; CRA = Concrete recycled aggregate;

The CRA and MRA present old mortar adhered to its surface, which leads to a greater absorption capacity due to its porosity [10]. Similar results in MRA water absorption were observed by Kou e Poon [47], Leite et al. [48], and da Silva e de Oliveira Andrade [28], which was 5.34%, 5.5%, and 5.23%, respectively. Alexandridou et al. [49] found results in two samples from different recycling plants, from 2.4% e 3.1% for CRA samples similar to that used in this research. The particle size distribution of the coarse aggregates (NA, MRA, and CRA) and sand is presented in Figure 2.

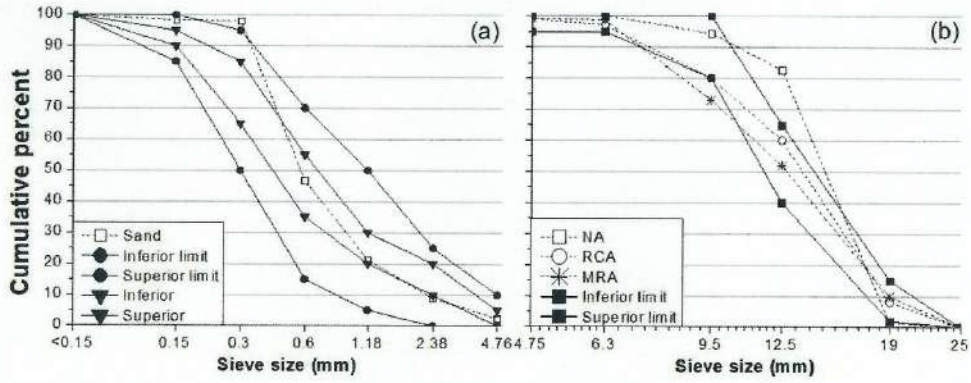

Figure 2: Particle size distribution: (a) Sand; (b) NA = natural aggregate, CRA = concrete recycled aggregate, MRA = mixed recycled aggregate

To prepare MRA for use as a coarse aggregate was necessary to remove heterogeneous materials such as glass, plastics, papers, woods, metals, and rubbers. After removing impurities, the MRA and CRA underwent crushing using the crusher with three simultaneous sieves (19, 12.5, and 4.8 mm). After crushing, 1 kg of each RA type was separated, and the classification was performed as shown in Table 4.

Table 4: RA compositions

Composition	MRA (%)	CRA (%)
Brick	28.81	0
Ceramic	4.99	0
Stone	9.26	12
Mortar	44.67	31
Mortar + Stone	8.81	81
Mortar + Brick	3.16	0
Others (paint, wood, plastic)	0.30	0

Where MRA = Mixed recycled aggregate; CRA = Recycled concrete aggregate

2.2 Experiment design

The experimental program was developed in two stages. The first stage elaborates a mix proportioning diagram for concretes with MRA and CRA. Based on the mix proportion diagram, a w/c ratio was fixed to define the concrete mixtures for the development of the second stage. Four mixes proportioning with different coarse aggregates (RC, MRA, and CRA) were elaborated, and the mix proportioning for reference concrete (with NA) is presented in Table 5.

Table 5: Mixing concrete with NA

Mass	Proportion	w/c	C (kg/m³)	Aggregates (kg/m³)	
				Sand	Coarse
2.5	1:0.86:1.65	0.35	631	543	1041
3.5	1:1.39:2.12	0.45	487	677	1032
5	1:2.18:2.82	0.55	369	804	1041
6.5	1:2.98:3.53	0.65	298	888	1052

Consistency was determined using the Brazilian standard NM 67 [50]. The consistency class adopted was Class S100, with values between 100 and 160 mm, according to the Brazilian standard NBR 7212 [51]. Dry material (cement and aggregates) was measured in mass, and the mortar content was fixed as 55% for all concretes. For the construction of the concrete mix proportion diagram with recycled aggregate (MRA and CRA), the base of the proportions was used (Table 6), and RA replaced the NA at the levels 25, 50, 75, and 100%. Due to the difference in the specific mass between the NA and RA, the volume compensation method suggested by Leite et al. [48] and used by Lovato et al. [52] and da Silva et al. [53] was used based on Equation 1.

$$M_{RA} = M_{NA} \times \frac{\gamma_{RA}}{\gamma_{NA}} \quad (1)$$

Where: M_{RA} = recycled aggregate mass, in kg; M_{NA} = natural aggregate mass, in kg; γ_{RA} = recycled aggregate bulk density, in kg/dm³; γ_{NA} = natural aggregate bulk density, in kg/dm³. The RA was mixed in the saturated with a dry surface to avoid water absorption due to their high porosity, as recommended by some authors [28][54]. The concretes mixtures for concretes with CRA are presented in Table 6.

Table 6: Mix proportion concrete with CRA

CRA content	Mass	Proportion* (C:S:NA:CRA)	w/c	C (kg/m³)	Sand (kg/m³)	Coarse aggregates (kg/m³)	
						NA	CRA
25%	2.5	1:0.86:1.23:0.36	0.35	601	517	739	186
	3.5	1:1.39:1.59:0.47	0.45	486	418	773	196
	5	1:2.18:2.12:0.63	0.55	369	317	782	200
	6.5	1:2.98:2.64:0.79	0.65	296	255	781	201
50%	2.5	1:0.86:0.82:0.73	0.35	609	524	499	382
	3.5	1:1.39:1.06:0.94	0.45	471	405	499	381
	5	1:2.18:1.41:1.25	0.55	357	307	503	384
	6.5	1:2.98:1.76:1.56	0.65	288	248	507	386
75%	2.5	1:0.86:0.41:1.09	0.35	590	507	242	553
	3.5	1:1.39:0.53:1.41	0.45	471	405	250	571
	5	1:2.18:0.71:1.88	0.55	356	306	253	576
	6.5	1:2.98:0.88:2.34	0.65	284	244	250	572
100%	2.5	1:0.86:0.00:1.46	0.35	584	502	0	733
	3.5	1:1.39:0.00:1.88	0.45	450	387	0	728
	5	1:2.18:0.00:2.50	0.55	355	305	0	763
	6.5	1:2.98:0.00:3.13	0.65	284	244	0	764

*Where: C = cement, S = sand, NA= natural coarse aggregate and CRA = recycled concrete aggregate

Based on the compressive strength results at 28 days of the concrete with CRA, the mix proportioning diagram was elaborated, as shown in Figure 3.

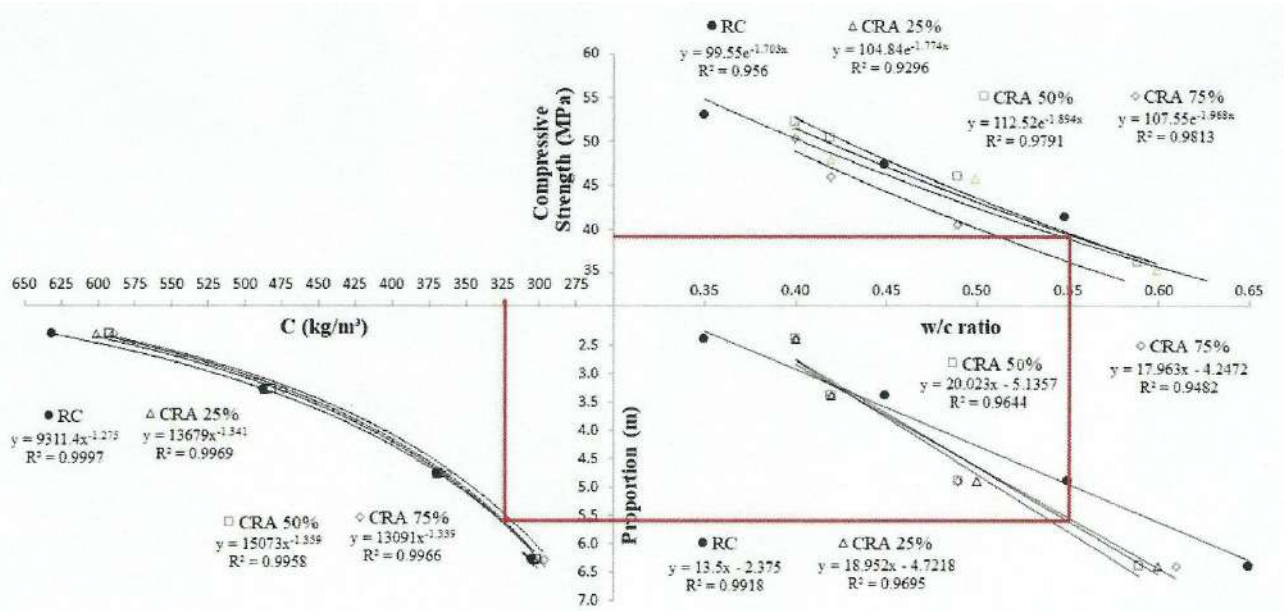

Figure 3: Mix proportioning diagram for concretes with CRA

The concrete mix proportion with MRA is shown in Table 7, and the mix proportion diagram is presented in Figure 5.

Table 7: Mix proportion concrete with MRA

MRA content	Mass	Proportion* (C:S:NA:MRA)	w/c	C (kg/m³)	Sand (kg/m³)	Coarse aggregates (kg/m³)	
						NA	MRA
25%	2.5	1:0.86:1.23:0.35	0.35	612	526	753	184
	3.5	1:1.39:1.59:0.46	0.45	481	414	765	190
	5	1:2.18:2.12:0.61	0.55	369	317	782	194
	6.5	1:2.98:2.64:0.76	0.65	293	252	774	192
0%	2.5	1:0.86:0.82:0.71	0.35	609	524	499	372
	3.5	1:1.39:1.06:0.92	0.45	471	405	499	373
	5	1:2.18:1.41:1.22	0.55	357	307	503	375
	6.5	1:2.98:1.76:1.52	0.65	288	248	507	376
75%	2.5	1:0.86:0.41:1.06	0.35	590	507	242	538
	3.5	1:1.39:0.53:1.38	0.45	471	405	250	559
	5	1:2.18:0.71:1.83	0.55	356	306	253	560
	6.5	1:2.98:0.88:2.28	0.65	284	244	250	557
100%	2.5	1:0.86:0.00:1.43	0.35	584	502	0	718
	3.5	1:1.39:0.00:1.83	0.45	450	387	0	708
	5	1:2.18:0.00:2.44	0.55	355	305	0	745
	6.5	1:2.98:0.00:3.05	0.65	284	244	0	745

*Where: C = cement, S = sand, NA = natural coarse aggregate and MRA = mixed recycled aggregate;

concretes with 50% CRA.

Similar behavior was also observed by Hoppe Filho [38]. The author observed that the increase in the f_{c91} of the concretes with 50% of FA in partial substitution to the PC and 20% of addition HL for the w/c 0.50 ratio was 12.29% higher than the concrete without HL. According to the author, the increase of f_c in concretes with FA and HL is associated with higher $Ca(OH)_2$ content, which increases the degree of FA reaction by pozzolanic activity. A similar trend was observed by Valcuende et al. [36] when analyzed concrete with 50% addition of FA in partial replacement to the PC and addition of 10% and 20% HL without RA. Concrete with 20% HL showed an increase of 29.73% in f_{c28} than concrete without HL. According to the authors, this increase in f_{c28} is due to the participation of HL in the FA pozzolanic reaction due to the formation of new calcium silicate hydrides (C-S-H).

Compressive strength compared to each concrete mixture between 63 and 28 days old allows for analysis of the rate of compressive strength development in a period, as shown in Figure 6. The growth rate of RC concrete was 1.03. When CRA was incorporated), the growth rate was 30% higher than reference concrete (RC).

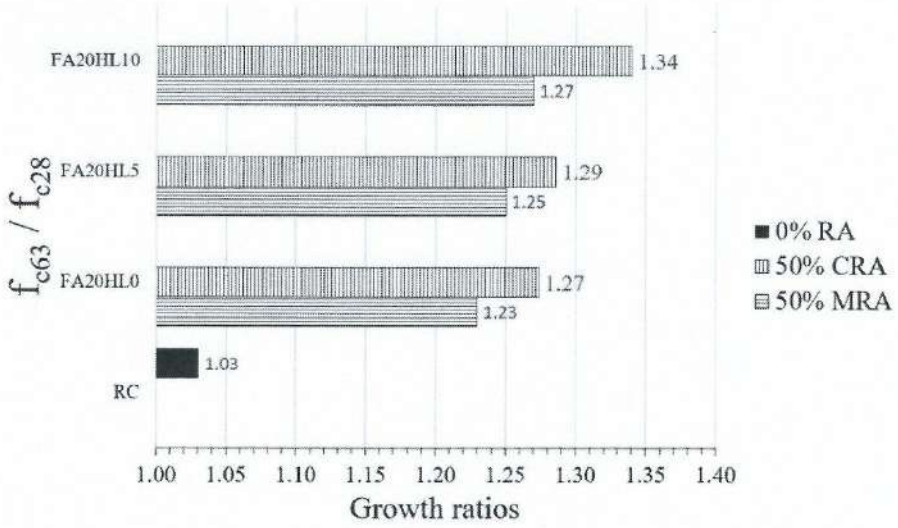

Figure 6: Relationship between 63-days-old concretes and 28-days-old concrete.

According to Lorca et al. [33], the FA reacts with the cement hydration product's $Ca(OH)_2$. The authors also noted that the role played by the added HL will depend on the proportion of PC and the FA because, according to the results obtained by authors, the addition of 40% HL in concrete with 20% FA showed a drop in compressive strength of 6.7% compared to concrete with 20% HL addition. Accordinig Lorca et al. [33], adding 40% HL in concrete with 20% FA showed the need to increase water demand in fresh conditions. This statement corroborates what was observed by Hoppe Filho [32]. Another very relevant factor is the chemical composition of the FA in question. Mira et al. [68] observed that adding 25% HL in concrete with 20% FA did not improve compressive strength because, according to the authors, the FA used in the study contained high calcium oxide (CaO) in its composition content.

3.2 Elastic modulus (E_c)

This item presents the E_{c28} results for concretes with 50% of RA (MRA and RCA) and 20% of FA, varying only the HL amount. The results of elastic modulus at 28 days old (E_{c28}) are presented in Figure 7.

Table 9: Mix proportions for concretes with RA, FA, and HL

Mixes	Proportion*	Binders (kg/m³)			Aggregates (kg/m³)			
		C (kg/m³)	FA	HL	Sand	NA	MRA	CRA
RC	1:0:0:2.40:3.02:0	355	0	0	852	1072	0	0
FA20HL0	0.8:0.2:0:2.40:3.02:0	363	73	0	1045	1316	0	0
MRA50FA0HL0	1:0:0:2.21:1.42:1.19	360	0	0	796	511	428	0
MRA50FA20HL0	0.8:0.2:0:2.21:1.42:1.19	368	74	0	976	627	526	0
MRA50FA20HL5	0.8:0.2:0.06:2.21:1.42:1.19	368	74	22	976	627	526	0
MRA50FA20HL10	0.8:0.2:0.12:1:2.21:1.42:1.19	368	74	44	976	627	526	0
CRA50FA0HL0	1:0:0:2.64:1.61:1.38	324	0	0	855	522	0	447
CRA50FA20H0L0	0.8:0.2:0:2.64:1.61:1.38	331	66	0	1049	639	0	548
CRA50FA20H0L5	0.8:0.2:0.06:2.64:1.61:1.38	331	66	20	1049	639	0	548
CRA50FA20H0L10	0.8:0.2:0.12:2.64:1.61:1.38	331	66	40	1049	639	0	548

*Cement: Fly Ash: HL: Sand: NA: MRA or CRA

To ensure an equal mixing method for all concretes, the mixture of binders (PC, FA, and HL) was first adopted for 5 s. After mixing, the binders and sand were inserted and mixed for 10 s. After this time, the aggregate was inserted and mixed for more than 10 s. After 25 s of the mixture, 80% of the mixing water was added and mixed for another 45 s. After the 45 s, the RA was added and mixed for another 15 s. The tests performed, specimens' amount, age of the tests for each mixture, and the Brazilian standards used are presented in Table 10.

Table 10: Mechanical and physical test methods

Property	Tests	Brazilian standard ABNT	Specimens	Amount	Age (days)
Mechanical	Compressive Strength	NBR 5739 [61]	cylindrical (10×20 cm)	3 3 3	7 28 63
	Elastic Modulus	NBR 8522 [62]	cylindrical (10×20 cm)	3	28
Physical	Water absorption and porosity	NBR 9778 [63]	cylindrical (10 × 20 cm)	2	28
	Carbonation Depth	The procedure adopted by da Silva and de Andrade [53]	prismatic (10 × 10 × 30 cm)	2	Reading up to 110 days
	Scanning electron microscopy	Specific procedure	Pieces (2-5 mm)	2	63
	Microtomography	Specific procedure	Cubes (2.5-2.5 inches)	2	63

2.4 Methods

2.4.1 Accelerated carbonation test

After 28 days of curing submerged in water, the prismatic specimens were introduced into a carbonation chamber with an internal concentration of CO_2 equal to 3% at room temperature. The chamber's internal pressure is equivalent to atmospheric pressure, and the relative humidity varies

between 65% and 75% manually controlled by water spray. To verify the evolution of carbonation, front a phenolphthalein solution with a concentration of 1% dissolved in 70% of ethyl and 30% dissolved aqueous alcohol was sprayed on the fractured surface of the prismatic specimen. The greatest and smallest depths were measured on both sides of each sample to analyze the carbonation depth. The average on each side represents the carbonation depth of the sample. The first reading was performed at 35 days of exposure to CO_2, and the other measures were performed every 35 days for a total of 110 days. Pauletti [64] and Kulakowski [66] proposed the method to determine the carbonation depth.

2.4.2 Scanning Electron Microscopy (SEM)

Scanning Electron Microscopy (SEM) was used to analyze the paste morphology of the concretes with FA and HL, the interface transition zone (ITZ) between the aggregate and the paste. The equipment used energy levels between 0.3 and 30 kV and a point resolution of 1.2 nm. The tests were carried out on concrete specimens at 63 days of wet curing.

2.4.3 X-ray microtomography

The microtomography images provide qualitative and quantitative information about the tested specimens. To quantitatively analyze the voids volume (VOI), each cylindrical sample was electronically cut into 1800 sections. Nine sections were selected, one of the upper extremities and one of the lower extremities, and seven sectors were established in the interval between the upper and lower extremities. To elaborate on the 3D rendering images that show the spatial distribution of the concrete paste pores with FA and HL, a cube was extracted from each size sample of 6.5 × 6.5 × 6.5 mm. The tests were performed on cylindrical samples at 63-day-old. The X-ray microtomography test is used to analyze the voids in concrete specimens [66] and to perform quantitative measurements in the pore system [67].

3 RESULTS AND DISCUSSION

3.1 Compressive strength (f_c)

The results for the compressive strength at 7, 28, and 63-day-old are shown in Figure 5. It can be observed that adding 20% of FA in partial replacement to PC (Figure 5-a) decreases f_c by approximately 32% compared to RC 28-day-old concrete (f_{c28}). However, a slight improvement was observed in concretes with 20% FA when adding HL. Concretes with 20% FA and 5% HL showed an increase in f_{c28} of 6.15% compared to concretes without HL. When adding 10% of HL, the increase in strength in concretes with 20% of FA was 12.47% compared to concrete without HL.

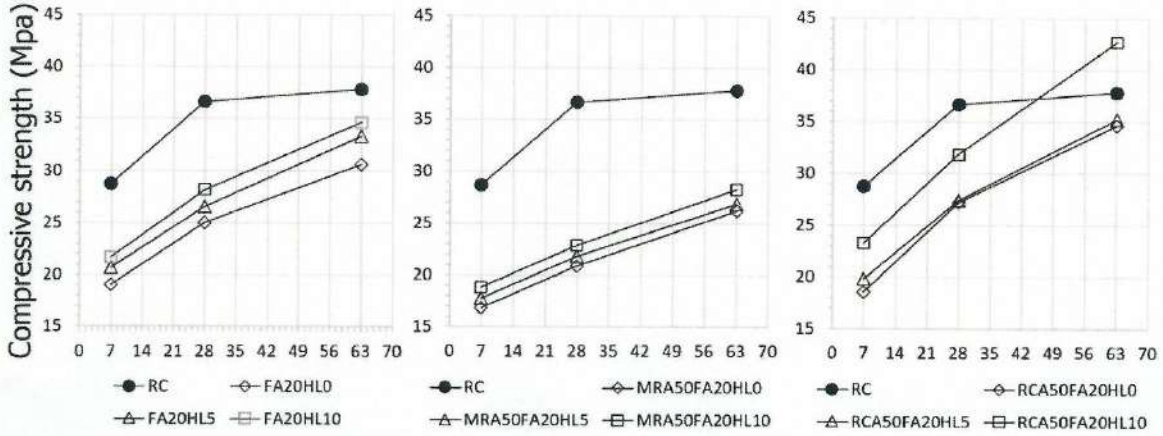

Figure 5: Concretes compressive strength at 7, 28, and 63-day-old, with 20% FA and with the addition of hydrated lime (HL) in proportions of 5 and 10%: (a) concrete without CDW; (b) concrete with 50% MRA; (c)

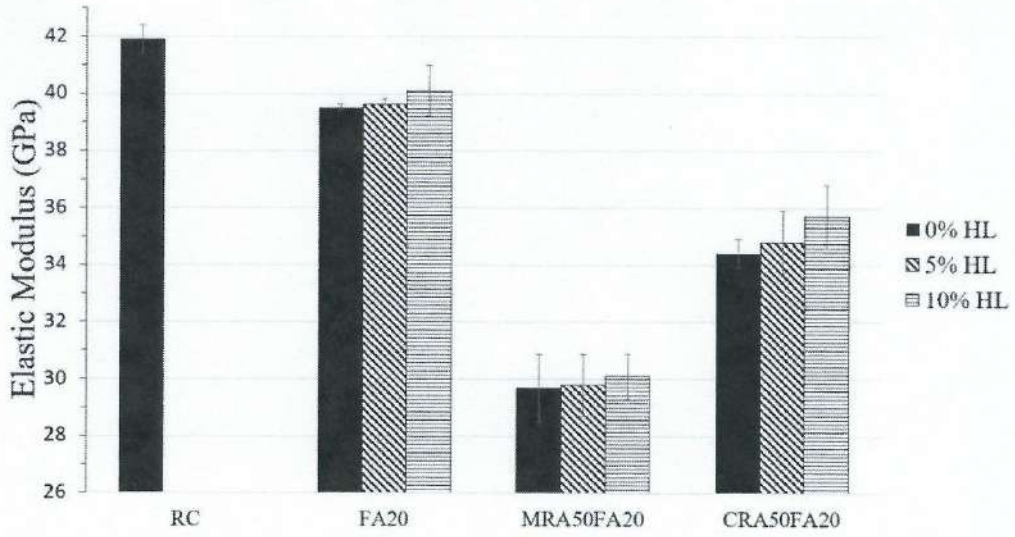

Figure 7: Elastic modulus of concretes at 28-day-old.

The concretes with MRA, FA, and 10% of HL showed an increase in the Ec_{28} of 1% more than concrete without HL, while the concretes with CRA, FA, and 10% HL showed an increase of 4% than concrete without HL. When E_{c28} is compared with RC, the concrete with MRA, FA, and 10% of HL decreased by 39%, and the concrete with RCA, FA, and 10% of HL decreased by 17%. According to Wang et al. [69] , the elastic modulus is influenced by the aggregate stiffness reduction and the aggregates' elastic properties. The transition zone (ITZ) between the paste and the aggregate has a strong influence on the elastic modulus of the concrete [70][71]. The presence of hydration products causes densification of the ITZ due to the slight increase in aluminum and silicon compounds, and the effect of porosity reduction tends to increase the stiffness of the ITZ [72] and corroborates the results obtained in this study.

3.3 Water absorption, porosity and bulk density

Water absorption, porosity, and bulk density are properties that indirectly have a relationship with concrete durability, whose results are presented are presented in Figure 8.

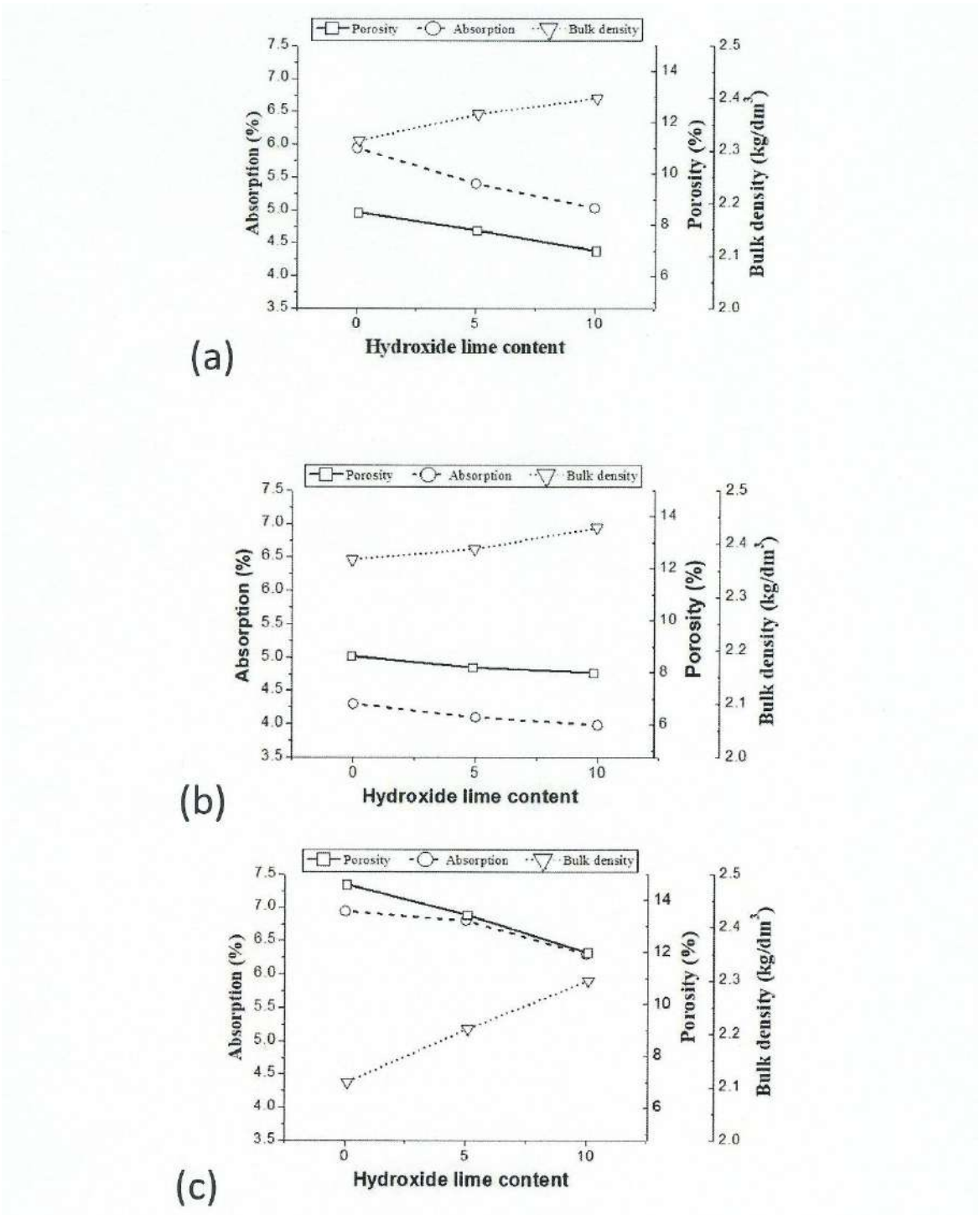

Figure 8: Water absorption, porosity, and bulk density concretes with RA, FA and HL at 28-days-old: (a) Concrete without RA and with 20% FA, (b) Concrete with 50% CRA and 20% FA, (c) Concrete with 50% MRA and 20% FA.

According to the results observed to concretes with 50% of MRA, 50% of CRA and 20% of FA, varying only the HL amount. Concrete with MRA, FA and 10% HL showed a decrease in water absorption of 10.16%, a reduction in porosity of 8%, and an increase in bulk density of 1.79% when

compared to concrete without HL. Concrete with CRA, FA and 10% HL reduced water absorption and porosity by 9.87% and 23.82%, respectively, and increased the bulk density by 8.77% when compared to concrete without HL. By reducing the amount of PC in the mixture due to the addition of FA, the concrete porosity is increased, and the pozzolanic reaction does not influence porosity but reduces the interconnectivity of the pore structure of the paste [73]. The addition of 10% HL showed a slight improvement in the physical properties (water absorption, specific mass, and porosity) of all investigated concretes, as observed by Valcuende et al. [36]. Mira et al. [68] suggest improving physical properties to the acceleration of pozzolanic activity when HL is added. The ettringite formation within the matrix as a function of the HL addition reduces voids and increases the density of paste [34][74][75]. The amount of the paste adhered to the RA directly influences the water absorption capacity of the concretes [28].

3.4 Scanning electron microscopy (SEM)

This section presents the microstructural characteristics for concretes with 50% of MRA and 20% of FA, varying only the HL amount. In Figure 9, for HL0 (a) and L10 (b), it can be observed that MRA contains old paste adhered, the old transition zone between interfaces (ITZ), and micro-cracks due to the crushing process. The identification of the old mortar was made through a visual analysis based on the color of the samples, whose old mortar has a slightly darker color compared to the new mortar.

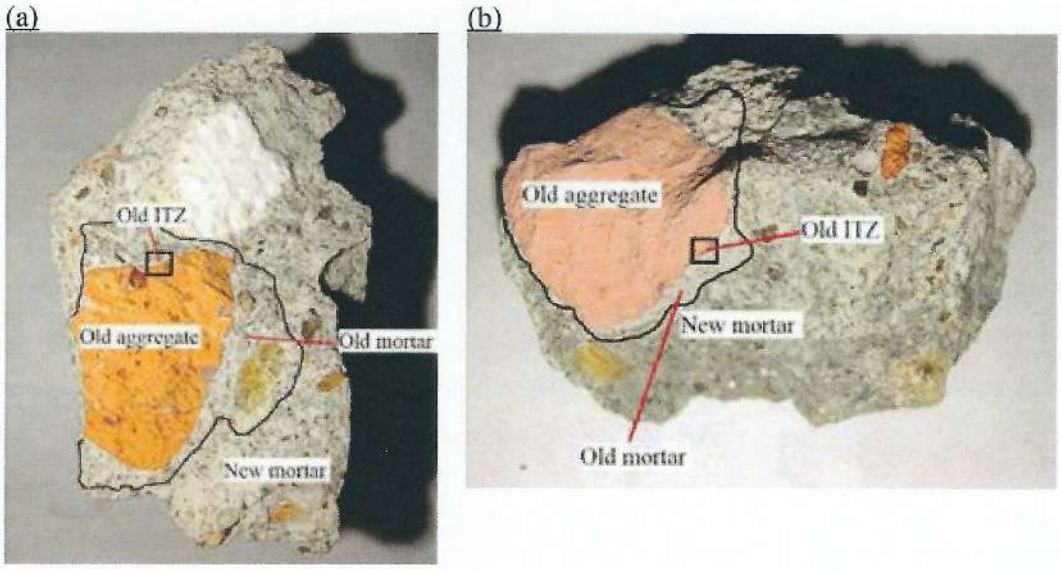

Figure 9: Images of concretes with 50% MRA and 20% of FA: HL0 (a) and HL10 (b) at 63-day-old.

Figure 10 shows the morphology of concrete without HL (a) and concrete with 10% of HL (b) concretes at 63-days-old. It is possible to visualize spherical FA particles that have not yet reacted. According to Mehta [24], FA oxides, when reacting with water and $Ca(OH)_2$, form a layer of C-S-H around the particle, and the pozzolanic reaction becomes slower. For the FA dissolution particle, there is a need for $Ca(OH)_2$ in sufficient concentration for hydroxide ions to activate the amorphous components and initiate the hydration process. Figure 10 shows the thickness measurements of concrete ITZ with MRA, FA, (a) without HL, and (b) with 10% HL.

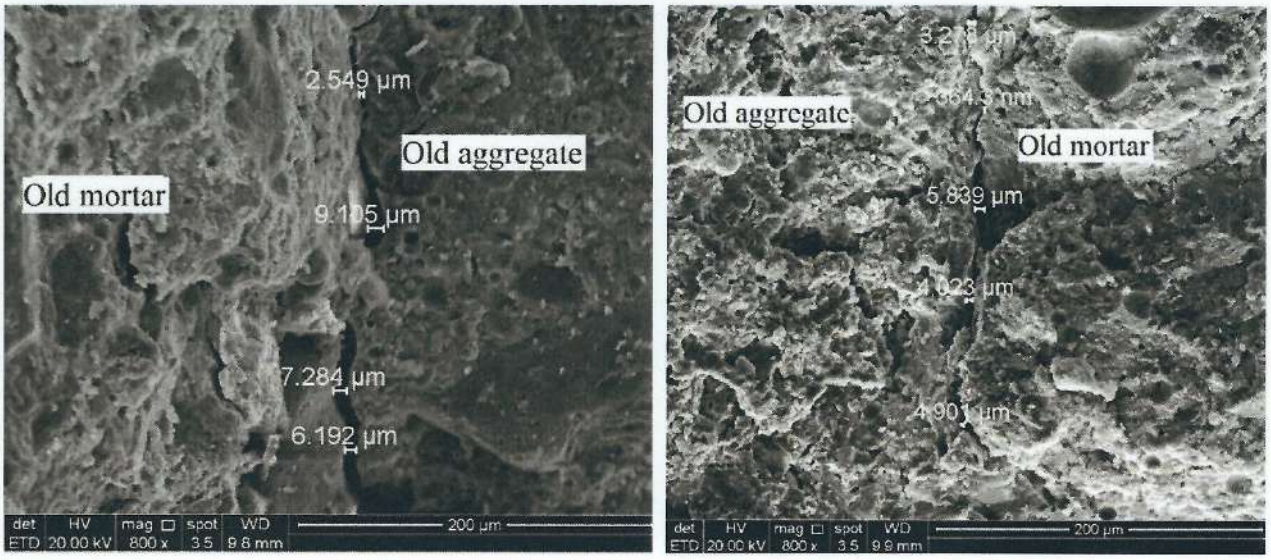

(a) (b)

Figure 10: Scanning electron microscopy micrographs for concretes with 50% of MRA and 20% of FA: HL0 (a) and HL10 (b) at 63-days-old.

Hydrated calcium silico-aluminates are formed in ITZ through the pozzolanic reaction with $Ca(OH)_2$, thus modifying the cement matrix's morphology, improving ITZ's characteristics when FA in concrete [32]. This microstructural modification replaces the $Ca(OH)_2$ with stable hydrates, and the pore refinement occurs, decreasing the capillary network and increase in ITZ density [76]. The mean thickness of the investigated ITZ of the concrete with 50% of MRA and 20% of FA (Figure 11-a) was 6.282 µm, and when 10% of HL was added, the mean thickness (Figure 11-b) was 3.614 µm. It was evidenced that the addition of HL contributed to the decrease in the thickness of the ITZ. This may be related to the early dissolution of FA particles for the formation of secondary C-S-H in regions close to ITZ. As shown in Figure 11-a, concrete without HL showed many spherical FA particles that have not yet reacted as well as a high concentration of micro-cracks and micro-cavities.

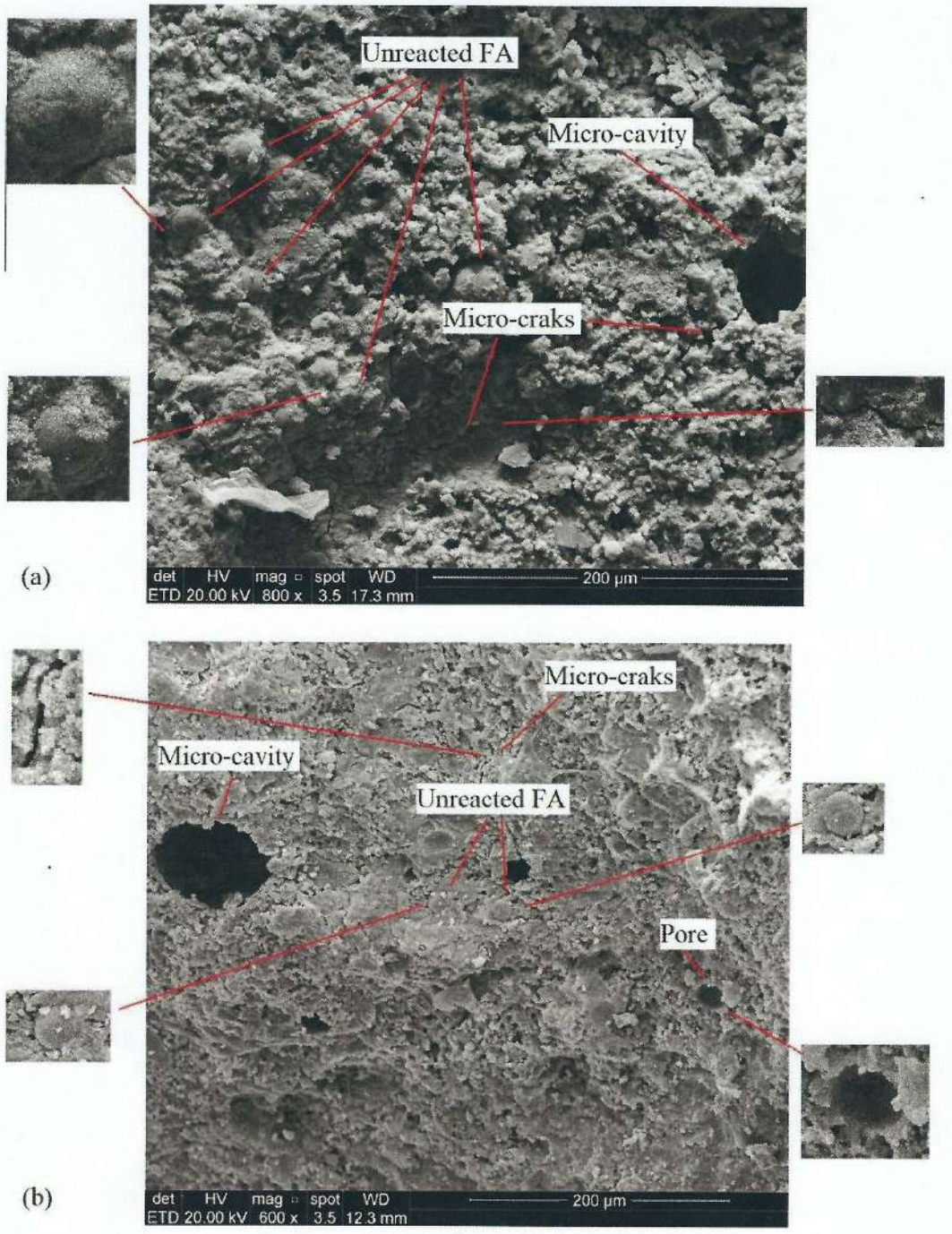

Figure 11: Scanning electron microscopy micrographs for concretes with 50% of MRA and 20% of FA: HL0 (a) and HL10 (b) at 63-days-old.

3.5 Spatial distribution of pores in cement matrices

Based on the method employed by Leite and Monteiro [67], 3D x-ray microtomography images (μ-CT) were saved in a series of slices from samples. Nine sections were selected from each 8.5 × 2.5 cm. The base and top sections were selected, and the other sections were randomly chosen between the bottom and the top. Based on the image intensity of each section, it was possible to determine the porous areas through the color intensity from the images obtained. The equipment used identifies the objects by the intensity of the color that varies from white to black, varying between this range of shades of gray. Objects with intensity 0 are represented by the color black, which corresponds to empty areas, and objects with intensity 1 correspond to areas with higher density. Objects with intensity greater than 0 and less than 1 correspond to areas with densities less than 1. In this way, a binary system can perform a quantitative analysis of the pore distribution of each section. The sum of the pore distribution of all selected sections represents the total pore volume in each sample. Based on the result obtained, it was possible to create histograms of pore's equivalent diameters. The pore structure is classified according to Huang et al. [77] and Ondrášik and Kopecký [78], where nanopores are classified as diameters < 0.05 μm, micropores in the range of 0.05 μm - 100 μm diameters and macropores are larger than 100 μm until 1000 μm diameters. However, the pore structure of the specimens in this study presented only micropores and macropores. This process was carried out through processing software packages to treat images. All empty equivalent to one pixel were eliminated according to the procedure adopted by Lu et al. [79]. According to the authors, the field of view in the tomography system limits the size of the specimen to spatial resolution.

It is possible to observe in histograms presented in Figures 12 and 13 that there is a different distribution between macropores and micropores. Micropores with diameters smaller than 30 μm are observed in greater quantity in RC, a behavior that is not observed in macropores. It is suggested that this behavior is associated with the rearrangement of pores as the pozzolanic reaction occurs because micropores tend to reduce their diameter as a function of the refinement process. The histograms of specimens' concrete with MRA are shown in Figure 12.

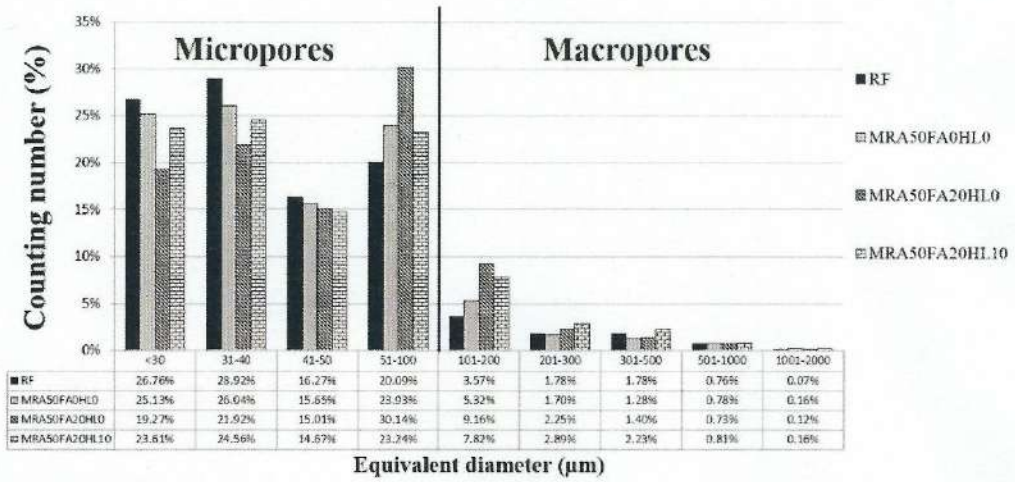

	<30	31-40	41-50	51-100	101-200	201-300	301-500	501-1000	1001-2000
RF	26.76%	28.92%	16.27%	20.09%	3.57%	1.78%	1.78%	0.76%	0.07%
MRA50FA0HL0	25.13%	26.04%	15.65%	23.93%	5.32%	1.70%	1.28%	0.78%	0.16%
MRA50FA20HL0	19.27%	21.92%	15.01%	30.14%	9.16%	2.25%	1.40%	0.73%	0.12%
MRA50FA20HL10	23.61%	24.56%	14.67%	23.24%	7.82%	2.89%	2.23%	0.81%	0.16%

Figure 12: Histogram corresponding to the pore size distribution of concrete mortars with MRA, FA, and HL in prisms with dimensions 6.550 × 6.550 × 6.550 μm at 63-days-old.

According to the results observed to concretes with 50% of MRA and 20% of FA, varying only the HL amount (Figure 12), the number of pores with diameters between 51 and 100 μm of the concretes without HL and concrete with 10% of HL was 30.14% and 23.25% respectively. Concretes showed the highest levels of pore sizes greater than 50μm. Concrete with 10% HL presented 37.15% of pores greater than 50μm, and concrete without HL presented 43.8%. Concrete without HL showed 17.90% more pores greater than 50μm. Pore size greater than 50μm may influence the compressive strength of

concrete. Concrete with 10% HL presented f_{c28} of 22.9 MPa, and concrete without HL presented 20.85 MPa. Leite and Monteiro [67] observed in their studies that macroporous negatively influences the mechanical properties of concrete. The authors observed that the amount of high porosity in concretes with recycled aggregate varied between 32.2% and 48.2% for pores larger than 50 μm, and the compressive strength was 5-8% lower than the reference concrete.

Figure 13-a shows the specimens of size 8.5 × 2.5 cm of MRA50FA20HL0 concrete cut electronically vertically to visualize pore sizes. Figure 13-b shows the dimensions and spatial distribution of the pores of the cubic specimens of the cement paste with a size of 6.55 × 6.55 × 6.55 mm.

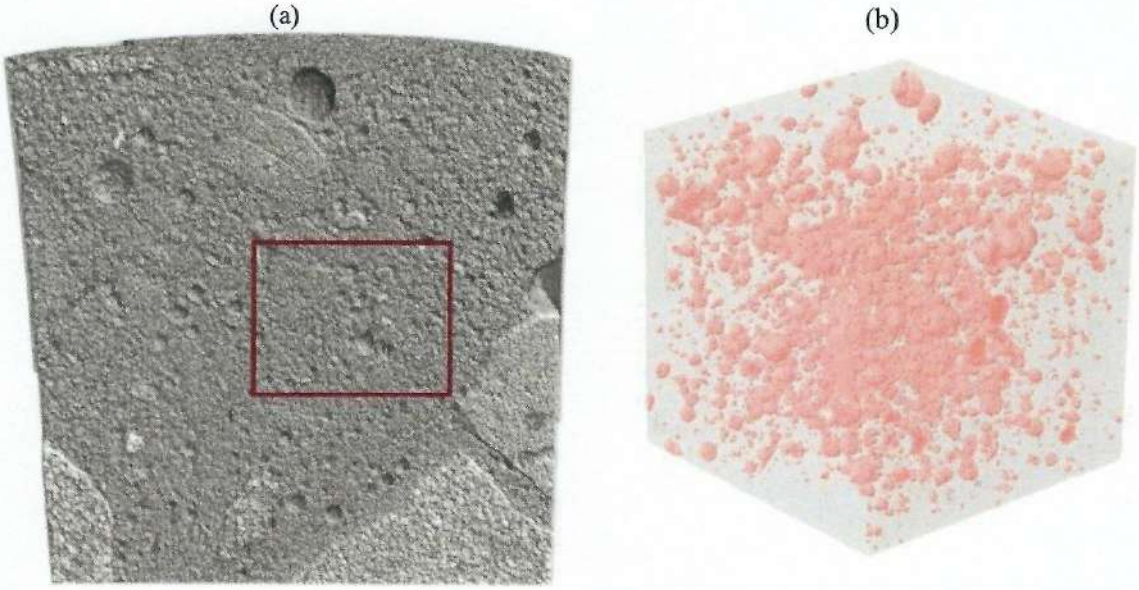

Figure 13: (a) 3D specimens' image of MRA50FA20HL0 concrete, (b) 3D image showing the size and spatial distribution of pores within the new concrete cement matrix MRA50FA20HL0.

The greater amount of pores with large equivalent diameters (>500 μm), according to Leite and Monteiro [67], may be related to the release of water from the inside of the pores of the CRA to the cement paste during the mixing process due to its heterogeneity, thus increasing the water/cement ratio since the CRA was used in the condition saturated with a dry surface (SSD). Figure 14 presents the pore distribution histogram of concrete with CRA, FA, and HL.

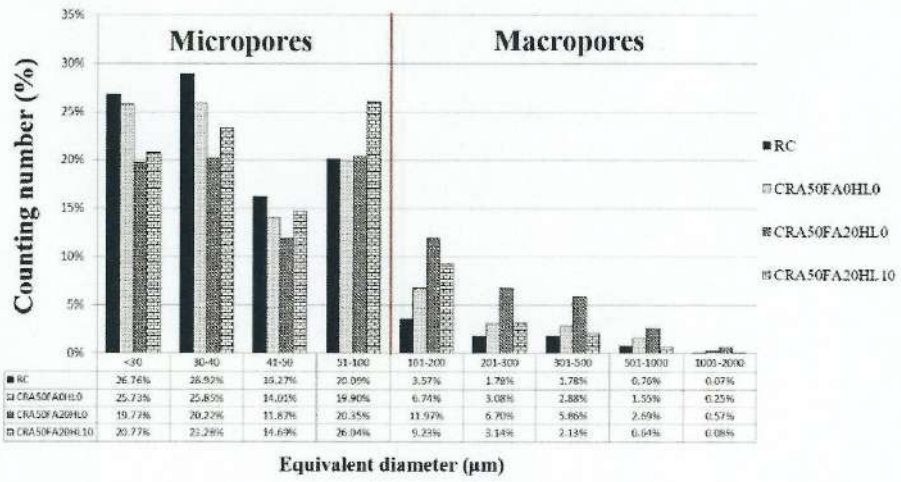

Figure 14: Histogram corresponding to the pore size distribution in prisms of concrete mortars with CRA, FA ash, and HL in prisms with dimensions 6.550 x 6.550 x 6.550 μm at 63 days old.

According to the results observed to concretes with 50% of CRA and 20% of FA, varying only the HL amount, the number of pores with diameters between 51 and 100 μm of the concretes without HL and concrete with 10% of HL was 20.09% and 26.04% respectively. Concrete with 10% HL presented 34.4% of pores greater than 50μm, and concrete without HL showed 41.26%. Concrete without HL presented 19.94% more pores greater than 50μm. Barbhuiya et al. [34] observed through the analysis of mercury intrusion porosimetry a reduction in the percentage of the total volume of pores in mortars with FA and HL, which may also be associated with the reaction product of the FA with HL. Figure 15-a shows the cylindrical specimens of size 8.5 × 2.5 cm of CRA50FA20HL0 concrete in which, in the cutting section, it is possible to visualize the pores. In Figure 15-b shows the cube specimen of size 6.55 × 6.55 × 6.55 mm, and it is possible to visualize the connectivity and tortuosity of pores that, according to Leite and Monteiro [67], can contribute to the propagation of cracks during the loading of the mechanical test. Lu et al. performed a study with microtomography in concretes with active silica, slag, and FA. The authors observed that pore connectivity in FA concrete is higher than in silica fume concrete and slag concrete.

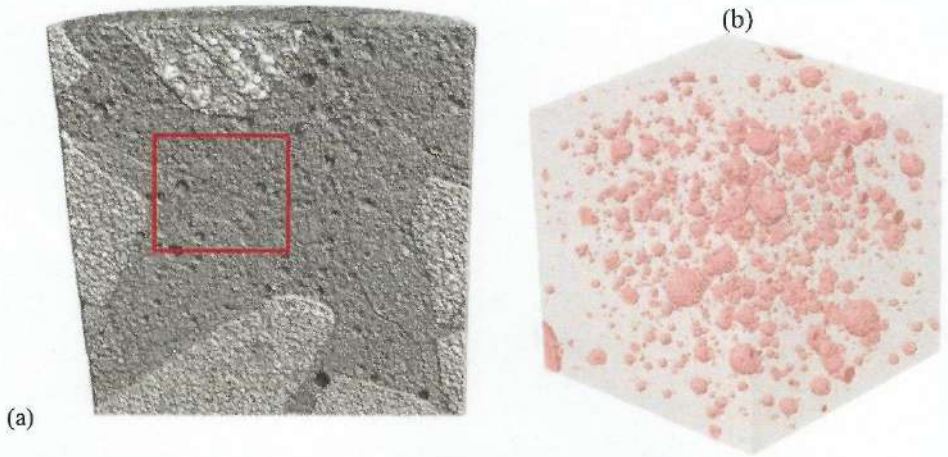

Figure 15: (a) 3D specimens' image of MRA50FA20HL0 concrete, (b) 3D image showing the size and spatial distribution of pores within the new cement matrix MRA50FA20HL0 concrete.

Based on the results, it is evidenced that the addition of HL in concretes with FA and RA influences the refinement of the pores of the concrete since concrete with CRA, FA, and 10% HL showed 19.94% lower than concrete without HL. Concrete with MRA, FA, and 10% HL presented 17.90%

lower than HL concrete. According to Hoppe Filho [32], the interaction between FA and HL does not reduce porosity during hydration. Still, it only refines the microstructure, and the reduction of porosity in pastes with FA depends solely and exclusively on the cement hydration process.

3.6 Carbonation depth

Figure 16 shows the carbonation depth as a function of time for concretes with RA, FA, and HL.

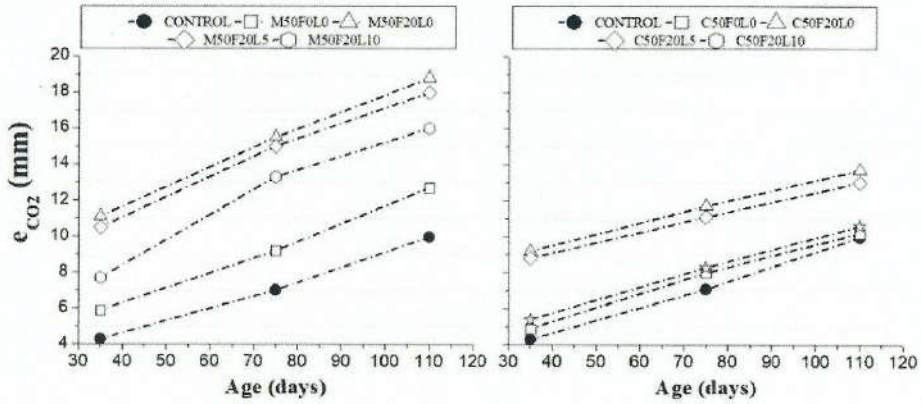

Figure 16: Carbonation depth with different types of recycled aggregate (MRA and CRA).

The effect of HL on carbonation depth is observed in concretes with 50% of RA (MRA and CRA) and with 20% of FA. By adding 10% HL to the concretes with MRA, the carbonation depth decreased to 44.16% at 35 days and 17.5% at 110 days of exposure to CO_2 when compared to concretes without HL. Similar behavior was also observed in concretes with CRA, where the carbonation depth decreased to 10.20% and 3.92% compared to concretes without HL. The carbonation fronts can be seen in Figure 17.

Days	RC	MRA		
		MRA50	MRA50FA20	MRA50FA20HL10
35				
110				
Age (days)	RC	RCA		
		CRA50	CRA50FA20	CRA50FA20HL10

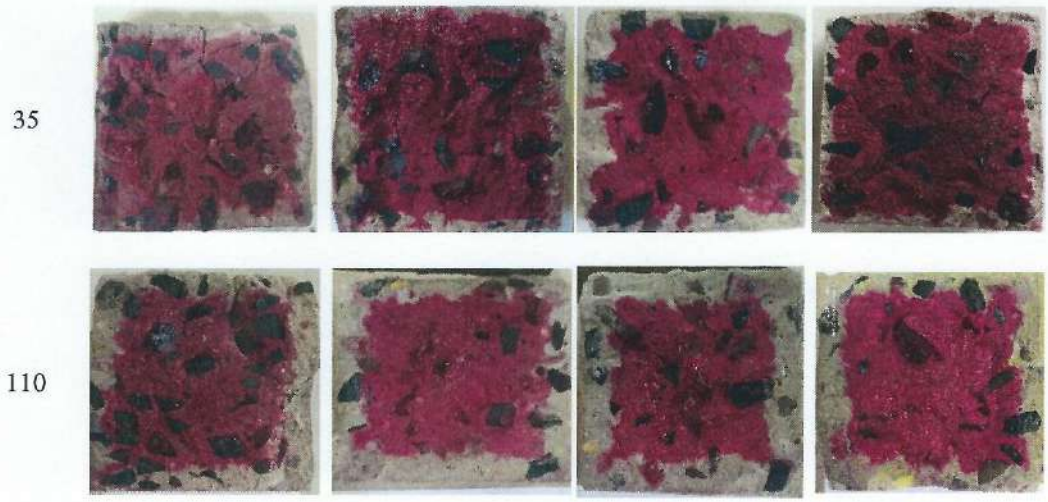

Figure 17: Carbonation front of the concretes with RC, RMA, and CRA with FA and HL at 35-day's-old and 110-days-old.

Recycled aggregates generally have higher permeability [80][81], water absorption and porosity [82][47][49]. Another factor that should be considered is the RA micro-crack due to the crushing process, usually located in the old transition zone (ITZ) between the paste and the aggregate, which is a preferential path for CO_2 diffusion [82]. Adding FA in partial replacement to PC is another factor contributing to the reduction of concrete carbonation resistance. The higher the content of replacing FA with Portland cement, the lower the availability of $Ca(OH)_2$ for the pozzolanic reaction. Thus, the refinement of pores at an early age is compromised while the ash is in the induction phase awaiting $Ca(OH)_2$, a PC reaction product, to react and, consequently, the carbonation speed is high [28][83]. It is evidenced, based on the results obtained in this study, that the 10% addition of HL tends to reduce the carbonation depth in concrete with FA because there will be the anticipation of the production of $Ca(OH)_2$ that contributes to the faster dissolution of these particles and, consequently, an early pozzolanic reaction that contributes to the refinement of pores and the reduction of the carbonation rate. The effect of adding HL in concrete with CRA was more pronounced when compared to the concretes with MRA, which is associated with RA characteristics. The carbonation depth increases as a function of the time in exposure to CO_2. However, according to Fick's second law [84], the carbonation rate tends to stabilize over time, as it corresponds to the square root of this time. The equation is presented in Equation 2.

$$\boldsymbol{X_c = K \times \sqrt{t}} \qquad (2)$$

where Xc = carbonation depth, in mm; K = Carbonation coefficient, in mm/month$^{0.5}$; t = exposure time, in months.

Based on Fick's second law, the relationship between the carbonation coefficient and the time of exposure of samples to CO_2 are shown in Figure 20 (with MRA) and Figure 18 (with CRA).

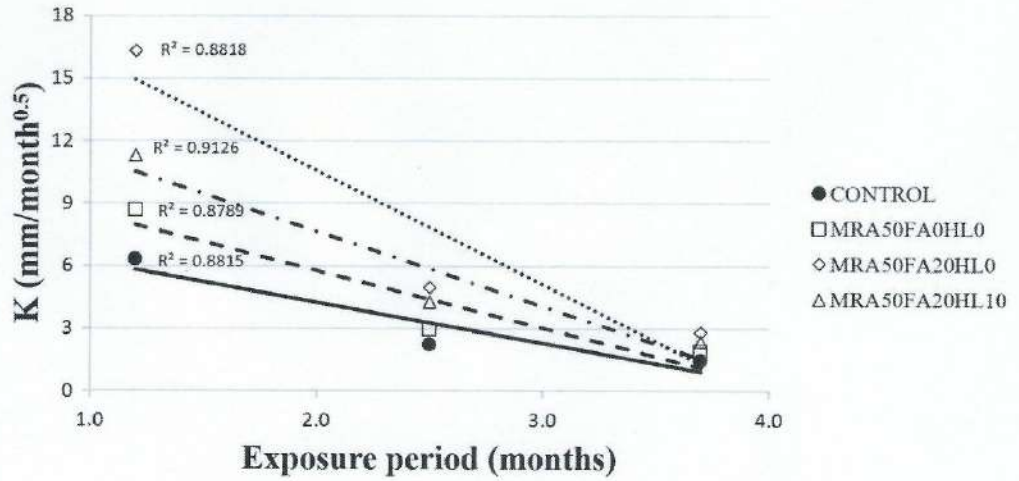

Figure 18: Relationship between K (mm/month$^{0.5}$) with MRA, FA, and HL

Based on the results of the tests, all concretes must present a carbonation coefficient close to the reference coefficient at 110 days of exposure to CO_2. However, in the first 35 days, the MRA50FA20HL0 concrete showed a carbonation coefficient of 158% higher compared to RC. By adding the HL, the concrete MRA50FA20HL10 concrete showed a carbonation coefficient of 44.5% lower compared to the MRA50FA20HL0 concrete. Adding HL in concrete with FA tends to reduce the carbonation coefficient of concrete at an early age. The results for concretes with CRA are shown in Figure 19.

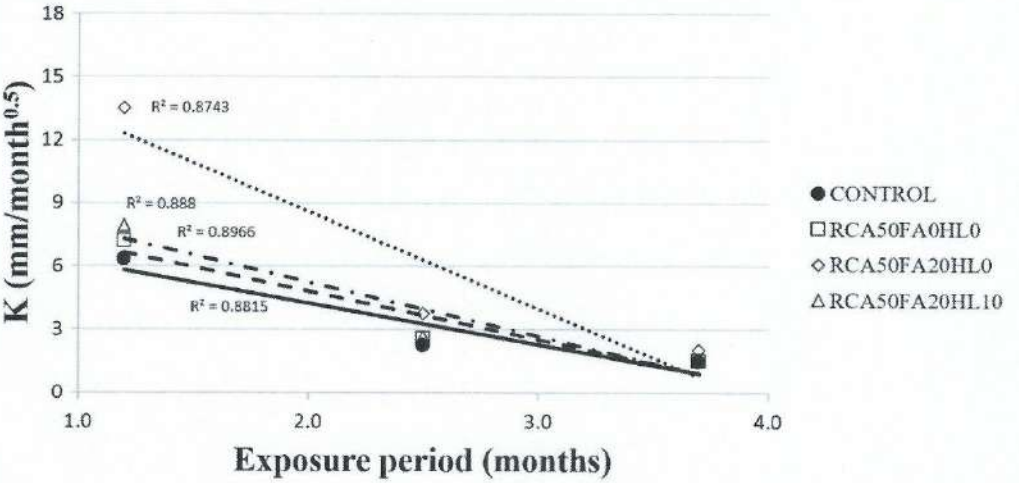

Figure 19: Relationship between K (mm/month$^{0.5}$) with CRA, FA, and HL

The concretes with CRA present similar behavior to those with MRA, which is the reduction of the carbonation coefficient over time. According to Sisonphon and Franke [84], the pore refinement that occurs during the carbonation process, which produces calcium carbonate, partially blocks the pore network of concrete and reduces the gas diffusivity. Consequently, the carbonation coefficient is reduced as a function of time. However, when the CRA has used, the carbonation coefficient of all samples tends to be lower when compared to the samples with MRA in the first 35 days of exposure. This behavior is associated with the physical characteristics of the RA, as already discussed in item 4.3. Based on the above, the RA type influences the carbonation coefficient in concrete with FA with HL.

3.7 Relations between mechanical properties and durability

The correlations between properties (physical and mechanical) are widely discussed in different studies [85][86][87]. The correlations between the physical and mechanical properties of concretes with MRA and CRA are shown in figures 20 and 21.

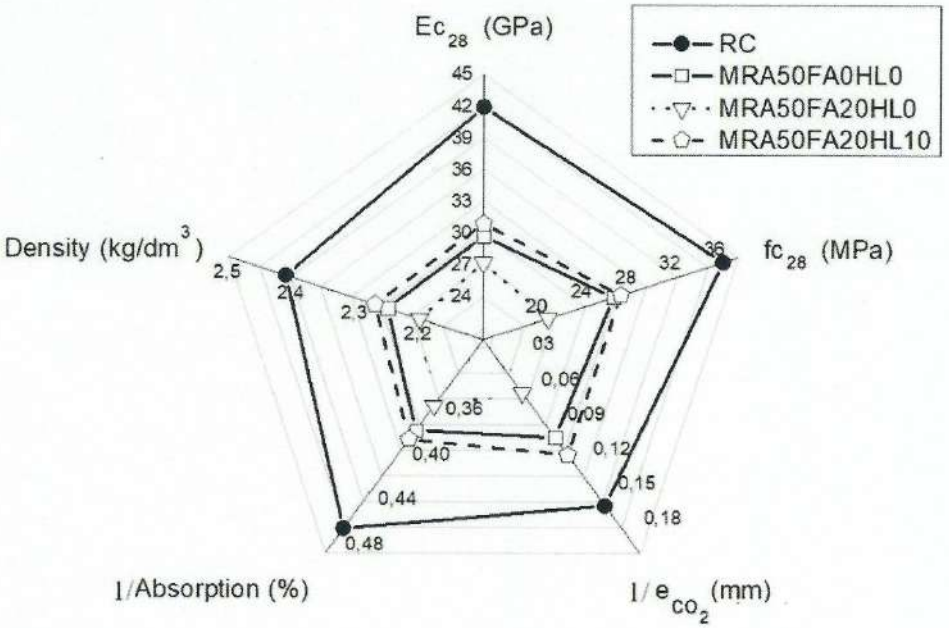

Figure 20: Correlation between the mechanical properties Ec_{28} (GPa), f_{c28} (MPa), and CO_2 (mm), Water absorption (%), and density (kg/dm³) of concretes with MRA, FA, and HL.

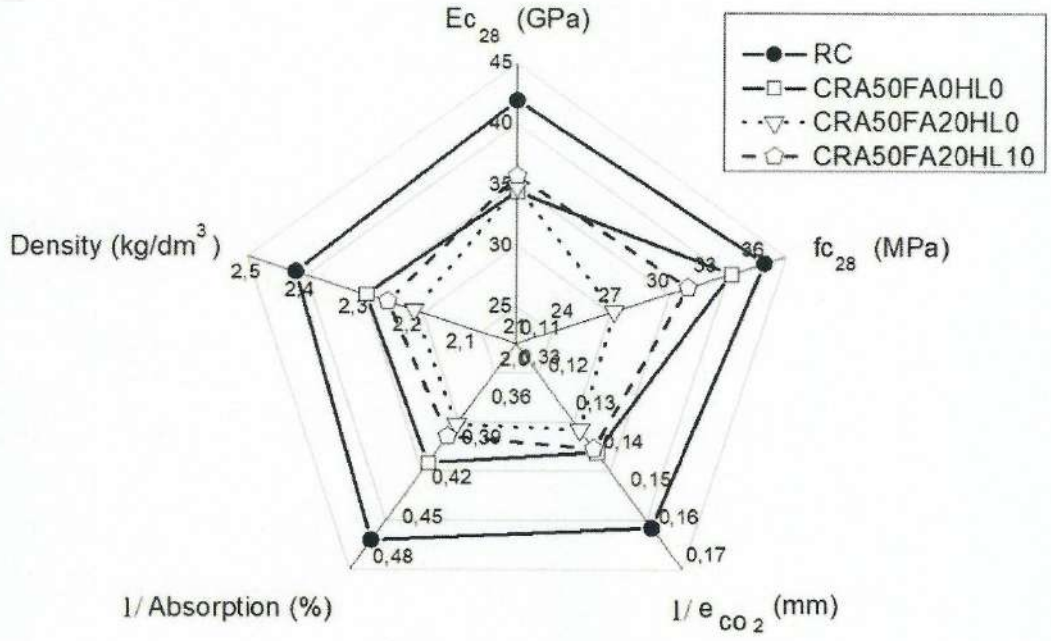

Figure 21: Correlation between the mechanical properties Ec_{28} (GPa), f_{c28} (MPa), and$_{CO2}$ (mm), Water absorption (%), and density (kg/dm³) of concretes with CRA, FA, and HL (all properties are measured at 28 days).

It is observed that the compressive strength (f_{c28}) of MRA50FA20HL10 concrete and CRA50FA20HL10 concrete shows a slight improvement (12.03% and 25.76%) when compared to concretes with FA and HL, respectively. This behavior is also observed in f_{c28}, which shows an improvement of 31.4%. This shows that adding HL in concrete with FA has an activation effect that allows the FA particles to react at the earliest ages due to the greater availability of $Ca(OH)_2$. According to Valcuende et al. [36], the improvement of the compressive strength of the FA with HL concretes is closely linked to acid-base self-neutralization of the matrix. The pozzolanic reaction of the FA with $Ca(OH)_2$ from PC and HL is the predominant factor for increasing compressive strength. Similar trends were obtained by Barbhuiya et al. [34]. MRA50FA20HL10 concrete and CRA50FA20HL10 concrete was 17.15% higher compressive strength compared to CRA50FA20HL0 concrete at 28-days-old and 23.27% higher at 63-days-old. However, the consumption of PC for concrete with MRA was 370 kg/m³, while for concrete with CRA, it was 331 kg/m³. In water absorption, porosity and density, and modulus of elasticity (Ec_{28}), it is possible to observe improvements in these properties when HL is added to all concretes (MRA, CRA).

4 CONCLUSIONS

Based on the analysis of the experimental results, the main conclusions will be presented below:

- The addition of 10% of hydrated lime in concrete with 50% recycled aggregate and 20% of fly ash showed improvements in the compressive strength of concrete being, for concretes with recycled concrete aggregate, an increase of 17.15%, and concretes with mixed recycled aggregate an increase of 41% when compared to concretes without hydrated lime.

- Improvements in the elastic modulus were also observed by adding 10% of hydrated lime, which in concretes with CRA showed an increase of 3.78%, and for concretes with mixed recycled aggregate the growth was 1.34% when compared to concretes without hydrated lime.

- Concrete with 50% recycled aggregate of concrete, 20% of fly ash, and 10% of hydrated lime showed a decrease in porosity and water absorption of 23.82% and 9.87%, respectively, when compared to concrete without the addition of 10% hydrated lime. The specific mass showed an increase of 5.02% when compared to concrete without the addition of 10% hydrated lime

- The concrete MRA50FA20HL10 concrete showed a carbonation coefficient of 44.5% lower compared to the MRA50FA20HL0 concrete. Adding HL in concrete with FA tends to reduce the carbonation coefficient of concrete at an early age.

- The concretes with 50% of MRA, 20% fly ash and without HL showed an average equivalent diameter of 68.20 μm of the pores. When 10% of HL was inserted, the average equivalent diameter was 69.92 μm. The effect of HL on concrete with RCA was more pronounced, as it showed a reduction in the average equivalent diameter of 62.29% when compared to concrete without HL.

5 SUGGESTIONS FOR IN-DEEP STUDIES

The results obtained in this study make attractive the development of more research involving concrete with recycled aggregate, fly ash, and hydrated lime. The addition of hydrated lime results in improvements in mechanical and durability properties. In addition to encouraging the use of this waste to reduce the consumption of natural resources and contribute to the reduction of CO_2 emissions in the environment, resulting in more sustainable concrete. Considering the results

obtained and few published papers focusing on the analysis of the effect of hydrated lime on concrete with fly ash and recycled aggregate, it is possible to draw some relevant suggestions for further in-depth studies on this subject:

- Analyze the amount of $Ca(OH)_2$ through the use of differential scanning calorimetry and thermogravimetric analysis to establish a more suitable content for the addition of hydrated lime for a given content of fly ash in Portland cement concrete.
- The concrete in the fresh state has the function of hydrating the cement to develop its resistance characteristics, however in excess, it will be evaded, and its path towards the surface of the concrete creates pore paths that will be the water of the concrete in the hardened state. Therefore, a capillary water absorption test in Portland cement concrete with fly ash, hydrated lime, and recycled aggregate should be considered to evaluate the addition of hydrated lime in this context.
- Follow the evolution of hydration, through X-ray diffraction, of Portland cement concretes with fly ash, hydrated lime and recycled aggregate, to assess whether there are changes in the hydrated compounds when hydrated lime is added.

ACKNOWLEDGMENTS

This study was financed in part by the Coordenação de Aperfeiçoamento de Pessoal de Nível Superior – Brasil (CAPES) – Finance Code 001 to the first author. The authors gratefully acknowledge the support from the A. H. Augustin from the IPR/PUCRS, Chemistry Laboratory of the Polytechnic School of PUCRS. The authors are very thankful to professors F. A. P. Recena, M. H. F. Medeiros, M. Mancio and E. M. da Costa for their valuable suggestion and J. E. Cruz from the Construction Materials Laboratory.

REFERENCES

[1] J. Solís-Guzmán, M. Marrero, M.V. Montes-Delgado, A. Ramírez-de-Arellano, A Spanish model for quantification and management of construction waste, Waste Manag. 29 (2009) 2542–2548. https://doi.org/10.1016/j.wasman.2009.05.009.

[2] ABRELPE, Panorama dos Resídos Sólidos no Brasil, Assoc. Bras. Empres. Limp. Pública e Resíduos Especiais - ABRELPE. (2021) 53 P. https://abrelpe.org.br/panorama/.

[3] R. V. Silva, J. De Brito, R.K. Dhir, Performance of cementitious renderings and masonry mortars containing recycled aggregates from construction and demolition wastes, Constr. Build. Mater. 105 (2016) 400–415. https://doi.org/10.1016/j.conbuildmat.2015.12.171.

[4] International Energy Agency, Global Energy Review: CO2 Emissions in 2021 Global emissions rebound sharply to highest ever level, Iea. (2022) 1–14. https://iea.blob.core.windows.net/assets/c3086240-732b-4f6a-89d7-db01be018f5e/GlobalEnergyReviewCO2Emissionsin2021.pdf.

[5] F. Cirilo, Reduction in CO2 Emissions is synonym of Competitiveness in the Global Cement Industry (in Portuguese), ABCP - Assoc. Bras. Cim. Portl. (2022) 1 p,. https://abcp.org.br/reducao-na-emissao-de-co2-e-sinonimo-de-competitividade-na-industria-global-do-cimento/.

[6] P.S. Martínez, M.G. Cortina, F.F. Martínez, A.R. Sánchez, Comparative study of three types of fine recycled aggregates from construction and demolition waste (CDW), and their use in masonry mortar fabrication, J. Clean. Prod. 118 (2016) 162–169. https://doi.org/10.1016/j.jclepro.2016.01.059.

[7] K. Robalo, H. Costa, R. do Carmo, E. Júlio, Experimental development of low cement content and recycled construction and demolition waste aggregates concrete, Constr. Build. Mater. 273 (2021) 121680. https://doi.org/10.1016/j.conbuildmat.2020.121680.

[8] M. Bravo, J. De Brito, J. Pontes, L. Evangelista, Mechanical performance of concrete made with aggregates from construction and demolition waste recycling plants, J. Clean. Prod. 99 (2015) 59–74. https://doi.org/10.1016/j.jclepro.2015.03.012.

[9] R.L.S. Ferreira, M.A.S. Anjos, A.K.C. Nóbrega, J.E.S. Pereira, E.F. Ledesma, The role of powder content of the recycled aggregates of CDW in the behaviour of rendering mortars, Constr. Build. Mater. 208 (2019) 601–612. https://doi.org/10.1016/j.conbuildmat.2019.03.058.

[10] K.P. Verian, W. Ashraf, Y. Cao, Properties of recycled concrete aggregate and their influence in new concrete production, Resour. Conserv. Recycl. 133 (2018) 30–49. https://doi.org/10.1016/j.resconrec.2018.02.005.

[11] L.W. Zhang, A.O. Sojobi, V.K.R. Kodur, K.M. Liew, Effective utilization and recycling of mixed recycled aggregates for a greener environment, J. Clean. Prod. 236 (2019) 117600. https://doi.org/10.1016/j.jclepro.2019.07.075.

[12] M.G.C. Cunha, Feasibility of using C&W from the generation of conventional and high-strength concrete through the use of the jig as a processing schedule (in Portuguese), UNIVERSIDADE FEDERAL DO RIO GRANDE DO SUL, 2017. https://lume.ufrgs.br/handle/10183/178221.

[13] X. Chen, L. Capiau, I. Reynaert, K. Zheng, E. Gruyaert, J. Li, Comparative study on modelling concrete properties using physical and mechanical properties of recycled coarse aggregate, Constr. Build. Mater. 345 (2022) 128249. https://doi.org/10.1016/j.conbuildmat.2022.128249.

[14] R.K. Dhir, J. de Brito, R. V Silva, C.Q. Lye, 15 - Epilogue, in: R.K. Dhir, J. de Brito, R. V Silva, C.Q.B.T.-S.C.M. Lye (Eds.), Woodhead Publ. Ser. Civ. Struct. Eng., Woodhead Publishing, 2019: pp. 603–608. https://doi.org/https://doi.org/10.1016/B978-0-08-100985-7.00015-7.

[15] E. Khoury, W. Ambrós, B. Cazacliu, C.H. Sampaio, S. Remond, Heterogeneity of recycled concrete aggregates, an intrinsic variability, Constr. Build. Mater. 175 (2018) 705–713. https://doi.org/10.1016/j.conbuildmat.2018.04.163.

[16] I.F. Sáez del Bosque, W. Zhu, T. Howind, A. Matías, M.I. Sánchez de Rojas, C. Medina, Properties of interfacial transition zones (ITZs) in concrete containing recycled mixed aggregate, Cem. Concr. Compos. 81 (2017) 25–34. https://doi.org/10.1016/j.cemconcomp.2017.04.011.

[17] I. Martínez-Lage, P. Vázquez-Burgo, M. Velay-Lizancos, Sustainability evaluation of concretes with mixed recycled aggregate based on holistic approach: Technical, economic and environmental analysis, Waste Manag. 104 (2020) 9–19. https://doi.org/10.1016/j.wasman.2019.12.044.

[18] C. Zhou, Z. Chen, Mechanical properties of recycled concrete made with different types of coarse aggregate, Constr. Build. Mater. 134 (2017) 497–506. https://doi.org/10.1016/j.conbuildmat.2016.12.163.

[19] K. Kapoor, S.P. Singh, B. Singh, Durability of self-compacting concrete made with Recycled Concrete Aggregates and mineral admixtures, Constr. Build. Mater. 128 (2016) 67–76. https://doi.org/10.1016/j.conbuildmat.2016.10.026.

[20] A. Adessina, A. Ben, J. Barthélémy, C. Chateau, Experimental and micromechanical investigation on the mechanical and durability properties of recycled aggregate concretes, Cem. Concr. Res. 126 (2019) 105900. https://doi.org/10.1016/j.cemconres.2019.105900.

[21] C. Meyer, The greening of the concrete industry, Cem. Concr. Compos. 31 (2009) 601–605. https://doi.org/10.1016/j.cemconcomp.2008.12.010.

[22] E. Aprianti, P. Shafigh, S. Bahri, J.N. Farahani, Supplementary cementitious materials origin from agricultural wastes - A review, Constr. Build. Mater. 74 (2015) 176–187. https://doi.org/10.1016/j.conbuildmat.2014.10.010.

[23] H. Plfdv, G.R. Frqfuhwr, X.P. Hvwxgr, G.H. Fdvr, Z. Kljk, P. Dgglwlrq, F.D. Fdvh, Perspectivas ambientais e econômicas do concreto com altos teores de adições minerais: um estudo de caso, Ambient. Construído. 4 (2008) 19–30.

[24] P. Kumar Mehta, Natural Pozzolan. In: Suplementary Cementing Materials., in: Ottawa V. M. Malhotra, 1987: p. 427p.

[25] V. Corinaldesi, G. Moriconi, Influence of mineral additions on the performance of 100% recycled aggregate concrete, Constr. Build. Mater. 23 (2009) 2869–2876. https://doi.org/10.1016/j.conbuildmat.2009.02.004.

[26] R. Kurad, J.D. Silvestre, J. de Brito, H. Ahmed, Effect of incorporation of high volume of recycled concrete aggregates and fly ash on the strength and global warming potential of concrete, J. Clean. Prod. 166 (2017) 485–502. https://doi.org/10.1016/j.jclepro.2017.07.236.

[27] S. Sunayana, S. V. Barai, Recycled aggregate concrete incorporating fly ash: Comparative study on particle packing and conventional method, Constr. Build. Mater. 156 (2017) 376–386. https://doi.org/10.1016/j.conbuildmat.2017.08.132.

[28] S.R. da Silva, J.J. de Oliveira Andrade, Investigation of mechanical properties and carbonation of concretes with construction and demolition waste and fly ash, Constr. Build. Mater. 153 (2017) 704–715. https://doi.org/10.1016/j.conbuildmat.2017.07.143.

[29] M.S. Barkhordari, D.J. Armaghani, A.S. Mohammed, Data-Driven Compressive Strength Prediction of Fly Ash, (2022). https://doi.org/10.3390/buildings12020132.

[30] J. Geng, J. Sun, Characteristics of the carbonation resistance of recycled fine aggregate concrete, Constr. Build. Mater. 49 (2013) 814–820. https://doi.org/10.1016/j.conbuildmat.2013.08.090.

[31] M. Limbachiya, M.S. Meddah, Y. Ouchagour, Use of recycled concrete aggregate in fly-ash concrete, Constr. Build. Mater. 27 (2012) 439–449. https://doi.org/10.1016/j.conbuildmat.2011.07.023.

[32] J. Hoppe Filho, Cement, Fly Ash and Hydrated Lime Systems: Hydration, Microstructure and concrete Carbonation Mechanism (in Portuguese), Escola Politécnica da Universidade de São Paulo, 2008.

[33] P. Lorca, R. Calabuig, J. Benlloch, L. Soriano, J. Payá, Microconcrete with partial replacement of Portland cement by fly ash and hydrated lime addition, Mater. Des. 64 (2014) 535–541. https://doi.org/10.1016/j.matdes.2014.08.022.

[34] S.A. Barbhuiya, J.K. Gbagbo, M.I. Russell, P.A.M. Basheer, Properties of fly ash concrete modified with hydrated lime and silica fume, Constr. Build. Mater. 23 (2009) 3233–3239. https://doi.org/10.1016/j.conbuildmat.2009.06.001.

[35] M. Kumar, S.K. Singh, N.P. Singh, Heat evolution during the hydration of Portland cement in the presence of fly ash, calcium hydroxide and super plasticizer, Thermochim. Acta. 548 (2012) 27–32. https://doi.org/10.1016/j.tca.2012.08.028.

[36] M. Valcuende, R. Calabuig, A. Martínez-Ibernón, J. Soto, Influence of hydrated lime on the chloride-induced reinforcement corrosion in eco-efficient concretes made with high-volume fly ash, Materials (Basel). 13 (2020) 1–16. https://doi.org/10.3390/ma13225135.

[37] C. Gunasekara, M. Sandanayake, Z. Zhou, D.W. Law, S. Setunge, Effect of nano-silica addition into

high volume fly ash–hydrated lime blended concrete, Constr. Build. Mater. 253 (2020) 119205. https://doi.org/10.1016/j.conbuildmat.2020.119205.

[38] J. Hoppe Filho, Cement, Fly Ash and Hydrated Lime Systems: Hydration Mechanism, Microstructure and Carbonation of Concrete (in portuguese), Escola Politécnica da Universidade de São Paulo, 2008. https://www.teses.usp.br/teses/disponiveis/3/3146/tde-19082008-172648/publico/TESE_DOUTORADO_JUAREZ_HOPPE_FILHO.pdf.

[39] O. Hurtado-Figueroa, F.J. Echavarria-Paez, J.A. Cárdenas-Gutiérrez, Influence of water/cement ratio on mechanical strength of concrete with partial addition of fly ash and hydrated lime, J. Phys. Conf. Ser. 1386 (2019). https://doi.org/10.1088/1742-6596/1386/1/012085.

[40] M.A.S. Anjos, A. Camões, P. Campos, G.A. Azeredo, R.L.S. Ferreira, Effect of high volume fly ash and metakaolin with and without hydrated lime on the properties of self-compacting concrete, J. Build. Eng. 27 (2020). https://doi.org/10.1016/j.jobe.2019.100985.

[41] S.H. Kang, Y. Jeong, M.O. Kim, J. Moon, Pozzolanic reaction on alkali-activated Class F fly ash for ambient condition curable structural materials, Constr. Build. Mater. 218 (2019) 235–244. https://doi.org/10.1016/j.conbuildmat.2019.05.129.

[42] P. Chindaprasirt, S. Homwuttiwong, V. Sirivivatnanon, Influence of fly ash fineness on strength, drying shrinkage and sulfate resistance of blended cement mortar, Cem. Concr. Res. (2004). https://doi.org/10.1016/j.cemconres.2003.11.021.

[43] ABNT, NBR 16605 - Cimento Portland e outros materiais em pó — Determinação da massa específica, Assoc. Bras. Normas Técnicas. (2017) 1–4.

[44] G.D. Moon, S. Oh, Y.C. Choi, Effects of the physicochemical properties of fly ash on the compressive strength of high-volume fly ash mortar, Constr. Build. Mater. 124 (2016) 1072–1080. https://doi.org/10.1016/j.conbuildmat.2016.08.148.

[45] ABNT, NBR NM 52 - Agregado miúdo - Determinação da massa específica e massa específica aparente, Assoc. Bras. Normas Técnicas. (2003) 6.

[46] ABNT, NBR NM 248 - Agregados-Determinação da composição granulométrica, Assoc. Bras. Normas Técnicas. (2003).

[47] S.C. Kou, C.S. Poon, Long-term mechanical and durability properties of recycled aggregate concrete prepared with the incorporation of fly ash, Cem. Concr. Compos. (2013). https://doi.org/10.1016/j.cemconcomp.2012.12.011.

[48] M.B. Leite, J.G.L. Figueire Do Filho, P.R.L. Lima, Workability study of concretes made with recycled mortar aggregate, Mater. Struct. Constr. 46 (2013) 1765–1778. https://doi.org/10.1617/s11527-012-0010-4.

[49] C. Alexandridou, G.N. Angelopoulos, F.A. Coutelieris, Mechanical and durability performance of concrete produced with recycled aggregates from Greek construction and demolition waste plants, J. Clean. Prod. 176 (2018) 745–757. https://doi.org/10.1016/j.jclepro.2017.12.081.

[50] ABNT, 6118 - 2014 Projeto de estruturas de concreto - Procedimento, Assoc. Bras. Normas Técnicas. (2014) 256. https://doi.org/01.080.10; 13.220.99.

[51] ABNT, NBR 7212 - Concreto dosado em central - Preparo, fornecimento e controle, Assoc. Bras. Normas Técnicas. (2021) 25p.

[52] P.S. Lovato, E. Possan, D.C.C.D. Molin, Â.B. Masuero, J.L.D. Ribeiro, Modeling of mechanical properties and durability of recycled aggregate concretes, Constr. Build. Mater. 26 (2012) 437–447. https://doi.org/10.1016/j.conbuildmat.2011.06.043.

[53] S.R. da Silva, F.N. Cimadon, P.M. Borges, J.Z. Schiavon, E. Possan, J.J. de O. Andrade, Relationship Between the mechanical properties and Carbonation of Concretes with construction and demolition waste, Case Stud. Constr. Mater. (2021) 104876. https://doi.org/10.1016/j.cscm.2021.e00860.

[54] M.B. Leite, Evaluation of the mechanical properties of concrete made with recycled aggregates from construction and demolition waste (in Portuguese), Federal University of Rio Grande do Sul, Porto Alegre, 270 p., 2001. https://doi.org/000292768.

[55] G. Dimitriou, P. Savva, M.F. Petrou, Enhancing mechanical and durability properties of recycled aggregate concrete, Constr. Build. Mater. 158 (2018) 228–235. https://doi.org/10.1016/j.conbuildmat.2017.09.137.

[56] A. Lotfy, M. Al-Fayez, Performance evaluation of structural concrete using controlled quality coarse and fine recycled concrete aggregate, Cem. Concr. Compos. 61 (2015) 36–43. https://doi.org/10.1016/j.cemconcomp.2015.02.009.

[57] G.L. Vieira, J.Z. Schiavon, P.M. Borges, S.R. da Silva, J.J. de Oliveira Andrade, Influence of recycled aggregate replacement and fly ash content in performance of pervious concrete mixtures, J. Clean. Prod. 271 (2020). https://doi.org/10.1016/j.jclepro.2020.122665.

[58] R. Ramkrishnan, B. Abilash, M. Trivedi, P. Varsha, P. Varun, S. Vishanth, Effect of Mineral Admixtures on Pervious Concrete, Mater. Today Proc. 5 (2018) 24014–24023. https://doi.org/10.1016/j.matpr.2018.10.194.

[59] X. Chen, H. Wang, H. Najm, G. Venkiteela, J. Hencken, Evaluating engineering properties and environmental impact of pervious concrete with fly ash and slag, J. Clean. Prod. 237 (2019) 117714. https://doi.org/10.1016/j.jclepro.2019.117714.

[60] N. Saboo, S. Shivhare, K.K. Kori, A.K. Chandrappa, Effect of fly ash and metakaolin on pervious concrete properties, Constr. Build. Mater. 223 (2019) 322–328. https://doi.org/10.1016/j.conbuildmat.2019.06.185.

[61] ABNT, NBR 5739 - Ensaios de compressão de corpos de prova cilíndricos., Assoc. Bras. Normas Técnicas. (2007) 14.

[62] ABNT, ABNT NBR 8522 - Concreto: Determinação dos módulos estáticos de elasticidade e de deformação à compressão, Assoc. Bras. Normas Técnicas. (2017) 20.

[63] ABNT, NBR 9778 - Argamassa e concreto endurecidos - Determinação da absorção de água, índice de vazios e massa específica, Assoc. Bras. Normas Técnicas. (2005) 4p.

[64] C. Pauletti, Estimation of the natural carbonation of cementitious materials from accelerated tests and prediction models (in Portuguese), Federal University of Rio Grande do Sul - UFRGS, 2009. https://www.lume.ufrgs.br/bitstream/handle/10183/30120/000778056.pdf?sequence=1&isAllowed=y.

[65] M.P. Kulakowski, Contribution to the study of carbonation in concrete and composite mortars with the addition of silica fume (in Portuguese), Universidade Federal do Rio Grande do Sul - UFRGS, 2002. http://hdl.handle.net/10183/3594.

[66] S.K. Saha, S. Pradhan, S. V. Barai, Use of machine learning based technique to X-ray microtomographic images of concrete for phase segmentation at meso-scale, Constr. Build. Mater. 249 (2020) 118744. https://doi.org/10.1016/j.conbuildmat.2020.118744.

[67] M.B. Leite, P.J.M. Monteiro, Microstructural analysis of recycled concrete using X-ray microtomography, Cem. Concr. Res. 81 (2016) 38–48. https://doi.org/10.1016/j.cemconres.2015.11.010.

[68] P. Mira, V.G. Papadakis, S. Tsimas, Effect of lime putty addition on structural and durability properties of concrete, Cem. Concr. Res. 32 (2002) 683–689. https://doi.org/10.1016/S0008-8846(01)00744-X.

[69] Y. Wang, H. Zhang, Y. Geng, Q. Wang, S. Zhang, Prediction of the elastic modulus and the splitting tensile strength of concrete incorporating both fine and coarse recycled aggregate, Constr. Build. Mater. 215 (2019) 332–346. https://doi.org/10.1016/j.conbuildmat.2019.04.212.

[70] M.G.A. and T.I. Milne, Influence of Cement Blend and Aggregate Type on the Stress-Strain Behavior and Elastic Modulus of Concrete, ACI Mater. J. 92 (n.d.). https://doi.org/10.14359/1114.

[71] M. Uysal, The influence of coarse aggregate type on mechanical properties of fly ash additive self-compacting concrete, Constr. Build. Mater. 37 (2012) 533–540. https://doi.org/10.1016/j.conbuildmat.2012.07.085.

[72] V. Nežerka, J. Němeček, Z. Slížková, P. Tesárek, Investigation of crushed brick-matrix interface in lime-based ancient mortar by microscopy and nanoindentation, Cem. Concr. Compos. 55 (2015) 122–128. https://doi.org/10.1016/j.cemconcomp.2014.07.023.

[73] J. Hoppe Filho, M.H.F. Medeiros, E. Pereira, P. Helene, G.C. Isaia, High-Volume Fly Ash Concrete with and without Hydrated Lime: Chloride Diffusion Coefficient from Accelerated Test, J. Mater. Civ. Eng. 25 (2013) 411–418. https://doi.org/10.1061/(asce)mt.1943-5533.0000596.

[74] N.S. Pandian, S. Balasubramonian, Permeability and consolidation behavior of fly ashes, J. Test. Eval. 27 (1999) 337–342.

[75] C. Lima, A. Caggiano, C. Faella, E. Martinelli, M. Pepe, R. Realfonzo, Physical properties and mechanical behaviour of concrete made with recycled aggregates and fly ash, Constr. Build. Mater. (2013). https://doi.org/10.1016/j.conbuildmat.2013.04.051.

[76] R. Vedalakshmi, A.S. Raj, S. Srinivasan, K.G. Babu, Quantification of hydrated cement products of blended cements in low and medium strength concrete using TG and DTA technique, Thermochim. Acta. 407 (2003) 49–60.

[77] S. Huang, S. Yu, Y. Ye, Z. Ye, A. Cheng, Pore structure change and physico-mechanical properties deterioration of sandstone suffering freeze-thaw actions, Constr. Build. Mater. 330 (2022) 127200. https://doi.org/10.1016/j.conbuildmat.2022.127200.

[78] M. Ondrášik, M. Kopecký, Rock Pore Structure as Main Reason of Rock Deterioration, Stud. Geotech. Mech. 36 (2014). https://doi.org/10.2478/sgem-2014-0010.

[79] S. Lu, E.N. Landis, D.T. Keane, X-ray microtomographic studies of pore structure and permeability in Portland cement concrete, Mater. Struct. Constr. 39 (2006) 611–620. https://doi.org/10.1617/s11527-006-9099-7.

[80] L. Zong, Z. Fei, S. Zhang, Permeability of recycled aggregate concrete containing fly ash and clay brick waste, J. Clean. Prod. (2014). https://doi.org/10.1016/j.jclepro.2014.02.040.

[81] I.F.S. Bosque, P. V. Heede, N. Belie, M.I.S. Rojas, C. Medina, Carbonation of concrete with construction and demolition waste based recycled aggregates and cement with recycled content, Constr. Build. Mater. 234 (2020) 117336. https://doi.org/10.1016/j.conbuildmat.2019.117336.

[82] M. Bravo, J. de Brito, L. Evangelista, J. Pacheco, Durability and shrinkage of concrete with CDW as recycled aggregates: Benefits from superplasticizer's incorporation and influence of CDW composition, Constr. Build. Mater. 168 (2018) 818–830. https://doi.org/10.1016/j.conbuildmat.2018.02.176.

[83] N. Singh, S.P. Singh, Carbonation and electrical resistance of self compacting concrete made with recycled concrete aggregates and metakaolin, Constr. Build. Mater. 121 (2016) 400–409. https://doi.org/10.1016/j.conbuildmat.2016.06.009.

[84] K. Sisomphon, L. Franke, Carbonation rates of concretes containing high volume of pozzolanic materials, Cem. Concr. Res. 37 (2007) 1647–1653. https://doi.org/10.1016/j.cemconres.2007.08.014.

[85] S.R. da Silva, F.N. Cimadon, P.M. Borges, J.Z. Schiavon, E. Possan, J.J. de O. Andrade, Relationship between the mechanical properties and carbonation of concretes with construction and demolition waste, Case Stud. Constr. Mater. 16 (2022). https://doi.org/10.1016/j.cscm.2021.e00860.

[86] S. Ghorbani, S. Sharifi, S. Ghorbani, V.W. Tam, J. de Brito, R. Kurda, Effect of crushed concrete waste's maximum size as partial replacement of natural coarse aggregate on the mechanical and durability properties of concrete, Resour. Conserv. Recycl. 149 (2019) 664–673. https://doi.org/10.1016/j.resconrec.2019.06.030.

[87] V. Carević, I. Ignjatović, J. Dragaš, Model for practical carbonation depth prediction for high volume fly ash concrete and recycled aggregate concrete, Constr. Build. Mater. 213 (2019) 194–208. https://doi.org/10.1016/j.conbuildmat.2019.03.267.

4. CONCLUSÕES

A adição da cal hidratada em concretos com adição de cinza volante em substituição ao cimento Portland e agregado reciclado aumenta o teor remanescente de $Ca(OH)_2$ na matriz. Quanto maior for a disponibilidade de cal, maior será a quantidade de hidratos e consumo de $Ca(OH)_2$ para um mesmo tempo de reação (HOPPE FILHO, 2008a). A análise da atividade pozolânica de cinza volante com cal hidratada, baseado nos experimentos realizados, permite as seguintes conclusões:

- A capacidade de absorção de água do agregado graúdo reciclado é alta e deve ser considerada na produção de concreto. Essa maior absorção está relacionada à menor massa específica do RA e à maior porosidade, que tem influência negativa sobre as propriedades mecânicas e durabilidade do concreto produzido.

- O concreto com RA de 100% e uma relação de a/c de 0,60 apresentaram redução na resistência à compressiva (f_{c28}) de 60,60% em relação à referência. No entanto, o concreto produzido com 25% de agregado reciclado aos 28 dias de idade e uma relação a/c de 0,50 apresentou redução na resistência à compressão de 8,7% em relação ao concreto de referência.

- Verificou-se que para o concreto com uma relação a/c de 0,60, o valor de E_c foi reduzido em 47,2% e 18,1% em relação ao concreto de referência, para teor de substituição de 100% e 25%, respectivamente. No entanto, para o concreto com uma relação a/c de 0,40 e 0,50, a queda no E_c quando comparada à referência foi inferior a 6%.

- O concreto com 100% de ARM e relação a/c de 0,60 mostrou profundidades de carbonatação (e_{co2}) em 45 e 120 dias 29,80% e 18,70% maiores, respectivamente, quando comparados ao concreto de referência com relação a/c de 0,60. O concreto com 50% de ARM e relação a/c de 0,40 mostrou e_{co2} em 45 e 120 dias 14,90% e 9,35% maiores, respectivamente, quando comparados ao concreto de referência com relação a/c de 0,40.

- A análise utilizando MEV demonstrou a predominância do vazios, $Ca(OH)_2$, e etringita no concreto com RA. Em contraste, o concreto de referência mostrou o C-S-H mais uniforme, embora contivesse poros entre as camadas características do gel C-S-H. Além disso, o RA mostrou a presença de uma pequena quantidade de pasta velha aderida à superfície agregada, mas a nova pasta era mais densa e uniforme.

- O aumento do teor de RA resulta em um claro aumento dos poros interligados do concreto. O alto volume de vazio está associado a uma alta taxa de absorção e menor densidade de RA. Observou-se boa correlação entre as propriedades mecânicas aos 28 dias de idade (f_c e E_c) e propriedades de durabilidade (volume vazios aos 28 dias e profundidade de carbonatação com 45 dias de exposição) ao CO_2.

- Os resultados do ensaio através da microtomografia de raios X indicam que a porosidade do concreto aumenta com a adição de RA. Para 0,50-R0 (Figura 20), o volume reduzido do vazio ocorre em espaços onde não há agregado presente. A diferença de porosidade entre agregados naturais e reciclados torna-se clara. O espaço ocupado pelo agregado natural não tem vazios aparentes, enquanto o volume preenchido por RA mostra maior concentração de vazios.

    - É possível estimar, através da modelagem matemática utilizando os dados amostrais deste estudo, o E_c de concreto com RA variando entre 0% e 100% para as relações a/c variando entre 0,4 e 0,6 e 28 dias de cura;

    - A adição de 10% de cal hidratado em concreto com 50% de agregado reciclado e 20% de cinzas de volante apresentou melhorias na resistência à compressão do concreto. Para concreto com agregado reciclado de concreto (ARC) o aumento foi de 17,15%, e para concretos com agregado reciclado misto (ARM) o aumento foi de 41% quando comparado ao concreto sem cal hidratado;

    - Também foram observadas melhorias no módulo de elasticidade quando 10% de cal hidratada é adicionada. Concreto com ARC apresentou um aumento de

3,78%, e concreto com ARM apresentou um crescimento de 1,34% quando comparado ao concreto sem cal hidratada;

- Também foram observadas melhorias no módulo de elasticidade quando 10% de cal hidratada é adicionada. Concreto com ARC apresentou um aumento de 3,78%, e concreto com ARM apresentou um crescimento de 1,34% quando comparado ao concreto sem cal hidratado;

- Concreto com 50% de ARC, 20% de cinzas de volante 10% de cal hidratada apresentou queda na porosidade e absorção de água de 23,82% e 9,87%, respectivamente, quando comparado ao concreto sem a adição de 10% de cal hidratada. A massa específica apresentou aumento de 5,02% quando comparada ao concreto sem a adição de 10% de cal hidratada;

- O concreto com MRA, FA e 10% de cal hidratada mostrou um coeficiente de carbonatação 44,5% menor em relação ao concreto sem cal hidratada. Adicionar cal hidratada no concreto com FA tende a reduzir o coeficiente de carbonatação do concreto logo aos 35 dias de exposição ao CO_2.

- Os concretos com MRA e FA e sem cal hidratada apresentaram diâmetro equivalente médio de 68,20 μm dos poros. Quando 10% do cal hidratada foi inserido, o diâmetro equivalente médio foi de 69,92 μm. O efeito da cal hidratada no concreto com RCA foi mais acentuado, pois mostrou uma redução no diâmetro equivalente médio de 62,29% quando comparado ao concreto sem cal hidratada.

5. SUGESTÕES PARA TRABALHOS FUTUROS

Os resultados obtidos neste estudo tornam atrativo o desenvolvimento de mais pesquisas envolvendo concreto com agregado reciclado, cinza volante e cal hidratada. A adição de cal hidratada resulta em melhorias nas propriedades mecânicas e de durabilidade, se comparada com concretos apenas com cinza volante. Além disso, deve-se incentivar o uso desses resíduos para reduzir o consumo de recursos naturais e contribuir para redução das missões de CO_2 no meio ambiente, resultando na possibilidade de produção de um concreto mais ecoeficiente. Considerando os resultados obtidos e poucos artigos publicados com foco na análise do efeito da cal hidratada no concreto com cinzas volante e agregado reciclado, é possível propor algumas sugestões relevantes para estudos mais aprofundados sobre o assunto:

- Analisar a quantidade de $Ca(OH)_2$ através do uso de calorimetria diferencial e análise termogravimétrica para estabelecer um conteúdo mais adequado para a adição de cal hidratada para um determinado teor de cinza volante em concretos de cimento Portland com agregado reciclado.

- Analisar o impacto da cal hidratada na corrosão da armadura.

- O concreto no estado fresco tem a função de hidratar o cimento para desenvolver suas características de resistência. Porém, a água em excesso poderá evaporar, criando uma interconexão entre os poros no estado endurecido. Portanto, um teste de absorção capilar de água em concreto de cimento Portland com cinzas volante, cal hidratada e agregado reciclado deve ser considerado para avaliar a adição de cal hidratada neste contexto.

- Acompanhar a evolução da hidratação dos concretos de cimento Portland com cinzas volante, cal hidratada e agregado reciclado, para avaliar se há alterações nos compostos hidratados quando a cal hidratada é adicionada.

REFERÊNCIAS

ABNT. NBR NM 52 - Agregado miúdo - Determinação da massa específica e massa específica aparente. **Associação Brasileira de Normas Técnicas**, p. 6, 2003a.

ABNT. NBR NM 248 - Agregados-Determinação da composição granulométrica. **Associação Brasileira de Normas Técnicas**, 2003b.

ABNT. NBR 9778 - Argamassa e concreto endurecidos - Determinação da absorção de água, índice de vazios e massa específica. **Associação Brasileira de Normas Técnicas**, p. 4p, 2005.

ABNT. NBR 5739 - Ensaios de compressão de corpos de prova cilíndricos. **Associação Brasileira de Normas Técnicas**, p. 14, 2007.

ABNT. 6118 - 2014 Projeto de estruturas de concreto - Procedimento. **Associação Brasileira de Normas Técnicas**, p. 256, 2014.

ABNT. NBR 16605 - Cimento Portland e outros materiais em pó — Determinação da massa específica. **Associação Brasileira de Normas Técnicas**, p. 1–4, 2017a.

ABNT. ABNT NBR 8522 - Concreto: Determinação dos módulos estáticos de elasticidade e de deformação à compressão. **Associação Brasileira de Normas Técnicas**, p. 20, 2017b.

ABNT. NBR 7212 - Concreto dosado em central - Preparo, fornecimento e controle. **Associação Brasileira de Normas Técnicas**, p. 25p, 2021.

ABNT NBR 12653. ABNT NBR 12653 - Materiais pozolânicos. **Molecular Reproduction and Development**, v. 74, n. 2, p. 172–177, 1992.

ABOUSTAIT, M. et al. Physical and chemical characteristics of fly ash using automated scanning electron microscopy. **Construction and Building Materials**, v. 106, p. 1–10, 2016.

ABRELPE. **Panorama dos Resídos Sólidos no Brasil**. Disponível em: <https://abrelpe.org.br/panorama/>.

ACAR, I.; ATALAY, M. U. Characterization of sintered class F fly ashes. **Fuel**, v. 106, p. 195–203, 2013.

ADESINA, P. A.; OLUTOGE, F. A. Structural properties of sustainable concrete developed using rice husk ash and hydrated lime. **Journal of Building Engineering**, v. 25, n. February, p. 100804, 2019.

ADESSINA, A. et al. Experimental and micromechanical investigation on the mechanical and durability properties of recycled aggregate concretes. **Cement and Concrete Research**, v. 126, n. September, p. 105900, 2019.

ALEXANDRIDOU, C.; ANGELOPOULOS, G. N.; COUTELIERIS, F. A. Mechanical and durability performance of concrete produced with recycled aggregates from Greek construction and demolition waste plants. **Journal of Cleaner Production**, v. 176, p. 745–757, 2018.

ALI, B.; GULZAR, M. A.; RAZA, A. Effect of sulfate activation of fly ash on mechanical and durability properties of recycled aggregate concrete. **Construction and Building Materials**, v. 277, p. 122329, 2021.

ALMEIDA, E. P. DE; GOMES, W. C. Reutilização das cinzas volantes de carvão mineral na fabricação de cimento de Portland Reuse of coal fly ash in the manufacture of Portland cement. **Revista Ibero-Americana de Ciências Ambientais**, v. v12, n.8, p. 375–386, 2021.

ANJOS, M. A. S. et al. Effect of high volume fly ash and metakaolin with and without hydrated lime on the properties of self-compacting concrete. **Journal of Building Engineering**, v. 27, n. October 2019, 2020.

APRIANTI, E. et al. Supplementary cementitious materials origin from agricultural wastes - A review. **Construction and Building Materials**, v. 74, p. 176–187, 2015.

BAGHABRA AL-AMOUDI, O. S. et al. Lime-activation of natural pozzolan for use as supplementary cementitious material in concrete. **Ain Shams Engineering Journal**, n. xxxx, 2021.

BARBHUIYA, S. A. et al. Properties of fly ash concrete modified with hydrated lime and silica fume. **Construction and Building Materials**, v. 23, n. 10, p. 3233–3239, 2009.

BARKHORDARI, M. S.; ARMAGHANI, D. J.; MOHAMMED, A. S. Data-Driven Compressive Strength Prediction of Fly Ash. n. January, 2022.

BISWAL, U. S.; DINAKAR, P. A mix design procedure for fly ash and ground granulated blast furnace slag based treated recycled aggregate concrete. **Cleaner Engineering and Technology**, v. 5, p. 100314, 2021.

BLISSETT, R. S.; ROWSON, N. A. A review of the multi-component utilisation of coal fly ash. **Fuel**, v. 97, p. 1–23, 2012.

BOSQUE, I. F. S. et al. Carbonation of concrete with construction and demolition waste based recycled aggregates and cement with recycled content. **Construction and Building Materials**, v. 234, p. 117336, 2020.

BRAVO, M. et al. Durability performance of concrete with recycled aggregates from construction and demolition waste plants. **Construction and Building Materials**, v. 77, p. 357–369, 2015a.

BRAVO, M. et al. Mechanical performance of concrete made with aggregates from construction and demolition waste recycling plants. **Journal of Cleaner Production**, v. 99, n. 2015, p. 59–74, 2015b.

BRAVO, M. et al. Superplasticizer's efficiency on the mechanical properties of recycled aggregates concrete: Influence of recycled aggregates composition and incorporation ratio. **Construction and Building Materials**, v. 153, p. 129–138, 2017.

BRAVO, M. et al. Durability and shrinkage of concrete with CDW as recycled aggregates: Benefits from superplasticizer's incorporation and influence of CDW composition. **Construction and Building Materials**, v. 168, p. 818–830, 2018.

BROUWERS, H. J. H.; EIJK, R. J. VAN. Chemical Reaction of Fly Ash. **11th International Congress on the Chemistry of Cement.**, n. May, p. 791–800, 2003.

CAMPOS, H. F. et al. Low-cement high-strength concrete with partial replacement of Portland cement with stone powder and silica fume designed by particle packing optimization. **Journal of Cleaner Production**, v. 261, p. 121228, 2020.

CAREVIĆ, V.; IGNJATOVIĆ, I.; DRAGAŠ, J. Model for practical carbonation depth prediction for high volume fly ash concrete and recycled aggregate concrete. **Construction and Building Materials**, v. 213, p. 194–208, 2019.

CHEN, X. et al. Evaluating engineering properties and environmental impact of pervious concrete with fly ash and slag. **Journal of Cleaner Production**, v. 237, p. 117714, 2019.

CHEN, X. et al. Comparative study on modelling concrete properties using physical and mechanical properties of recycled coarse aggregate. **Construction and Building Materials**, v. 345, n. June, p. 128249, 2022.

CHINDAPRASIRT, P.; HOMWUTTIWONG, S.; SIRIVIVATNANON, V. Influence of fly ash fineness on strength, drying shrinkage and sulfate resistance of blended cement mortar. **Cement and Concrete Research**, 2004.

CHOUSIDIS, N. et al. Effect of fly ash chemical composition on the reinforcement corrosion, thermal diffusion and strength of blended cement concretes. **Construction and Building Materials**, v. 126, p. 86–97, 2016.

CIRILO, F. Reduction in CO2 Emissions is synonym of Competitiveness in the Global Cement Industry (in Portuguese). **ABCP - Associação Brasileira de Cimento Portland**, p. 1 p, abr. 2022.

CIRINO, M. A. G. et al. Caracterização e avaliação da atividade pozolânica das cinzas provenientes da queima de carvão mineral das termelétricas do Pecém, Ceará, Brasil. **Matéria (Rio de Janeiro)**, v. 26, n. 4, 2021.

CORINALDESI, V.; MORICONI, G. Influence of mineral additions on the performance of 100% recycled aggregate concrete. **Construction and Building Materials**, v. 23, n. 8, p. 2869–2876, 2009.

CUNHA, M. G. C. **Feasibility of using C&W from the generation of conventional and high-strength concrete through the use of the jig as a processing schedule (in Portuguese)**. [s.l.] UNIVERSIDADE FEDERAL DO RIO GRANDE DO SUL, 2017.

DA SILVA, S. R. et al. Relationship Between the mechanical properties and Carbonation of Concretes with construction and demolition waste. **Case Studies in Construction Materials**, p. 104876, 2021.

DA SILVA, S. R. et al. Relationship between the mechanical properties and carbonation of concretes with construction and demolition waste. **Case Studies in Construction Materials**, v. 16, n. September 2021, 2022.

DA SILVA, S. R.; DE OLIVEIRA ANDRADE, J. J. Investigation of mechanical properties and carbonation of concretes with construction and demolition waste and fly ash. **Construction and Building Materials**, v. 153, p. 704–715, 2017.

DAL MOLIN, D. C. C. Adições Minerais. In: **Concreto: Ciência e Tecnologia**. IBRACON ed. São Paulo: [s.n.]. p. 48p.

DE VARGAS, A. S. et al. The effects of Na2O/SiO2 molar ratio, curing temperature and age on compressive strength, morphology and microstructure of alkali-activated fly ash-based geopolymers. **Cement and Concrete Composites**, v. 33, n. 6, p. 653–660, 2011.

DHIR, R. K. et al. 15 - Epilogue. In: DHIR, R. K. et al. (Eds.). . **Woodhead Publishing Series in Civil and Structural Engineering**. [s.l.] Woodhead Publishing, 2019. p. 603–608.

DIMITRIOU, G.; SAVVA, P.; PETROU, M. F. Enhancing mechanical and durability properties of recycled aggregate concrete. **Construction and Building Materials**, v. 158, p. 228–235, 2018.

DING, Y.; DAI, J. G.; SHI, C. J. Mechanical properties of alkali-activated concrete: A state-of-the-art review. **Construction and Building Materials**, v. 127, p. 68–79, 2016.

DUAN, P. et al. Effects of metakaolin, silica fume and slag on pore structure, interfacial transition zone and compressive strength of concrete. **Construction and Building Materials**, v. 44, p. 1–6, 2013.

DURDZIŃSKI, P. T. et al. A new quantification method based on SEM-EDS to assess fly ash composition and study the reaction of its individual components in hydrating cement paste. **Cement and Concrete Research**, v. 73, p. 111–122, 2015.

FERREIRA, R. L. S. et al. The role of powder content of the recycled aggregates of CDW in the behaviour of rendering mortars. **Construction and Building Materials**, v. 208, p. 601–612, 2019.

GENG, J.; SUN, J. Characteristics of the carbonation resistance of recycled fine aggregate concrete. **Construction and Building Materials**, v. 49, p. 814–820, 2013.

GETTU, R. et al. Influence of supplementary cementitious materials on the sustainability parameters of cements and concretes in the Indian context. **Materials and Structures/Materiaux et Constructions**, v. 52, n. 1, p. 1–11, 2019.

GHORBANI, S. et al. Effect of crushed concrete waste's maximum size as partial replacement of natural coarse aggregate on the mechanical and durability properties of concrete. **Resources, Conservation and Recycling**, v. 149, n. November 2018, p. 664–673, 2019.

GONZALEZ-COROMINAS, A.; ETXEBERRIA, M.; POON, C. S. Influence of steam curing on the pore structures and mechanical properties of fly-ash high performance concrete prepared with recycled aggregates. **Cement and Concrete Composites**, v. 71, p. 77–84, 2016.

GUNASEKARA, C. et al. Zeta potential, gel formation and compressive strength of low calcium fly ash geopolymers. **Construction and Building Materials**, v. 95, p. 592–599, 2015.

GUNASEKARA, C. et al. Effect of nano-silica addition into high volume fly ash–hydrated lime blended concrete. **Construction and Building Materials**, v. 253, p. 119205, 2020.

HABERT, G. et al. Environmental impacts and decarbonization strategies in the cement and concrete industries. **Nature Reviews Earth and Environment**, v. 1, n. 11, p. 559–573, 2020.

HANUMANTHA RAO, B. et al. A mix design procedure for geopolymer concrete with fly ash. **Journal of Cleaner Production**, v. 133, p. 117–125, 2016.

HEFNI, Y.; ZAHER, Y. A. EL; WAHAB, M. A. Influence of activation of fly ash on the mechanical properties of concrete. **Construction and Building Materials**, v. 172, p. 728–734, 2018.

HOPPE FILHO, J. **Cement, Fly Ash and Hydrated Lime Systems: Hydration Mechanism, Microstructure and Carbonation of Concrete (in portuguese)**. [s.l.] Escola Politécnica da Universidade de São Paulo, 2008a.

HOPPE FILHO, J. **Cement, Fly Ash and Hydrated Lime Systems: Hydration, Microstructure and concrete Carbonation Mechanism (in Portuguese)**. [s.l.] Escola Politécnica da Universidade de Sâo Paulo, 2008b.

HOPPE FILHO, J. et al. High-Volume Fly Ash Concrete with and without Hydrated Lime: Chloride Diffusion Coefficient from Accelerated Test. **Journal of Materials in Civil Engineering**, v. 25, n. 3, p. 411–418, 2013.

HUANG, Q. et al. Modification of water absorption and pore structure of high-volume fly ash cement pastes by incorporating nanosilica. **Journal of Building Engineering**, v. 33, n. July 2020, p. 101638, 2021.

HUANG, S. et al. Pore structure change and physico-mechanical properties deterioration of sandstone suffering freeze-thaw actions. **Construction and Building Materials**, v. 330, n. November 2021, p. 127200, 2022.

HURTADO-FIGUEROA, O.; ECHAVARRIA-PAEZ, F. J.; CÁRDENAS-GUTIÉRREZ, J.

A. Influence of water/cement ratio on mechanical strength of concrete with partial addition of fly ash and hydrated lime. **Journal of Physics: Conference Series**, v. 1386, n. 1, 2019.

HUSEIEN, G. F. et al. Evaluation of alkali-activated mortars containing high volume waste ceramic powder and fly ash replacing GBFS. **Construction and Building Materials**, v. 210, p. 78–92, 2019.

INTERNATIONAL ENERGY AGENCY. Global Energy Review: CO2 Emissions in 2021 Global emissions rebound sharply to highest ever level. **Iea**, p. 1–14, 2022.

JUAN-VALDÉS, A. et al. Mechanical and microstructural characterization of non-structural precast concrete made with recycled mixed ceramic aggregates from construction and demolition wastes. **Journal of Cleaner Production**, v. 180, p. 482–493, 2018.

KANG, S. H. et al. Pozzolanic reaction on alkali-activated Class F fly ash for ambient condition curable structural materials. **Construction and Building Materials**, v. 218, p. 235–244, 2019.

KAPOOR, K.; SINGH, S. P.; SINGH, B. Durability of self-compacting concrete made with Recycled Concrete Aggregates and mineral admixtures. **Construction and Building Materials**, v. 128, p. 67–76, 2016.

KHOURY, E. et al. Heterogeneity of recycled concrete aggregates, an intrinsic variability. **Construction and Building Materials**, v. 175, p. 705–713, 2018.

KIATTIKOMOL, K. et al. A study of ground coarse fly ashes with different finenesses from various sources as pozzolanic materials. **Composites**, v. 23, p. 335–343, 2001.

KISKU, N. et al. A critical review and assessment for usage of recycled aggregate as sustainable construction material. **Construction and Building Materials**, v. 131, p. 721–740, 2017.

KONG, D. et al. Effect and mechanism of surface-coating pozzalanics materials around aggregate on properties and ITZ microstructure of recycled aggregate concrete. **Construction and Building Materials**, v. 24, n. 5, p. 701–708, 2010.

KOU, S. C.; POON, C. S. Enhancing the durability properties of concrete prepared with coarse recycled aggregate. **Construction and Building Materials**, v. 35, p. 69–76, 2012.

KOU, S. C.; POON, C. S. Long-term mechanical and durability properties of recycled aggregate concrete prepared with the incorporation of fly ash. **Cement and Concrete Composites**, 2013.

KULAKOWSKI, M. P. **Contribution to the study of carbonation in concrete and composite mortars with the addition of silica fume (in Portuguese)**. [s.l.] Universidade Federal do Rio Grande do Sul - UFRGS, 2002.

KUMAR, M.; SINGH, S. K.; SINGH, N. P. Heat evolution during the hydration of Portland cement in the presence of fly ash, calcium hydroxide and super plasticizer. **Thermochimica Acta**, v. 548, p. 27–32, 2012.

KUMAR MEHTA, P. Natural Pozzolan. In: Suplementary Cementing Materials. In: **Ottawa: V. M. Malhotra**. [s.l: s.n.]. p. 427p.

KURAD, R. et al. Effect of incorporation of high volume of recycled concrete aggregates and fly ash on the strength and global warming potential of concrete. **Journal of Cleaner Production**, v. 166, p. 485–502, 2017.

LEITE, M. B. **Evaluation of the mechanical properties of concrete made with recycled aggregates from construction and demolition waste (in Portuguese)**. [s.l.] Federal University of Rio Grande do Sul, Porto Alegre, 270 p., 2001.

LEITE, M. B.; FIGUEIRE DO FILHO, J. G. L.; LIMA, P. R. L. Workability study of concretes made with recycled mortar aggregate. **Materials and Structures/Materiaux et Constructions**, v. 46, n. 10, p. 1765–1778, 2013.

LEITE, M. B.; MONTEIRO, P. J. M. Microstructural analysis of recycled concrete using X-ray microtomography. **Cement and Concrete Research**, v. 81, p. 38–48, 2016a.

LEITE, M. B.; MONTEIRO, P. J. M. Microstructural analysis of recycled concrete using X-ray microtomography. **Cement and Concrete Research**, v. 81, p. 38–48, 2016b.

LIMA, C. et al. Physical properties and mechanical behaviour of concrete made with recycled aggregates and fly ash. **Construction and Building Materials**, 2013.

LIMBACHIYA, M.; MEDDAH, M. S.; OUCHAGOUR, Y. Use of recycled concrete aggregate in fly-ash concrete. **Construction and Building Materials**, 2012a.

LIMBACHIYA, M.; MEDDAH, M. S.; OUCHAGOUR, Y. Use of recycled concrete aggregate in fly-ash concrete. **Construction and Building Materials**, v. 27, n. 1, p. 439–449, 2012b.

LIU, C.; ZHANG, M. Effect of curing temperature on hydration, microstructure and ionic diffusivity of fly ash blended cement paste: A modelling study. **Construction and Building Materials**, v. 297, p. 123834, 2021.

LORCA, P. et al. Microconcrete with partial replacement of Portland cement by fly ash and hydrated lime addition. **Materials and Design**, v. 64, p. 535–541, 2014.

LOTFI, S. et al. Performance of recycled aggregate concrete based on a new concrete recycling technology. **Construction and Building Materials**, v. 95, p. 243–256, 2015.

LOTFY, A.; AL-FAYEZ, M. Performance evaluation of structural concrete using controlled quality coarse and fine recycled concrete aggregate. **Cement and Concrete Composites**, v. 61, p. 36–43, 2015.

LOVATO, P. S. et al. Modeling of mechanical properties and durability of recycled

aggregate concretes. **Construction and Building Materials**, v. 26, n. 1, p. 437–447, 2012.

LU, S.; LANDIS, E. N.; KEANE, D. T. X-ray microtomographic studies of pore structure and permeability in Portland cement concrete. **Materials and Structures/Materiaux et Constructions**, v. 39, n. 6, p. 611–620, 2006.

MARTÍN-MORALES, M. et al. Characterization of recycled aggregates construction and demolition waste for concrete production following the Spanish Structural Concrete Code EHE-08. **Construction and Building Materials**, v. 25, n. 2, p. 742–748, 2011.

MARTÍNEZ-LAGE, I. et al. Properties of plain concrete made with mixed recycled coarse aggregate. **Construction and Building Materials**, v. 37, p. 171–176, 2012.

MARTÍNEZ-LAGE, I.; VÁZQUEZ-BURGO, P.; VELAY-LIZANCOS, M. Sustainability evaluation of concretes with mixed recycled aggregate based on holistic approach: Technical, economic and environmental analysis. **Waste Management**, v. 104, p. 9–19, 2020.

MARTÍNEZ, P. S. et al. Comparative study of three types of fine recycled aggregates from construction and demolition waste (CDW), and their use in masonry mortar fabrication. **Journal of cleaner production**, v. 118, p. 162–169, 2016.

MASSAZZA, F. Pozzolana and Pozzolanic Cements. In: **LEA's Chemistry of Cement and Concrete**. [s.l: s.n.]. p. 471–635.

MEYER, C. The greening of the concrete industry. **Cement and Concrete Composites**, v. 31, n. 8, p. 601–605, 2009.

MILNE, M. G. A. AND T. I. Influence of Cement Blend and Aggregate Type on the Stress-Strain Behavior and Elastic Modulus of Concrete. **ACI Materials Journal**, v. 92, n. 3, [s.d.].

MIRA, P.; PAPADAKIS, V. G.; TSIMAS, S. Effect of lime putty addition on structural and durability properties of concrete. **Cement and Concrete Research**, v. 32, n. 5, p. 683–689, 2002.

MOON, G. D.; OH, S.; CHOI, Y. C. Effects of the physicochemical properties of fly ash on the compressive strength of high-volume fly ash mortar. **Construction and Building Materials**, v. 124, p. 1072–1080, 2016.

MYADRABOINA, H.; SETUNGE, S.; PATNAIKUNI, I. Pozzolanic Index and lime requirement of low calcium fly ashes in high volume fly ash mortar. **Construction and Building Materials**, v. 131, p. 690–695, 2017.

NEŽERKA, V. et al. Investigation of crushed brick-matrix interface in lime-based ancient mortar by microscopy and nanoindentation. **Cement and Concrete Composites**, v. 55, p. 122–128, 2015.

ONDRÁŠIK, M.; KOPECKÝ, M. Rock Pore Structure as Main Reason of Rock Deterioration. **Studia Geotechnica et Mechanica**, v. 36, 13 jun. 2014.

PANDIAN, N. S.; BALASUBRAMONIAN, S. Permeability and consolidation behavior of fly ashes. **Journal of Testing and Evaluation**, v. 27, p. 337–342, 1999.

PAULETTI, C. **Estimation of the natural carbonation of cementitious materials from accelerated tests and prediction models (in Portuguese)**. [s.l.] Federal University of Rio Grande do Sul - UFRGS, 2009.

PLFDV, H. et al. Perspectivas ambientais e econômicas do concreto com altos teores de adições minerais: um estudo de caso. **Ambiente Construído**, v. 4, n. 2, p. 19–30, 2008.

POON, C. S.; SHUI, Z. H.; LAM, L. Effect of microstructure of ITZ on compressive strength of concrete prepared with recycled aggregates. **Construction and Building Materials**, v. 18, n. 6, p. 461–468, 2004.

RAKNGAN, W. et al. Controlling workability in alkali-activated Class C fly ash. **Construction and Building Materials**, v. 183, p. 226–233, 2018.

RAMKRISHNAN, R. et al. Effect of Mineral Admixtures on Pervious Concrete. **Materials Today: Proceedings**, v. 5, n. 11, p. 24014–24023, 2018.

ROBALO, K. et al. Experimental development of low cement content and recycled construction and demolition waste aggregates concrete. **Construction and Building Materials**, v. 273, p. 121680, 2021.

RODRIGUE, A. et al. Influence of added water and fly ash content on the characteristics, properties and early-age cracking sensitivity of alkali-activated slag/fly ash concrete cured at ambient temperature. **Construction and Building Materials**, v. 171, p. 929–941, 2018.

SABOO, N. et al. Effect of fly ash and metakaolin on pervious concrete properties. **Construction and Building Materials**, v. 223, p. 322–328, 2019.

SÁEZ DEL BOSQUE, I. F. et al. Properties of interfacial transition zones (ITZs) in concrete containing recycled mixed aggregate. **Cement and Concrete Composites**, v. 81, p. 25–34, 2017.

SAHA, S. K.; PRADHAN, S.; BARAI, S. V. Use of machine learning based technique to X-ray microtomographic images of concrete for phase segmentation at meso-scale. **Construction and Building Materials**, v. 249, p. 118744, 2020.

SEDDIK MEDDAH, M. Recycled aggregates in concrete production: engineering properties and environmental impact. **MATEC Web of Conferences**, v. 101, p. 05021, 2017.

SHAFAATIAN, S. M. H. et al. How does fly ash mitigate alkali-silica reaction (ASR) in accelerated mortar bar test (ASTM C1567)? **Cement and Concrete Composites**, v.

37, n. 1, p. 143–153, 2013.

SHAIKH, F. U. A. Effect of ultrafine fly ash on the properties of concretes containing construction and demolition wastes as coarse aggregates. **Structural Concrete**, 2016.

SILVA, R. V.; DE BRITO, J.; DHIR, R. K. Properties and composition of recycled aggregates from construction and demolition waste suitable for concrete production. **Construction and Building Materials**, v. 65, p. 201–217, 2014.

SILVA, R. V.; DE BRITO, J.; DHIR, R. K. Performance of cementitious renderings and masonry mortars containing recycled aggregates from construction and demolition wastes. **Construction and Building Materials**, v. 105, p. 400–415, 2016.

SINGH, N.; SINGH, S. P. Carbonation and electrical resistance of self compacting concrete made with recycled concrete aggregates and metakaolin. **Construction and Building Materials**, v. 121, p. 400–409, 2016.

SISOMPHON, K.; FRANKE, L. Carbonation rates of concretes containing high volume of pozzolanic materials. **Cement and Concrete Research**, v. 37, n. 12, p. 1647–1653, 2007.

SOLÍS-GUZMÁN, J. et al. A Spanish model for quantification and management of construction waste. **Waste Management**, v. 29, n. 9, p. 2542–2548, 2009.

SUNAYANA, S.; BARAI, S. V. Recycled aggregate concrete incorporating fly ash: Comparative study on particle packing and conventional method. **Construction and Building Materials**, v. 156, p. 376–386, 2017.

SUPIT, S. W. M.; SHAIKH, F. U. A.; SARKER, P. K. Effect of ultrafine fly ash on mechanical properties of high volume fly ash mortar. **Construction and Building Materials**, v. 51, p. 278–286, 2014.

TOSUN-FELEKOĞLU, K. et al. Utilization and selection of proper fly ash in cost effective green HTPP-ECC design. **Journal of Cleaner Production**, v. 149, n. x, p. 557–568, 2017.

UYSAL, M. The influence of coarse aggregate type on mechanical properties of fly ash additive self-compacting concrete. **Construction and Building Materials**, v. 37, p. 533–540, 2012.

VALCUENDE, M. et al. Influence of hydrated lime on the chloride-induced reinforcement corrosion in eco-efficient concretes made with high-volume fly ash. **Materials**, v. 13, n. 22, p. 1–16, 2020.

VEDALAKSHMI, R. et al. Quantification of hydrated cement products of blended cements in low and medium strength concrete using TG and DTA technique. **Thermochimica Acta**, v. 407, p. 49–60, 2003.

VERIAN, K. P.; ASHRAF, W.; CAO, Y. Properties of recycled concrete aggregate and their influence in new concrete production. **Resources, Conservation and Recycling**,

v. 133, n. October 2017, p. 30–49, 2018.

VIEIRA, G. L. et al. Influence of recycled aggregate replacement and fly ash content in performance of pervious concrete mixtures. **Journal of Cleaner Production**, v. 271, 2020.

WANG, X.-Y.; PARK, K.-B. Analysis of compressive strength development of concrete containing high volume fly ash. **Construction and Building Materials**, v. 98, p. 810–819, 2015.

WANG, Y. et al. Prediction of the elastic modulus and the splitting tensile strength of concrete incorporating both fine and coarse recycled aggregate. **Construction and Building Materials**, v. 215, p. 332–346, 2019.

WRIGHT, J. R.; SHAFAATIAN, S.; RAJABIPOUR, F. Reliability of chemical index model in determining fly ash effectiveness against alkali-silica reaction induced by highly reactive glass aggregates. **Construction and Building Materials**, v. 64, p. 166–171, 2014.

XIAO, J. et al. Properties of interfacial transition zones in recycled aggregate concrete tested by nanoindentation. **Cement and Concrete Composites**, v. 37, n. 1, p. 276–292, 2013.

ZHANG, L. W. et al. Effective utilization and recycling of mixed recycled aggregates for a greener environment. **Journal of Cleaner Production**, v. 236, p. 117600, 2019.

ZHAO, Q. et al. Long-age wet curing effect on performance of carbonation resistance of fly ash concrete. **Construction and Building Materials**, v. 127, p. 577–587, 2016.

ZHAO, Y.; ZENG, W.; ZHANG, H. Properties of recycled aggregate concrete with different water control methods. **Construction and Building Materials**, v. 152, p. 539–546, 2017.

ZHOU, C.; CHEN, Z. Mechanical properties of recycled concrete made with different types of coarse aggregate. **Construction and Building Materials**, v. 134, p. 497–506, 2017.

ZONG, L.; FEI, Z.; ZHANG, S. Permeability of recycled aggregate concrete containing fly ash and clay brick waste. **Journal of Cleaner Production**, 2014.

ANEXO A

Gmail

Sergio Roberto Da Silva <sergio.roberto@acad.pucrs.br>

A manuscript number has been assigned: CONBUILDMAT-D-22-07932

1 message

Construction & Building Materials <em@editorialmanager.com> Wed, Aug 17, 2022 at 7:30 AM
Reply-To: Construction & Building Materials <support@elsevier.com>
To: Sergio da Silva <sergio.roberto@acad.pucrs.br>

ELSEVIER

This is an automated message

Dear Mr. da Silva,

Your submission entitled "SYNERGIC EFFECT OF RECYCLED AGGREGATES, FLY ASH, AND HYDRATED LIME FOR PRODUCTION OF ECO-FRIENDLY CONCRETE" has been been assigned the following manuscript number: **CONBUILDMAT-D-22-07932**. Please reference this manuscript number for your future enquiries on the status of the manuscript.

You will be able to check on the progress of your paper by logging on to Editorial Manager as an author.

Thank you for submitting your work to this journal.

Kind regards,

Swathi Ramalingam

Administrative Support Agent [17-Jan-11]

Construction and Building Materials

Have questions or need assistance?
Please do not reply to this automated message.
For further assistance, please visit Elsevier Support Center for Author Support.
You can also talk to our customer support team 24/7 by live chat, email and phone.

#AU_CONBUILDMAT#

To ensure this email reaches the intended recipient, please do not delete the above code

ELSEVIER

RELX™

Pontifícia Universidade Católica do Rio Grande do Sul
Pró-Reitoria de Graduação
Av. Ipiranga, 6681 - Prédio 1 - 3º. andar
Porto Alegre - RS - Brasil
Fone: (51) 3320-3500 - Fax: (51) 3339-1564
E-mail: prograd@pucrs.br
Site: www.pucrs.br